# Distribution Fault Location

## Field Data and Analysis

*Technical Report*

# Distribution Fault Location

## Field Data and Analysis

**1012438**

Final Report, December, 2006

EPRI Project Manager
A. Sundaram

## DISCLAIMER OF WARRANTIES AND LIMITATION OF LIABILITIES

THIS DOCUMENT WAS PREPARED BY THE ORGANIZATION(S) NAMED BELOW AS AN ACCOUNT OF WORK SPONSORED OR COSPONSORED BY THE BWR VESSEL AND INTERNALS PROJECT (BWRVIP) AND ELECTRIC POWER RESEARCH INSTITUTE, INC. (EPRI). NEITHER BWRVIP, EPRI, ANY MEMBER OF EPRI, ANY COSPONSOR, THE ORGANIZATION(S) BELOW, NOR ANY PERSON ACTING ON BEHALF OF ANY OF THEM:

(A) MAKES ANY WARRANTY OR REPRESENTATION WHATSOEVER, EXPRESS OR IMPLIED, (I) WITH RESPECT TO THE USE OF ANY INFORMATION, APPARATUS, METHOD, PROCESS, OR SIMILAR ITEM DISCLOSED IN THIS DOCUMENT, INCLUDING MERCHANTABILITY AND FITNESS FOR A PARTICULAR PURPOSE, OR (II) THAT SUCH USE DOES NOT INFRINGE ON OR INTERFERE WITH PRIVATELY OWNED RIGHTS, INCLUDING ANY PARTY'S INTELLECTUAL PROPERTY, OR (III) THAT THIS DOCUMENT IS SUITABLE TO ANY PARTICULAR USER'S CIRCUMSTANCE; OR

(B) ASSUMES RESPONSIBILITY FOR ANY DAMAGES OR OTHER LIABILITY WHATSOEVER (INCLUDING ANY CONSEQUENTIAL DAMAGES, EVEN IF BWRVIP, EPRI OR ANY EPRI REPRESENTATIVE HAS BEEN ADVISED OF THE POSSIBILITY OF SUCH DAMAGES) RESULTING FROM YOUR SELECTION OR USE OF THIS DOCUMENT OR ANY INFORMATION, APPARATUS, METHOD, PROCESS, OR SIMILAR ITEM DISCLOSED IN THIS DOCUMENT.

ORGANIZATION(S) THAT PREPARED THIS DOCUMENT

**EPRI Solutions, Inc.**

| |
|---|
| **NOTICE**:　　THIS REPORT CONTAINS PROPRIETARY INFORMATION THAT IS THE INTELLECTUAL PROPERTY OF BWRVIP UTILITY MEMBERS AND EPRI. ACCORDINGLY, IT IS AVAILABLE ONLY UNDER LICENSE FROM EPRI AND MAY NOT BE REPRODUCED OR DISCLOSED, WHOLLY OR IN PART, BY ANY LICENSEE TO ANY OTHER PERSON OR ORGANIZATION. |

## NOTE

For further information about EPRI, call the EPRI Customer Assistance Center at 800.313.3774 or e-mail askepri@epri.com.

Electric Power Research Institute and EPRI are registered service marks of the Electric Power Research Institute, Inc.

# CITATIONS

This report was prepared by

The report is a corporate document that should be cited in the literature in the following manner:

*Distribution Fault Location: Field Data and Analysis.* EPRI, Palo Alto, CA: 2006. 1012438.

# PRODUCT DESCRIPTION

---

Distribution faults are normally located manually without any measurements. Location is made primarily through field line inspections. Automated fault location algorithms have not been widely used because of the complexity and lack of monitoring equipment.

Practical fault location methods based on the use of current and voltage phasors have recently been implemented in feeder protection devices. Both Progress Carolina and Con Edison have implemented fault location systems using fairly simple Ohms-law fault-locating techniques along with feeder circuit impedances. This project builds on their work by gathering fault and outage data to test a variety of fault location approaches for the goal of developing a commercial-grade fault location system.

## Results & Findings

The project's main conclusion is that fault location can work well on a variety of circuits (urban and rural) and a variety of voltages with different types of monitors (relays and power quality monitors) at different measuring locations (bus level and feeder level). The best approaches for signal processing, fault identification, and location algorithms were developed.

One surprising and important outcome of this project is finding that it is possible to use monitoring waveforms to predict arc voltage during a fault. Being able to estimate arc voltage could help utilities in several ways:

- *Improving fault location algorithms*—An important outcome of this project, accounting for the impact of arc voltages can possibly improve the accuracy of fault locations.

- *Estimating arc power and energy*—Equipment explosions, manhole explosions, and arc flash are fundamentally a function of the power and energy in an arc.

- *Fault type estimation*—It may be possible to use arc voltage to help differentiate between types of faults. Preliminary data show a marked difference between splice failures and cable failures. Arc voltage also may help to differentiate between tree faults and lightning, for example.

## Challenges & Objective(s)

The ultimate goal of this series of projects is to develop a commercial-grade fault-locating system that utilities can integrate into their systems. A large set of fault data was gathered to make sure approaches were developed that would work with real monitoring data and real faults. In identifying the best approaches to fault location, a number of decisions were needed, including which fault location algorithms work best in different scenarios, what monitoring equipment works best, and where measurements are needed.

## Applications, Values & Use

Giving operators relatively accurate and reliable information on fault locations will improve restoration times. The most dramatic improvements will be for main feeder lockouts where the whole mainline would normally have to be patrolled. Progress Carolina reduced their average restoration time from 80 minutes to 60 minutes, mainly because of their fault-locating system. Automated fault location systems also will help circuits with repeated momentary interruptions—a fault location system will help pinpoint what section of the circuit has the problem causing repeated operations.

## EPRI Perspective

Monitoring has become more widespread recently with use of digital relays, power quality recorders, and advanced meters. Much of the data recorded by those devices is not being used to the full extent. These data are prime for utility use in fault location, fault identification, fault type classification, and arc voltage and energy estimation. Such uses will improve outage restoration, power quality, reliability, and safety. This fault location project will further advance the use and application of monitoring data.

## Approach

Monitoring data and outage information were gathered on over 1500 events from seven utilities. For each event, the project team collected voltage and current waveforms from a monitoring device (relays or power-quality recorders), a known outage location for outage data, and a circuit model. This process allowed the team to compare known locations with estimates from monitoring. Data included records from GE and Schweitzer relays, the Distribution Fault Anticipator (DFA), and Drantetz/BMI power quality recorders. Monitoring took place at substation bus monitors, substation feeder monitors, and line reclosers. Circuit data were in a number of formats, including Cyme, GIS, FeederAll, and PSS/Adept. The wide range of data will help in developing a system that can plug into a wide range of utility data sources.

## Keywords

Fault location
Distribution reliability
Short circuits
Faults
Arcs
Power quality

# EXECUTIVE SUMMARY

## EPRI Distribution Fault Location Study

This project is the first of a three-year set of projects with the ultimate goal of developing a commercial-grade fault-locating tool. To that end, a large amount of fault data has been collected and analyzed with various fault-location approaches.

## Fault-Location Approaches

Several impedance-based fault-location algorithms have been evaluated on the fault data collected. The main methods evaluated in this project include:

- Impedance to the fault—The absolute value of the impedance is estimated from $V/I$ from the monitoring waveshapes, and the fault possibilities are those where the magnitude of this impedance equals the cumulative impedance in the circuit model.

- Reactance to the fault—This is the same as the impedance method, but only the reactive portion is used. This avoids any resistance added by the fault arc.

- Current estimation—The available fault current at various points is compared with the measured fault current to identify location candidates.

- Voltage-sag estimation—The voltage sag during the event relative to the prefault voltage is used along with a voltage divider model along the circuit to estimate fault locations. The advantage of this method is that currents do not need to be measured.

- Takagi method—This method attempts to factor out the prefault load current and a linear arc resistance in estimating fault locations.

- Nonlinear arc method—The fault arc is highly nonlinear, and this model factors that in to derive an impedance of the line separately from the fault arc voltage.

All can provide useful estimates of fault location. The nonlinear arc method and the fault-current method have proved to be the most accurate. In addition to the algorithms used, important considerations are how to find magnitude and phase angle from waveform signals, whether to filter signals, and how to differentiate faults from inrush, voltage sags, and other events.

Beyond impedance-based methods, other approaches have been suggested, including traveling-wave methods and various learning systems like neural networks. These methods have not been proven yet, but more research is worthy to see if they can be used to improve fault locations.

## Existing Fault Location Systems

Progress Carolina has an advanced monitoring system that they use to locate faults. Progress Carolina records steady-state trend data and fault events on all of their feeders using a remote-terminal unit (RTU) that can sample at 16 samples per cycle. Progress Carolina uses the fault-current method of fault locating. They use the fault current from the measurement and use a fault-current profile from the given circuit to select possible fault locations. They assume a bolted fault (no fault resistance). They have web-based interfaces that their operators can use. The results of their program have been very good:

- *Accuracy*—Lampley[1] reported that their locations were accurate to within 0.5 miles 75% of the time; and in most of the remaining cases, the fault was usually no more than one to two miles from the estimate.

- *Restoration improvement*—Progress Carolina as reduced their CAIDI (average restoration time) from about 80 minutes to 60 minutes since 1998 when they started using their system for fault location.

Con Edison has recently implemented a fault location system in the New York City area with goals of reducing fault locating time and cost, directing crews more efficiently, and maintaining network reliability. For monitors, they use power quality monitors that are monitoring voltages and currents on a substation transformer. The monitors sample at 128 points per cycle. They use the reactance-to-the fault method of locating faults. Con Edison has been happy with their fault-location system. Stergio[2] reported that in an examination of 27 events at one location, 70% were within three manholes.

## Data Collection and Analysis

Utilities provided over 1500 fault events for analysis. Each event has monitoring data, a system circuit model, and a known outage location from an outage management database. Table ES-1 summarizes the data provided by seven utilities. This dataset has already allowed us to analyze a variety of fault types and a variety of monitoring instruments on a variety of different distribution systems. Such a wide range of data will help in developing a more commercial implementation.

Each dataset was analyzed using one or more fault-location algorithms. Figure ES-1 shows the example of one analysis done for Utility A for double-line-to-ground faults. This case showed a good relationship between the impedance to the fault predicted by the monitors and the impedance to the known fault location from the circuit database. The relationship was unaffected by the load current at the time of the fault. The relationship is not quite a 1:1 fit, but it is a linear relationship that can be corrected with a constant multiplier.

---

[1] Lampley, G. C., "Fault Detection and Location on Electrical Distribution System Case Study," presented at IEEE Rural Electric Power Conference, 2002.

[2] Stergiou, P. V., "Fault Location for Underground Systems," presented at PQA, 2006.

**Table ES-1**
**Fault Data Set Summary**

| Utility | Number of Events | Monitor | Samples Per Cycle | Voltage | System Type | Circuit Data |
|---------|------------------|---------|-------------------|---------|-------------|--------------|
| A | 211 | Bus PQ monitors | 128 | 13.8 kV | Suburban | Cyme/ArcGIS |
| B | 401 | Bus PQ monitors<br>GE feeder relays<br>SEL feeder relays | 128<br>32<br>16 | 13.8 and 27 kV | Urban | Custom format |
| C | 23 | Bus PQ monitors | 128 | 12 kV | Urban | SynerGEE |
| D | 10 | SEL feeder relays | 4 & 16 | 13 and 25 kV | Suburban/rural | FeederAll |
| E | 32 | SEL feeder relays<br>SEL recloser relay<br>DFA | 16<br>32<br>256 | 12 and 34 kV | Suburban/rural | Cyme |
| F | 1124 | Feeder and bus-level RTU | 16 | 12 and 23 kV | Suburban/rural | Cyme |
| G | 12 | SEL feeder relays | 4 | 12 kV | Suburban | PSS/Adept |



**Figure ES-1**
**Utility A: Impact of Load on Impedance Estimated from the Waveform Versus Impedance to the Fault from the Circuit Database**

*Executive Summary*

Figure ES-2 shows a typical line-to-ground fault that caused a feeder lockout. Figure ES-3 shows the circuit that was faulted with the known fault location. Location estimates from the waveform are also shown. Multiple locations are estimated because the radial circuit has a number of branches. Because the circuit breaker locked out, an operator could narrow the choices just to those on the mainline—assuming coordination of downstream protective devices. As with many of the faults at utility A, this prediction is an overestimate. The overestimate can be factored out of the model by including a multiplying factor.



```
                        prefault                    LG
    Va    8149.6 *an(  -18.2 )     6534.3 *an( -151.0 )
    Vb    8101.9 *an( -138.2 )     8598.4 *an(   94.7 )
    Vc    8203.5 *an(  101.4 )     8158.5 *an(  -19.0 )
    Ia    1181.7 *an(  -26.5 )     3711.9 *an(  169.9 )
    Ib    1281.5 *an( -145.6 )     1282.3 *an(   73.6 )
    Ic    1312.1 *an(   93.3 )     1545.7 *an(  -35.2 )
    V0      45.0 *an(   49.1 )     1013.2 *an(  -64.8 )
    V1    8151.6 *an(  -18.3 )     7736.8 *an( -144.7 )
    V2      25.8 *an( -156.8 )      422.2 *an(   66.9 )
    I0      31.8 *an(  142.6 )      752.7 *an(  154.0 )
    I1    1258.4 *an(  -26.3 )     2103.6 *an( -177.3 )
    I2      47.0 *an(  167.9 )      972.4 *an(  154.4 )
    Ir      95.3 *an(  142.6 )     2258.0 *an(  154.0 )
 Zfault                    NA                 1.66+2.37i
 Zfault3                   NA                        NA
```

**Figure ES-2**
**Example Line-to-Ground Fault**

X

$$z1 = 0.493+0.53i \quad z0 = 2.64+2.16i \quad zs = 1.21+1.07i$$
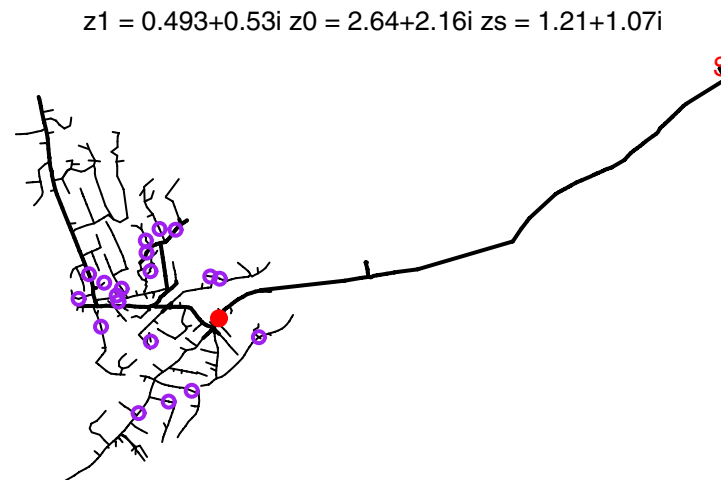


**Figure ES-3**
**Fault Estimates Relative to a Known Location (for the Event Plotted in Figure ES-2)**

Solid red: Known fault location

Purple circles: Location estimates

## Nonlinear Arc Estimation

One of the surprising and important outcomes of this project is finding that it is possible to use monitoring waveforms to predict the arc voltage during a fault. Being able to estimate the arc voltage could help utilities in several ways:

- *Improving fault location algorithms*—Of most interest for this project, accounting for the impact of arc voltages can possibly improve the accuracy of fault locations.

- *Estimating arc power and energy*—Equipment explosions, manhole explosions, and arc flash are fundamentally a function of the power and energy in an arc. Monitoring can provide better knowledge of arc energies in these situations. Monitoring to estimate arc energies can be used to develop better estimates of safety hazards, design arc flash boundaries or clothing requirements, or help perform failure forensics.

- *Fault type estimation*—It may be possible to use the arc voltage to help differentiate between different types of faults. Preliminary data shows a marked difference between splice failures and cable failures. It may also help to differentiate between tree faults and lightning for example. Such knowledge can help field crews when searching for the fault.

EPRI's Distribution Power Quality (DPQ) project (see EPRI TR-106294-V2 and EPRI TR-106294-V3) provided data that confirms that it is possible to accurately account for a nonlinear arc. Figure ES-4 shows two example events where the predicted arc voltage obtained from substation measurements matched well with the arc voltage measured downstream of the fault. This algorithm works by assuming that the arc voltage has the classic square-wave shape.
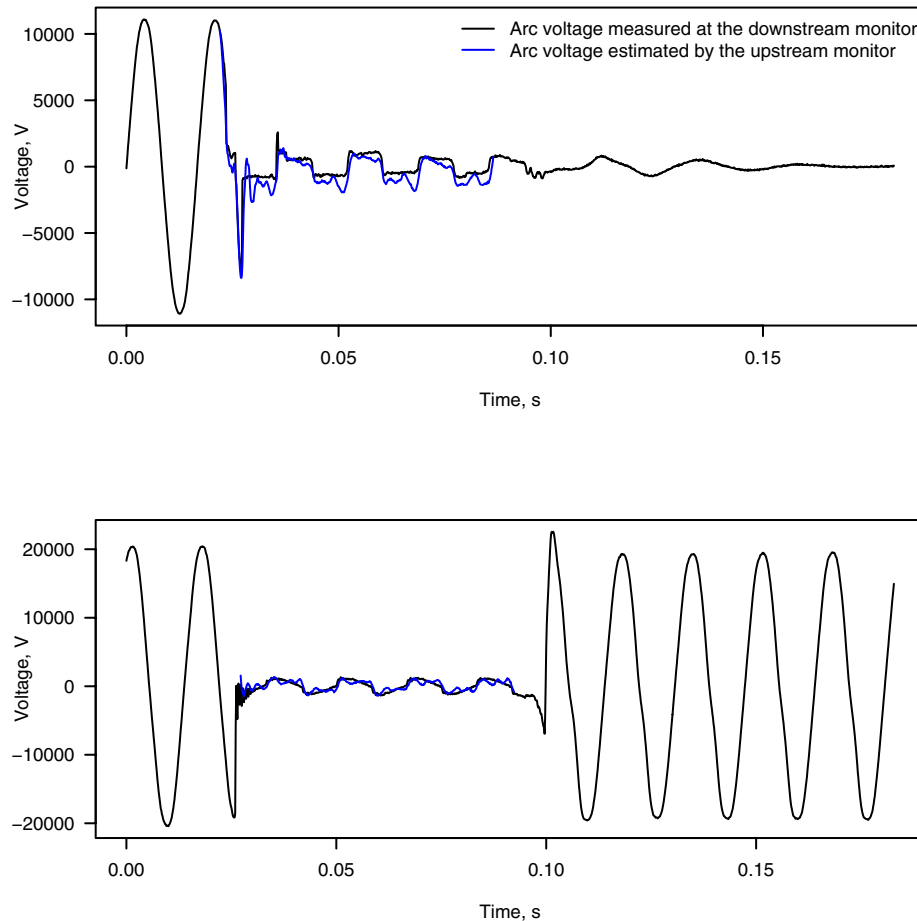
**Figure ES-4**
**Comparing Arc Voltages With Estimates from Feeder Monitors for Two Different Events (EPRI DPQ Study)**

Preliminary results with arc voltage estimations suggests that it may be possible to predict probabilities of fault type based on arc voltage. This was especially apparent on underground circuits which showed significant differences between joints, cables, and transformers, and even significant differences between solid joints, stop joints, and paper joints.

## Discussion Points

A number of issues related to fault-location systems were investigated during the study:

- *Feeder-level monitors versus bus monitors*—Feeder-level monitors are the best, but good fault location can be achieved with bus-level monitors. For line-to-ground faults, the key to achieving good location accuracy is using the residual current ($I_A + I_B + I_C$). This avoids most of the load current. For line-to-ground faults, the bus-level currents and the feeder-level currents are consistent within a multiplier factor for 70% of events. For multiphase faults, using a constant-impedance load model works reasonably well, but there is room for more research to investigate better load models for fault location.

- *Voltage-only fault location*—Measuring both voltage and current is the best, but voltage-only fault location is possible. Voltage-only fault location is less predictable because a prefault voltage is needed as a reference to the faulted voltage during the fault. If the prefault voltage is missing or misidentified, it will add error to the location, possibly even giving a nonsense answer. A nonsense answer may actually be better than a severely wrong but reasonable answer. Given that, a voltage-only algorithm can have uses on instrumentation where currents are unavailable.

- *Arc impedance*—Fault impedance is normally low and does not cause dramatic errors in fault locations. One drawback of many published fault-location algorithms is that they attempt to model the arc effect as a linear resistance. That is not a reasonable approximation. The arc impedance is highly nonlinear. The nonlinear arc modeling more accurately models arc characteristics and leads to one of the better fault-locating algorithms.

- *Underground and urban systems*—Impedance-based fault location works well on urban, underground systems as well as more suburban and rural systems. Both Utility B and Utility C are urban, mainly underground utilities. Accuracy gets better closer to the substation where circuit impedances between the substation and the fault are in the same range as the substation source impedance. In urban areas with high load, multiphase faults are the most difficult to locate because of the difficulty of separating load and fault current. The most difficult faults to identify are distant faults on rural circuits. As the fault current drops, the fault-current profile flattens out. The flat portion is where the location is most difficult (far from the substation).

- *Capacitors and regulators—*Circuit capacitors do not appear to influence fault-location results. The analysis of the data in this report was done without regard to capacitors—they were ignored, and that did not seem to impact the accuracy. While no rigorous investigations were done, checks on circuits with capacitors did not reveal anything unique on the impacts of capacitors. On circuits with capacitors, a ringing after the circuit faults can be pronounced, but as long as that part of the waveform is not used for fault location, it should not impact location estimates. Likewise, voltage regulators are not expected to significantly upset location estimates. Again, they were ignored in the analysis done in this report. A regulator at its neutral position does not add any impedance to the line.

- *Load current—*Load current can impact results, especially for bus-level monitors. The main ways to account for load current are (1) for line-to-ground faults, use the residual current $(I_A + I_B + I_C)$ to avoid all but the zero-sequence unbalance, and (2) use a constant-impedance (or other suitable load model) to divide out the load for multi-phase faults.

- *Built-in locating algorithms in relays*—The built-in algorithms in relays can give useful location estimates. It is certainly among the easiest ways to get fault location estimates, but it has limitations. For example, the SEL relays must have both voltage and current, and the Takagi algorithm that they use is one of the poorer methods for distribution faults based on the data we have evaluated.

## Implementation Vision

Fault-location algorithms are only one component of an integrated system to locate faults. In fact, the algorithms may be the easiest part. A fault location system must be integrated with the monitoring event database and the system circuit information (see Figure ES-5). This must be brought together and presented to the operator. The event data must be made available within minutes to be most useful to dispatchers.
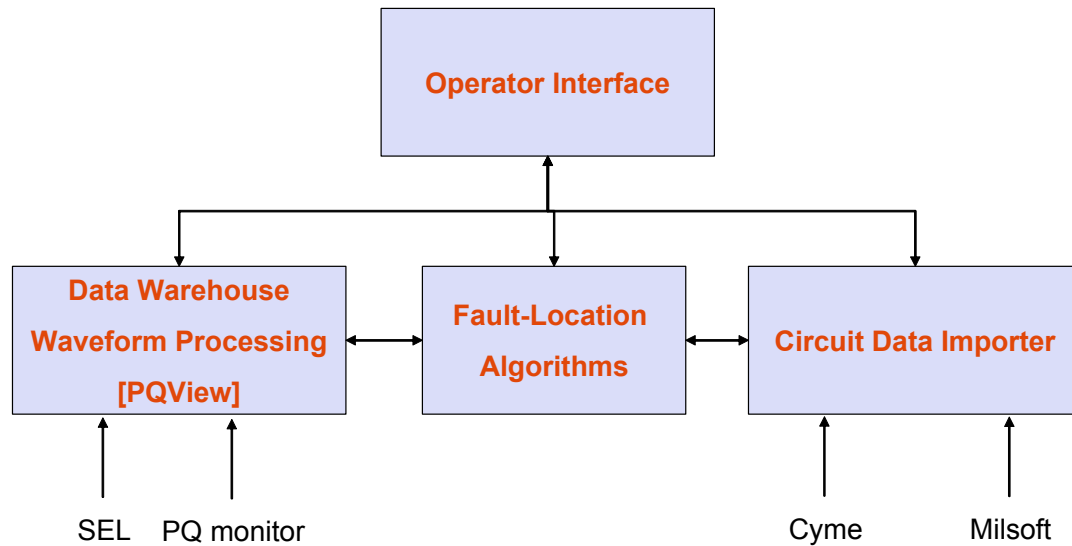
```
                    ┌─────────────────────┐
                    │  Operator Interface │
                    └─────────────────────┘

┌──────────────────┐   ┌──────────────┐   ┌─────────────────────┐
│ Data Warehouse   │   │Fault-Location│   │Circuit Data Importer│
│Waveform Processing│◄─►│  Algorithms  │◄─►│                     │
│    [PQView]      │   │              │   │                     │
└──────────────────┘   └──────────────┘   └─────────────────────┘

   SEL   PQ monitor                        Cyme      Milsoft
```

**Figure ES-5**
**Fault-Location System Components**

The highlights of these main components include:

- *Monitor Interfacing and Event Data Storage*—PQView will serve as the focal point for data storage and data collection. PQView can interface with many recording devices, including a large number of relays, power-quality recorders, and meters. PQView can now handle or will soon be able to handle a number of formats, including Comtrade, PQDIF, SEL formats, and a number of PQ recorders.

- *Interfacing with Circuit Models*—Utilities have circuit data in a variety of formats that would need to be accessed by a fault-location system. A number of distribution analysis programs are used widely, including those by Cyme, Milsoft, and Advantica. Database storage is the most common, and most of the database table structures are straightforward, so writing data-import or conversion routines should not be complicated for most distribution analysis programs.

- *Fault-Identification and Location Algorithm(s)*—A fault identification algorithm is needed to separate fault events and nonfault events recorded by the monitors. The main components of a fault-identification algorithm include: (1) determine if the event is actually a fault, (2) filter out and/or possibly classify voltage sags and inrush, (3) determine the phase or phases faulted, (4) locate the fault using the monitoring voltages and currents, and (5) provide a concise summary of fault parameters for the system operator. The fault-identification and location system will likely be implemented as a standalone library that interfaces with the PQView data warehousing application and the operator interface.

- *Operator Interface*—The operator interface is the focal point of the system. The interface should display recent fault events. As much as possible, the selection of fault events and location of faults should be automatic. For a fault location, the interface should display the fault and circuit graphically as well as provide pole numbers or manhole numbers or other physical location notation. If operators normally use some mapping software, one possibility is to forward fault-location information to the operator's normal mapping software for display and manipulation there. We envision that the operator interface will be a relatively simple web-based program. Ease of use and simplicity are important.

## Future Work

As part of the commercialization of the fault-location technology, work will proceed in 2007 with the following tasks:

*Prototypes*—The major effort for 2007 will include prototyping the modules in a fault-location system. We will finalize the best fault identification and location algorithms through more testing. Interfacing to PQView will allow us to directly interface with a large number of monitors. For the circuit data, we will test one or more converter services, depending on the direction of volunteer funders.

*Data collection*—While we already have a fantastic collection of data, we will follow up and try to fill some areas. We could use longer term data accumulated over several years at a small number of locations. This would let us test ways to "tune" fault locations to improve performance once we get a certain number of events, and it might tell us how many events are needed for "tuning." Data from multiple sources on a circuit is also something we are looking for; this will help us explore how to incorporate multiple data sources to improve fault locations. Lines with significant branching are where the most benefit could be gained from downline devices. We could also use more fault data from relays and more 34.5-kV fault data.

*Advanced algorithms*—Most of the algorithms tested to date have been relatively simple (except perhaps for the nonlinear arc model). We may try more advanced algorithms published in the literature if they seem to offer improvements.

# CONTENTS

# LIST OF FIGURES

# LIST OF TABLES

# *1*
# INTRODUCTION

## Project Overview

This is the first of a three-year set of projects with the ultimate goal of developing a commercial-grade fault-locating tool. The project plan is to proceed as follows:

- 2006 – Data collection, algorithm analysis, and implementation vision
- 2007 – Finalize algorithms, develop prototype version
- 2008 – Develop commercial-grade system

The three main components of this year's project are:

1. *Data Collection* – Collect data from sponsoring utilities including monitoring data, circuit impedances, circuit maps, and fault location data. Monitoring data will normally be from substation monitors: digital relays, power quality recorders, or other devices that record waveforms. Substation data is the most likely source of monitoring data for fault locating, but if utilities have data available from other sources, it will also be considered. Possibilities include data from down-line reclosers or from customer meters.

2. *Analyzing with Simple Algorithms* – Each fault will be located using the monitoring information. That will be compared with the known location provided by the utility. One or more simple fault-location algorithms will be used. By evaluating data from several utilities, several different monitoring data sources, several different types of feeders with different voltages and feeder layouts and load densities, sponsoring utilities will be able to optimize their approach to fault location. This project may answer several questions about the fault-locating algorithms.

3. *Identify Future Work and Implementation Vision* – Based on the reviews and analysis in 2006, future research needs will be identified. The 2006 work will identify how well the simplified algorithms work and needs for advanced algorithms. Of particular concern is how the results can be best implemented in solutions easily available to utilities. Particular needs include:

    - Interfacing with measurement data: Schweitzer relays and PQView databases are prime targets.

    - Interfacing with circuit models.

A main goal of the 2006 project is to find out what is feasible in a fault-location system and find out where to focus research efforts to develop more practical and more accurate location systems. We also want to verify approaches with field measurement data from monitoring whenever possible.

## Literature Overview on Distribution Fault Location

The literature review by Diaz and Lopez [5] provides a good overview of 89 papers and other citations. Most distribution fault-location approaches concentrate on impedance-based fault location techniques where fundamental-frequency parameters are used to estimate fault locations. Some commonly cited references on distribution circuits are by Girgis et al. [13], Schweitzer [32], and Santoso et al. [30]. Many of the impedance-based algorithms developed for distribution circuits are outgrowths of single-ended transmission-line location algorithms. Some commonly cited works include those by Takagi [39], Eriksson [10], and Sachdev [29].

Beyond impedance-based methods, other approaches have been suggested. Traveling-wave methods use timing difference between multiple monitors to arrive at a location estimate. That method is more applicable to transmission lines where lines are longer, and monitors may be available at two ends of a circuit. For distribution circuits, lines are too short to make this generally practical. It may be possible to use the transient component of waves oscillating on a distribution circuit to help estimate a fault location. Some references include Hizman et al. [16] and Xiangjun [40]. While some leads along these lines may prove fruitful, it appears unproven at this stage.

Another category of fault location algorithms is various learning systems. These can include expert systems, fuzzy logic, neural networks, and other trainable algorithms. These can be used in conjunction with other methods or as standalone algorithms. A key issue is getting a suitable training data set. Examples of learning systems include Jarventausta et al. [18] and Glinkowski et al. [14].

The IEEE has approved a guide on fault location, IEEE C37.114-2004 [17]. The guide covers impedance-based approaches to fault location as well as distribution location. The section on distribution has applicable information but is relatively weak on the overall approach to distribution fault location.

Most literature on fault location does not use field data. The most common approach is to develop, check, and analyze fault-locating algorithms with EMTP models (EMTP is used here as a generic name for electromagnetic transient programs, including ATP, DCG-EMTP, EMTP-RV, PSCAD, and others). The glaring limitation of this approach is that the EMTP models normally match the assumptions made when deriving the algorithm. Few researchers use actual measurement data from fault measurements. One of the main purposes of this project is to gather fault measurements to avoid that problem when analyzing and reviewing fault-locating algorithms.

## Progress Carolina's Experience With Fault Location

Progress Carolina has an advanced monitoring system that they use to locate faults. For further reference, see Lampley [21] and Peele [22, 23] plus some of the analysis done at NC State based on their data by Kim et al. [19] and Baran et al. [1]. Progress Carolina records steady-state trend data and fault events on all of their feeders using a remote-terminal unit (RTU) that can sample at 16 samples per cycle (see the block diagram of their arrangement in Figure 1-1). Their fault-location "system" started as a spreadsheet that assumed a constant conductor size for a given circuit. When the fault current and type of fault was entered, the spreadsheet would estimate a distance. Success with that led to development of several more automated systems to locate faults, including:

- *Fault Distance Tool*—This is a web tool available to all that provides distance to the fault assuming a constant wire size for each feeder.

- *Cyme software*—This provides several possible locations. They have found this to be the most accurate. It uses actual wire sizes from their GIS. This requires more manual processing.

- *OMS*—This interface provides locations to operators. It uses actual wire sizes from GIS, and the OMS is updated the most frequently to reflect the system connectivity in the field. It has the ability to locate automatically for feeder lockouts. Other outages must be initiated manually.
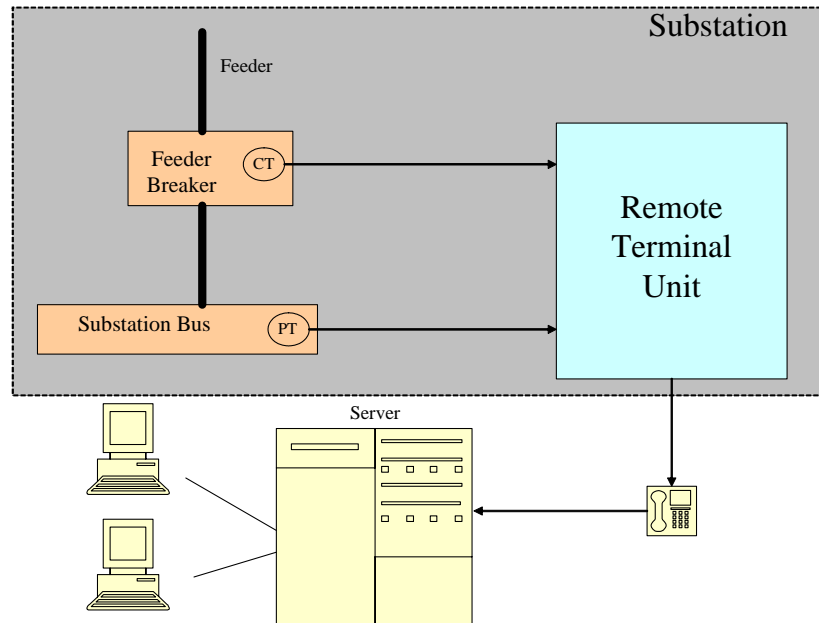


**Figure 1-1**
**Progress Energy's Carolina Monitoring Setup for Fault Location**

**Source**: Lampley, G. C., "Feeder Monitoring System Overview," internal Progress Energy Carolina presentation, 2006.

The web interface allows personnel to select the company region, substation, and circuit. From there, a list of fault events is given with the type of fault event and estimated distance. From there, the operator can go to a map view shown in Figure 1-4.
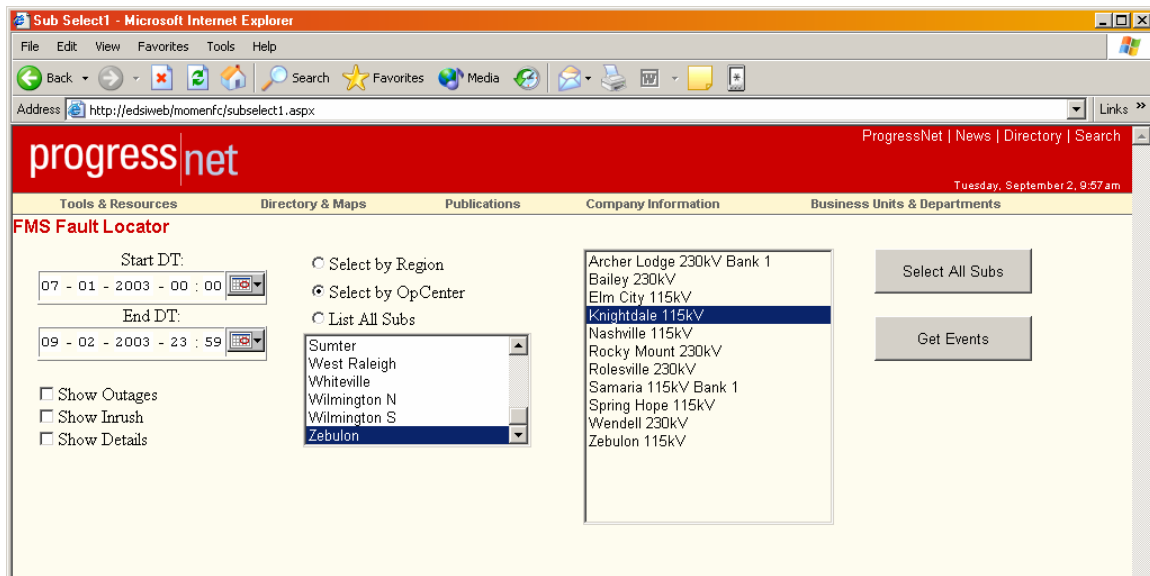
**Figure 1-2**
**Progress Energy's Fault Location Web Application: Location Drilldown**

**Source**: Lampley, G. C., "Feeder Monitoring System Overview," internal Progress Energy Carolina presentation, 2006.



**Figure 1-3**
**Progress Energy's Fault Location Web Application: Event List**

**Source**: Lampley, G. C., "Feeder Monitoring System Overview," internal Progress Energy Carolina presentation, 2006.
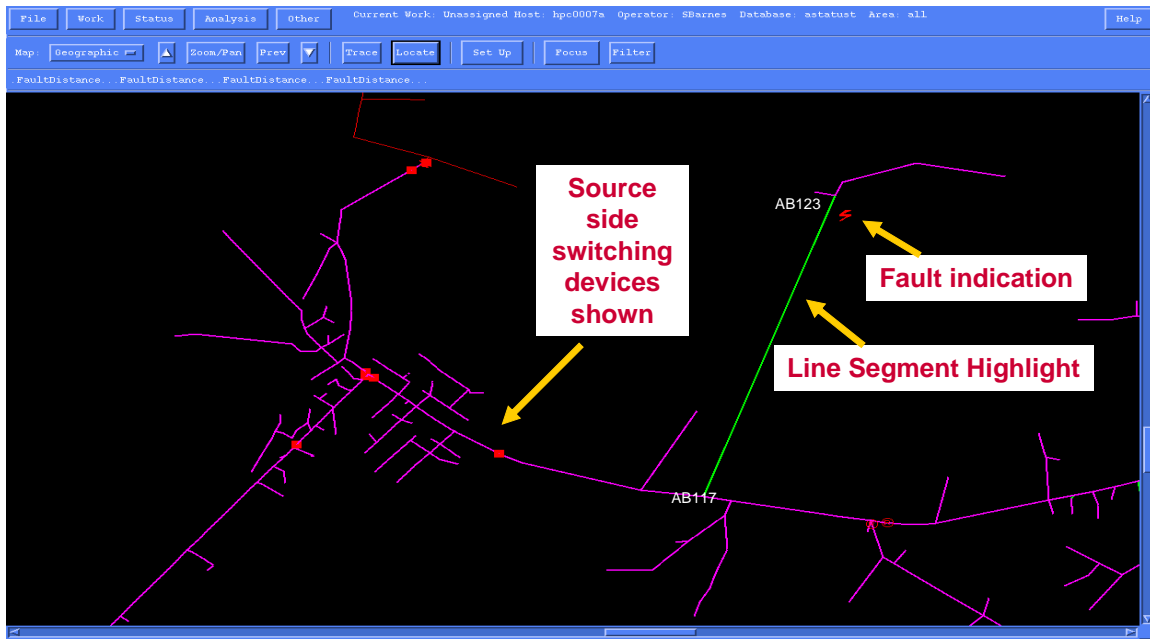
**Figure 1-4**
**Progress Energy's Fault Mapping System**

**Source**: Lampley, G. C., "Feeder Monitoring System Overview," internal Progress Energy Carolina presentation, 2006.

Progress Carolina uses the fault-current method of fault locating. They use the fault current from the measurement and use a fault-current profile from the given circuit to select possible fault locations. They assume a bolted fault (no fault resistance).

The results of their program have been very good:

- *Accuracy*—Lampley [21] reported that their locations were accurate to within 0.5 miles 75% of the time; and in most of the remaining cases, the fault was usually no more than one to two miles from the estimate.

- *Restoration improvement*—Progress Carolina as reduced their CAIDI (average restoration time) from about 80 minutes to 60 minutes since 1998 when they started using their system for fault location.

Progress Energy plans to implement a similar monitoring and fault-location system in their Progress Florida company. To do this, they plan to use digital relays with a data concentrator in the substation as shown in Figure 1-5.
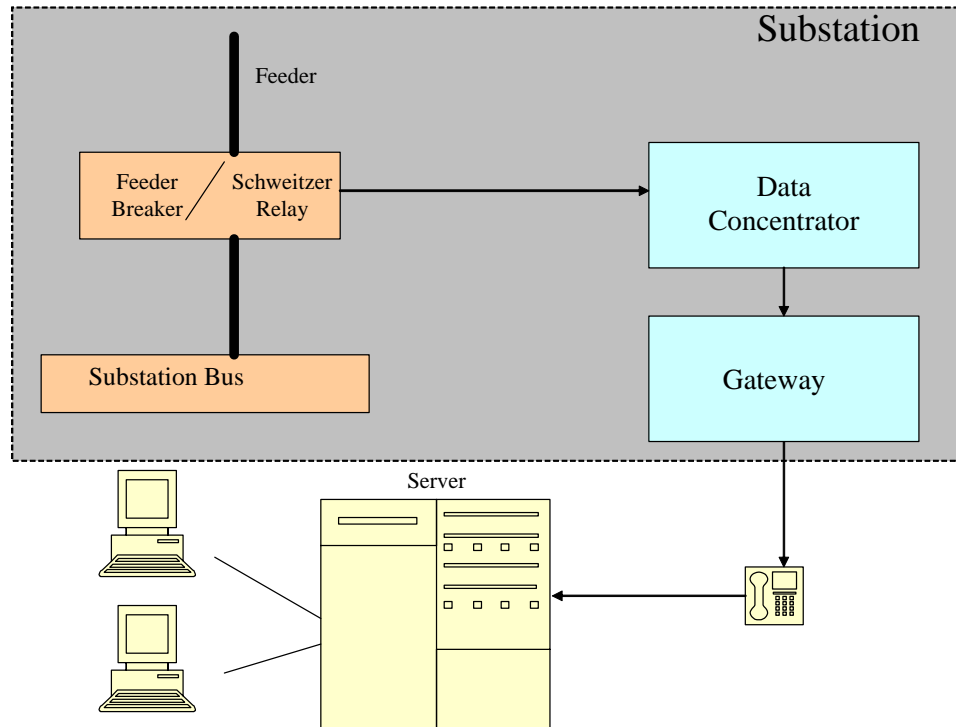
**Figure 1-5**
**Progress Energy's Planned Fault-Location System for their Florida Territory**

**Source**: Lampley, G. C., "Feeder Monitoring System Overview," internal Progress Energy Carolina presentation, 2006.

## Con Edison's Experience With Fault Location

Con Edison has recently implemented a fault location system in the New York City area with goals of reducing fault locating time and cost, directing crews more efficiently, and maintaining network reliability. For monitors, they use power quality monitors that are monitoring voltages and currents on a substation transformer. The monitors sample at 128 points per cycle. They use the reactance-to-the fault method of locating faults. They find the reactive part of the impedance to the fault and compare that with the reactance from the substation to the fault based on their circuit models. They use the residual current to pick out ground faults. This is particularly effective for them because their load is mainly secondary network load connected through line-to-ground transformers. Because the load is connected phase to phase, the ground current does not have load current mixed in. Their system models do not include zero-sequence impedances, so they use adjustment factors (k-factors) tuned for each site to adjust for the differences between the loop impedance to line-to-ground faults and the positive-sequence impedance. For further information on the implementation and performance of their system, see Stergio [36, 37].

They use PQView (http://www.pqview.com/) to download data from the recorders, act as a storage repository for the event data, and estimate the reactance to the fault for fault events. An operator interface is provided by an internal web application. Figure 1-6 shows the initial event and outage list from the interface. From there, the operator can open up a map-based visual locator shown in Figure 1-7.
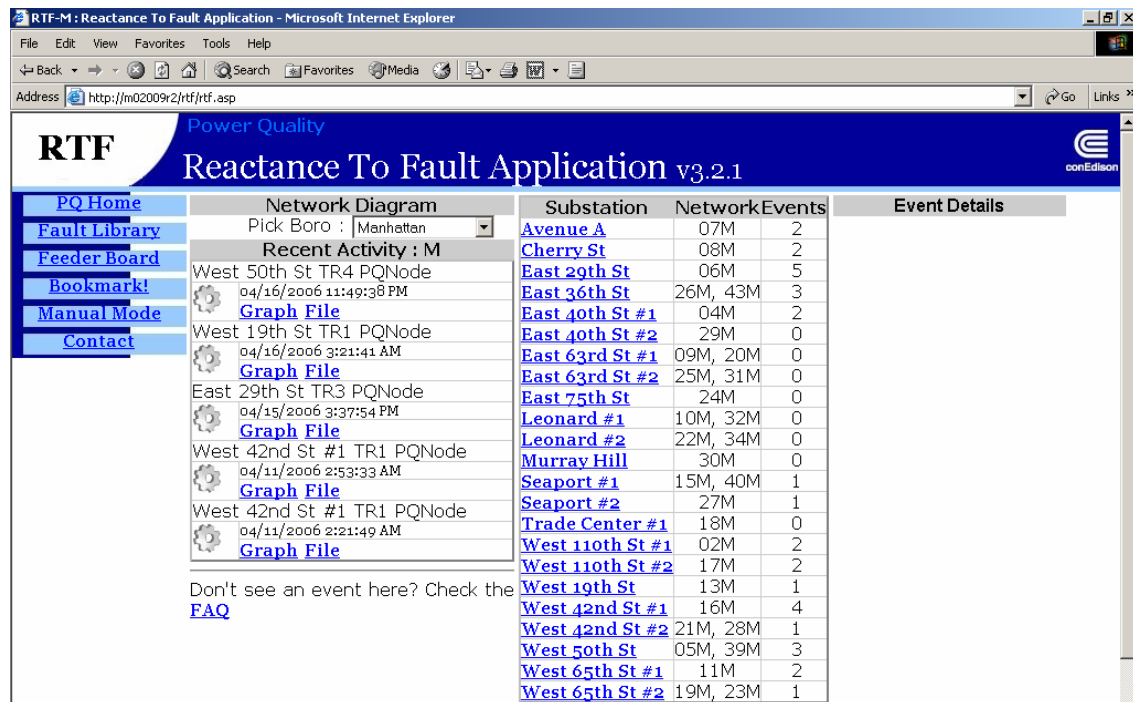
**Figure 1-6**
**Con Edison's Reactance-to-Fault Application**

**Source**: Stergiou, P. V., "Fault Location for Underground Systems," PQA, 2006.
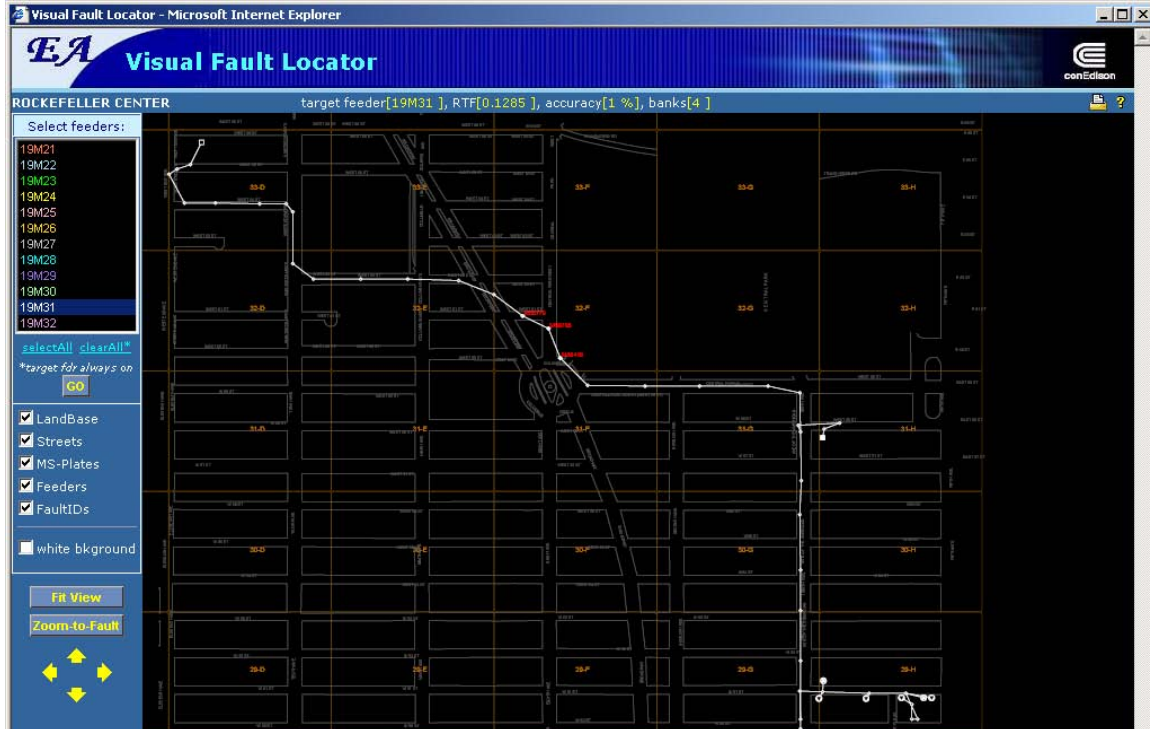


**Figure 1-7**
**Con Edison's Visual Fault Locator**

**Source**: Stergiou, P. V., "Fault Location for Underground Systems," PQA, 2006.

Con Edison has been happy with their performance to date. Stergio [37] reported that in an examination of 27 events at one location, the accuracy of the events was as follows:

- 10 (37%) were within 0 or 1 manholes (direct hits)
- 9 (33%) were within 1 – 3 manholes
- 4 (15%) were within 3 – 5 manholes
- 3 (11%) were within 5 – 10 manholes
- 1 (4%) was more than 10 manholes

70% were within three manholes.

# 2
# IMPEDANCE-BASED FAULT LOCATION

## Absolute Value of Impedance Method

If we know the voltages and currents during a fault, we can use these to estimate the distance to the fault. The equation is very simple, just Ohms Law (see Figure 2-1):

$$d = \frac{V}{I \cdot Z_l}$$

where,

$V$ = voltage during the fault, V

$I$ = current during the fault, A

$Z_l$ = line impedance, ohms per length unit

$d$ = distance to the fault, length unit such as miles

With complex values entered for the voltages and impedances and currents, the distance estimate should come out as a complex number. The real component should be a realistic estimate of the distance to the fault; the imaginary component should be close to zero. If not, then something is wrong.

A simplification of this approach is to use the reactance to the fault as:

$$d = \frac{\operatorname{Im}\left(\dfrac{V}{I}\right)}{\operatorname{Im}(Z_l)}$$

Using the reactance has the advantage of avoiding the arc impedance which is mainly resistive.



$$d = \frac{V}{I \cdot Z_l}$$
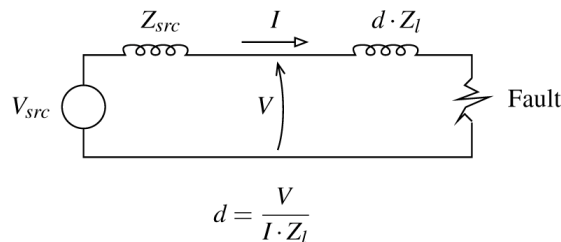
**Figure 2-1**
**Fault Location Calculations**

While the idea is simple, a useful implementation is more difficult. Different fault types are possible (phase-to-phase, phase-to-ground, etc.), and each type of fault sees a different impedance. Fault currents may have offsets. The fault may add impedance. There are uncertainties in the impedances, especially the ground return path. Conductor size changes also make location more difficult. With changing conductor sizes, we need to compare the estimated impedances with the impedances along various fault paths possible on the distribution circuit. For comparison, the absolute value, real part, or imaginary part may be used.

Many relays or power quality recorders or other instruments record fault waveforms. Some relays have fault-locating algorithms built in.

The Ohms Law equation is actually overdetermined—we have more information than we really need. The distance is a real quantity, but the voltages, currents, and impedances are complex, so the real part of the result is the distance, and the reactive part is zero. Most fault-locating algorithms use this extra information and allow the fault resistance to vary and find the distance that provides the optimal fit [13, 30]. The problem with that approach is that the fault resistance soaks up the error in other parts of the data—it does not necessarily mean a better distance estimation. Most fault arcs have a resistance that is very close to zero. In most cases, we're better off assuming zero fault resistance.

The most critical input to a fault impedance algorithm is the impedance data. Be sure to use the impedances and voltages and currents appropriate for the type of fault. For line-to-ground faults, use line-to-ground quantities; and for others, use phase-to-phase quantities:

Line-to-ground fault

$$V=V_a, \ I=I_a, \ Z=Z_S=(2Z_1+Z_0)/3$$

Line-to-line, line-to-line-to-ground, or three-phase faults

$$V=V_{ab}, \ I=I_a - I_b, \ Z=Z_1$$

Remember that these are all complex quantities. It helps to have software that automatically calculates vector quantities from a waveform. Several methods are available to calculate the rms values from a waveform; a Fourier transform is most common. Some currents have significant offset that can add error to the result. Try to find the magnitudes and angles after the offset has decayed (this is not possible on some faults cleared quickly by fuses).

Although the voltages and currents are complex, we can also estimate the distance just using the absolute values. Although we lose some information on how accurate our solution is because we lose the phase angle information, in many cases, it is as good as using the complex quantities. So, the simple fault location solution with absolute values is:

$$d = \frac{V}{I \cdot Z_1}$$

where,

$V$   =   absolute value of the rms voltage during the fault, V

$I$   =   absolute value of the rms current during the fault, A

$Z_l$   =   absolute value of the line impedance, ohms per length unit

$d$   =   distance to the fault, length unit such as miles

With this simple equation, we can estimate answers with voltage and current magnitudes. For a ground fault, $Z_l = Z_s$ is about one ohm per mile. If the line-to-ground voltage, $V$=5000 V, and the fault current, $I$=1500 A, the fault is at about 3.3 miles (5000/1500). Remember to use the phase-to-phase voltage and $|I_a - I_b|$ (and not $|I_a| - |I_b|$) for faults involving more than one phase.

## Current-Profile Location Method

We can calculate the distance to the fault using only the magnitude of the current (no phase angles needed and only prefault voltage needed) and the line and source impedances involved. If we know the absolute value of the fault current and the prefault voltage and the source impedance, the distance to the fault is a solution to the quadratic equation (Short [34]):

$$d = \frac{-b + \sqrt{b^2 - 4ac}}{2a}$$

where,

$$a = Z_l{}^2$$

$$b = 2R_l R_{src} + 2X_l X_{src}$$

$$c = Z_{src}{}^2 - \left(\frac{V_{prefault}}{I_{fault}}\right)^2$$

and,

$R_{src}$   =   source resistance, ohms

$X_{src}$   =   source reactance, ohms

$Z_{src}$   =   absolute value of the source impedance, ohms

$R_l$   =   line resistance, ohms per unit distance

$X_l$   =   line reactance, ohms per unit distance

$Z_l$   =   absolute value of the line impedance, ohms per unit distance

$I_{fault}$   =   absolute value of the rms current during the fault, amperes

$V_{prefault}$   =   absolute value of the rms voltage just prior to the fault, volts

In this case, we're doing the same thing as taking a fault current profile (such as Figure 2-2 and Figure 2-3) and interpolating the distance. In fact, it is often much easier to use a fault current profile developed from a computer output rather than this messy set of equations. If the prefault

voltage is missing, assume that it is equal to the nominal voltage. If we have the prefault voltage, divide the current by the per-unit prefault voltage before interpolating on the fault current profile. Using a fault current profile also allows changes in line impedances along the length of the line. Progress Carolina (formerly Carolina Power & Light) used this approach, and Lampley [21] reported that their locations were accurate to within 0.5 miles 75% of the time; and in most of the remaining cases, the fault was usually no more than one to two miles from the estimate.
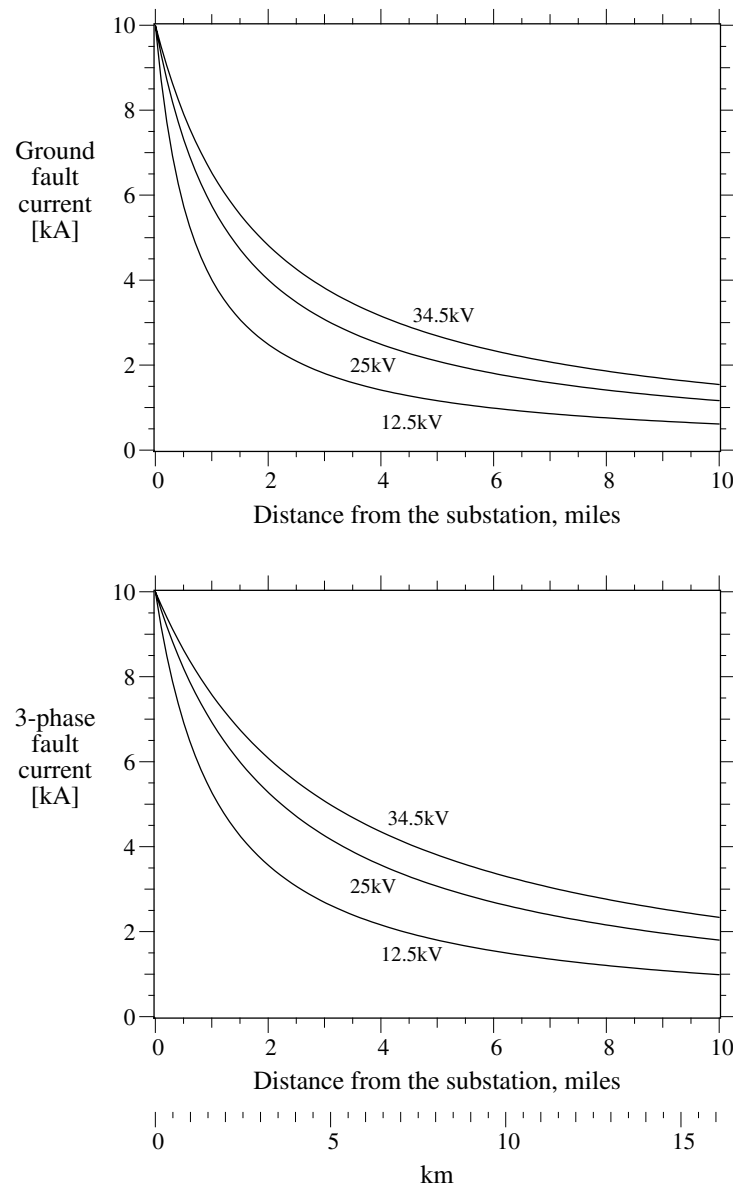


**Figure 2-2**
**Fault-Current Profiles for Line-to-Ground Faults and for Three-Phase Faults for an Overhead Circuit**

Phase characteristics: 500 kcmil, all-aluminum, GMD = 4.69 ft (1.43 m)
Neutral characteristics: 3/0 all-aluminum, 4-ft (1.22-m) line-neutral spacing
$Z_1$=0.207 + $j$0.628 Ω/mile (0.1286 + j0.3901 Ω/km)
$Z_0$=0.720 + $j$1.849 Ω/mile (0.4475 + j1.1489 Ω/km)
$Z_s$=0.378 + $j$1.035 Ω/mile (0.2350 + j0.6430 Ω/km)
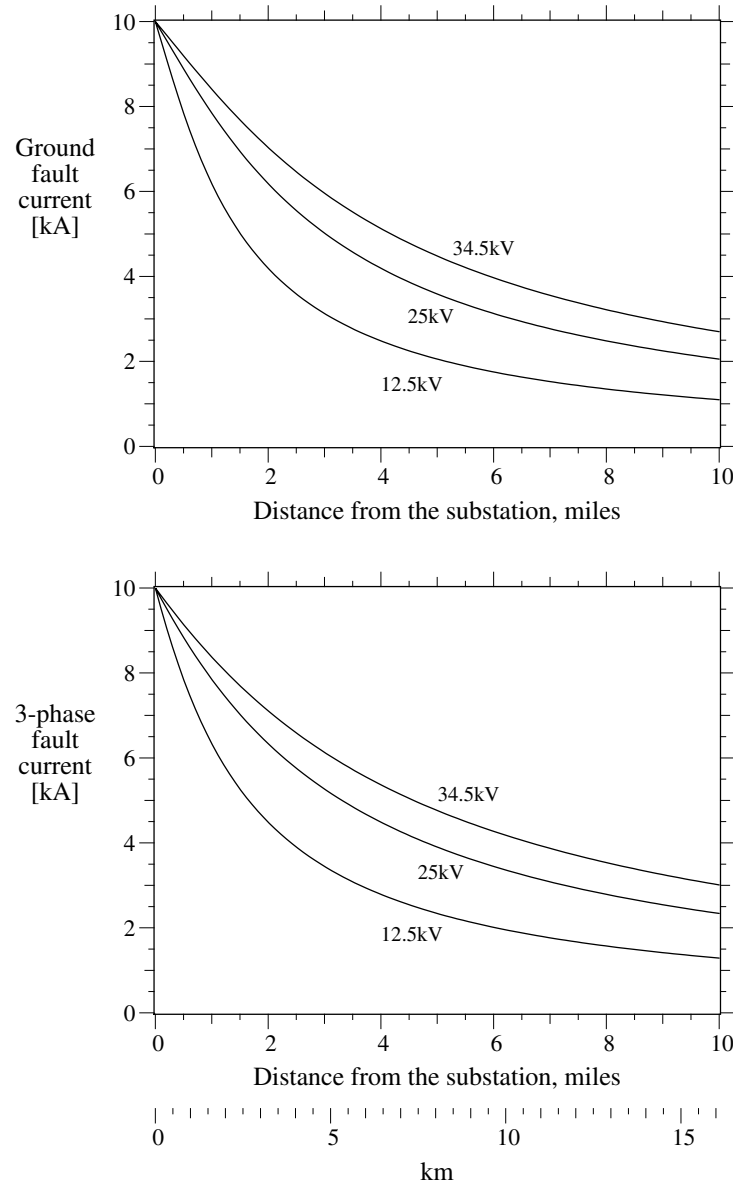
**Figure 2-3**
**Fault-Current Profiles for Line-to-Ground Faults and for Three-Phase Faults for an Underground Cable Circuit**

500-kcmil aluminum conductor, 220-mil XLPE insulation, 1/3 neutrals, flat spacing, 7.5 in between cables
$Z_1$=0.3543 + $j$0.3596 Ω/mile (0.2201 + j0.2234 Ω/km)
$Z_0$=0.8728 + $j$0.2344 Ω/mile (0.5423 + j0.1456 Ω/km)
$Z_s$=0.5271 + $j$0.3178 Ω/mile (0.3275 + j0.1975 Ω/km)

## Voltage-Profile Method

We can also just use voltages—if we know the source impedance, we do not need current. The circuit is a voltage divider as shown in Figure 2-4. The distance calculation is another quadratic formula solution, this time with (Short [34]):

$$d = \frac{-b - \sqrt{b^2 - 4ac}}{2a} \quad \text{(the negative root because } a \text{ is negative)}$$

where,

$$a = Z_l^{\;2} - Z_l^{\;2}\left(\frac{V_{prefault}}{V_{fault}}\right)^2$$

$$b = 2R_l R_{src} + 2X_l X_{src}$$

$$c = Z_{src}^{\;\;2}$$

and,

$V_{fault}$ = absolute value of the rms voltage during the fault, volts



$$V_{bus} = \frac{Z_f}{Z_f + Z_s}$$
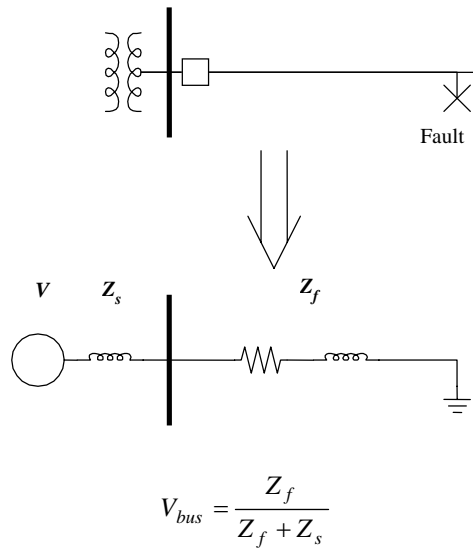
**Figure 2-4**
**Voltage Divider Equation Giving the Voltage at the Bus for a Fault Downstream**
**(This can be the Substation Bus or Another Location on the Power System)**

As with the fault current approach, rather than using this equation, we can interpolate a voltage profile graph to find the distance to the fault (such as those in Figure 2-5 or Figure 2-6). Again, we're assuming that the arc impedance is zero.
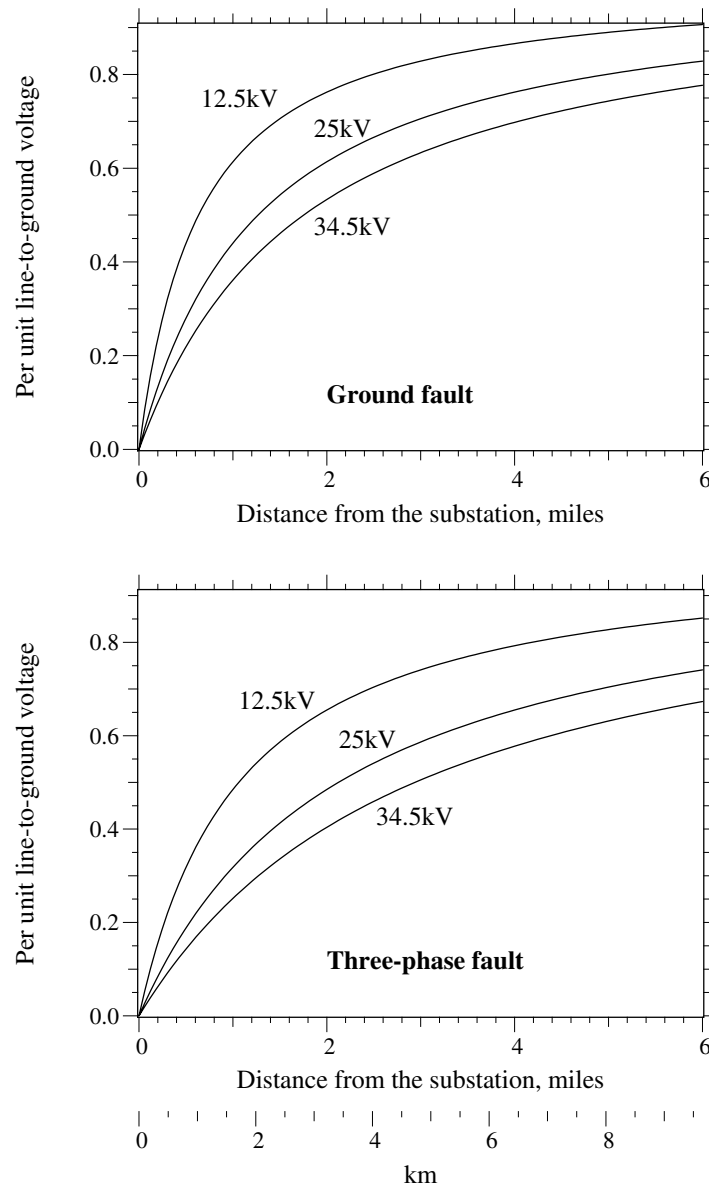
**Figure 2-5**
**Substation Voltage Profile for Faults at the Given Distance**

Single-phase and three-phase faults are shown for each voltage—the circuit parameters for the 500-kcmil circuit are the same as those in Figure 2-2.
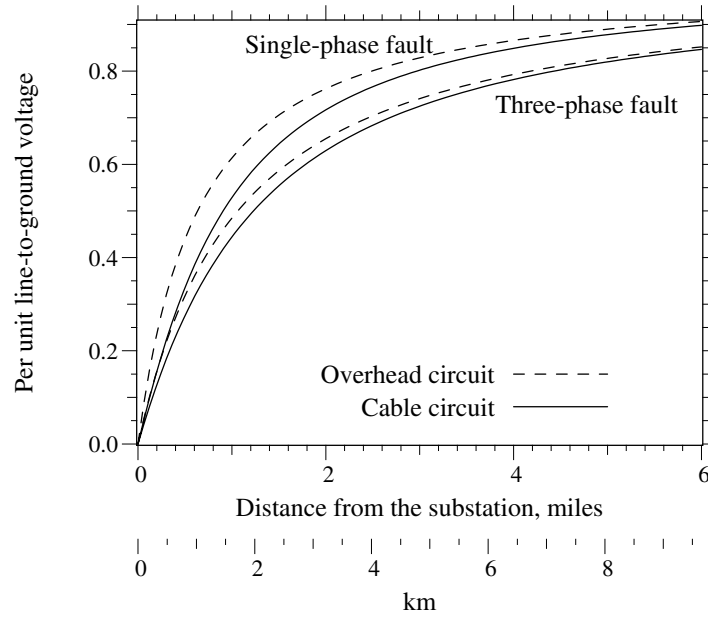
**Figure 2-6**
**Comparison of Substation Voltage for Faults on Overhead Circuits and Cable Circuits at the Given Distance**

Single-phase and three-phase faults are shown; the circuit parameters are the same as those in Figure 2-2 and Figure 2-3.

With source impedances, we can also recreate the line currents during a fault. Finding the current for line-to-ground faults is easiest as follows:

$$I_0 = -\frac{V_0}{Z_{0,src}}$$

where,

$I_0 = (I_A + I_B + I_C)/3 = $ zero sequence current

$V_0 = (V_A + V_B + V_C)/3 = $ zero sequence voltage

Therefore, the phase current is:

$$I_F = 3 \cdot I_0 = -\frac{3 \cdot V_0}{Z_{0,src}}$$

For multi-phase faults, it is more difficult to find the currents. You need to solve for $I_A$ - $I_B$ (or whichever two phases are faulted; for three-phase faults, it can be any two of the three currents). For this, start with the following:

$$I_1 = \frac{V_P - V_1}{Z_{1,src}}$$

$$I_2 = -\frac{V_2}{Z_{2,src}}$$

$$I_A - I_B = (a^2 - a)I_1 + (a - a^2)I_2$$

Where $V_1$ and $V_2$ are the sequence voltages (line-to-ground) during the fault, $V_P$ is the positive-sequence (line-to-ground) prefault voltage, and $Z_{1,src}$ and $Z_{2,src}$ are the positive and negative-sequence source impedances. The difficult parts when dealing with real waveforms are:

- $V_1$ and $V_2$ need to be calculated with the unfaulted phase as phase "A". That means if phase B is unfaulted, you need to calculate $V_1$ and $V_2$ as: $V_1 = (V_B + aV_C + a^2V_A)/3$ and $V_2 = (V_B + a^2V_C + aV_A)/3$.

- Since $V_P$ will be from the first cycle, and $V_1$ will be at some time during the fault, their phase angles will not align. You need to shift $V_P$ by a phase angle equal to the time difference between them.

For multiphase faults, there won't be an easy way to account for load current. It is partly accounted for by using the prefault voltage (since the voltage reflects the loading).

## Takagi Method

The Takagi method [39] is used in Schweitzer relays. It attempts to account for system load and for arc resistance. The distanced estimate is derived using:

$$d = \frac{\mathrm{Im}(V \cdot I_S^*)}{\mathrm{Im}(Z_t \cdot I \cdot I_S^*)}$$

Where,

$V$ = voltage during the fault, V

$I$ = current during the fault, A

$I_S^*$ = complex conjugate of $(I - I_L)$ where $I_L$ is the prefault load current, A

$Z_t$ = total line impedance, ohms

$d$ = distance to the fault, length unit such as miles

The main drawback of the Takagi method is that the linear arc resistance model for distribution faults is unrealistic. The constant-current load model may also not be accurate for distribution circuits. Another drawback to the Takagi method is that it uses the actual line current rather than the residual current $(I_A + I_B + I_C)$ for line-to-ground faults. The residual current allows for easier and more accurate load current reduction. Applying the Takagi method to a line with changing conductors is more difficult. To apply the Takagi method on lines with changing conductor sizes, the $Z_t$ needs to be calculated at each node, and the fault location is the point where the numerator and denominator of the equation above are equal.

## Accounting for System Load

To locate faults, the fault current must be separated from the load current to locate most accurately. During a fault, the voltage will sag. The response of the load current to the voltage sag can be used to "subtract out" the effect of the load. The standard models for load response are constant power, constant current, and constant impedance. Consider the constant-impedance model shown in Figure 2-7. With the constant-impedance load model, the impedance of the load is determined from the prefault voltage and prefault current:

$$Z_{load} = V_{prefault}/I_{prefault}$$

The total impedance ($Z_{total}$) is determined from the voltage and current during the fault:

$$Z_{total} = V_{fault}/I_{fault}$$

With these two parameters, the impedance to the fault can be found using a current divider equation.
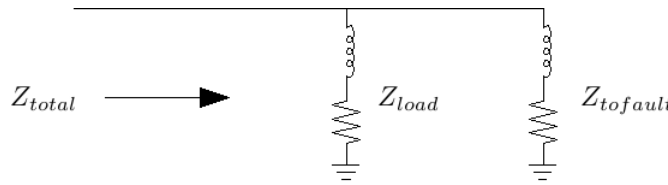


$$Z_{tofault} = \cfrac{1}{\cfrac{1}{Z_{total}} - \cfrac{1}{Z_{load}}}$$

**Figure 2-7**
**Constant-Impedance Load Model**

The constant-current model is also commonly assumed. For example, the Takagi fault-location model uses this to subtract out the load current (see the previous section).

Reineri and Alvarez [27] did several tests on various end-use equipment to better determine load models for use in fault-locating algorithms. They found that on devices with motors, current can increase during a voltage sag. On devices with dc power supplies like computers, the current can drop significantly during a deep sag. Figure 2-8 shows some of their results with two different load mixes evaluated. The graphs show what happens to the resistive portion (B) and reactive portion (G) of the load admittance Y. The admittance Y is the inverse of the load impedance Z. For moderate sags to about 60%, a constant impedance model is relatively accurate for the third and fifth cycle. For sags below that, it varies more depending on load mix. With high air-conditioner load, air conditioners can stall and pull in more current. Without high air-conditioning load, the load current can decrease significantly. For deep voltage sags, the fault current is normally going to be high enough to swamp out the load current anyway, so this reduces the uncertainty in this range.

Load mix 1: summer night

Load mix 2: winter night
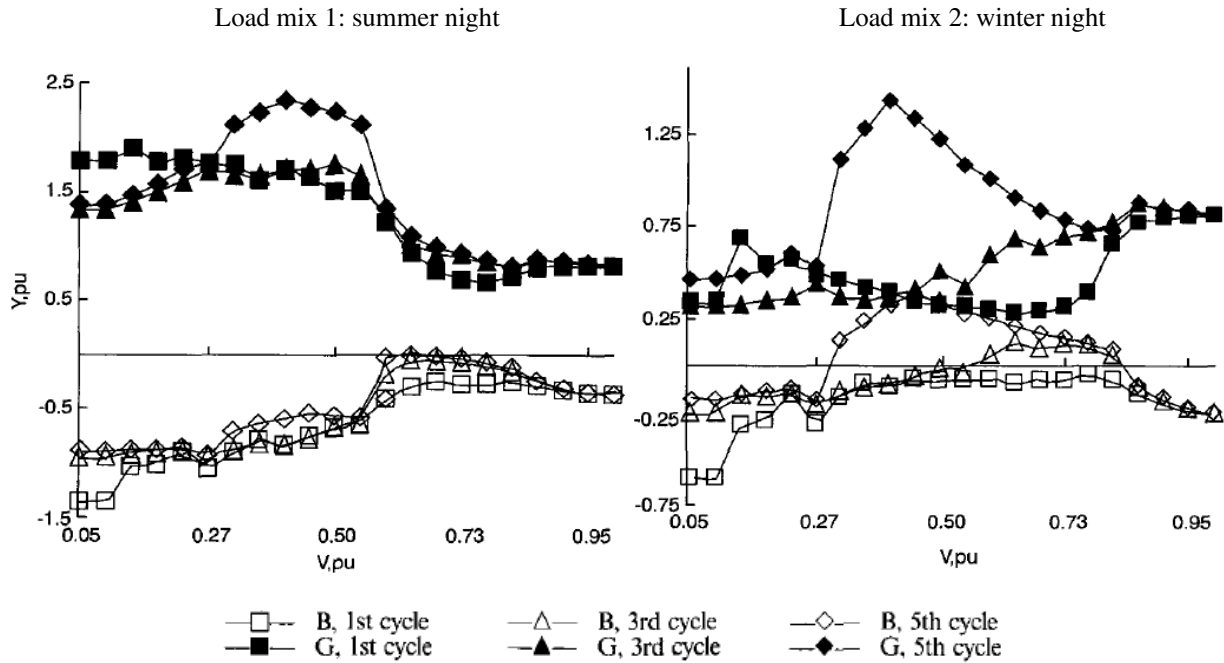


*Load mix 1*: summer night: 35% air conditioner; 15% refrigerators; 25% lighting (10% hp Na, 10% Hg, 5% fluorescent); 20% electronic load (15% TV, 5% PC); 5% microwave oven.

*Load mix 2*: winter night: 15% refrigerator; 45% lighting (20% hp Na, 20% Hg, 5% fluorescent); 35% electronic load (25% TV, 10% PC); 5% microwave oven.

**Figure 2-8**
**Response of Load to Voltage Sags of the Given Magnitude**

Source: Reineri, C. A. and Alvarez, C., "Load research for fault location in distribution feeders," *Generation, Transmission and Distribution, IEE Proceedings*-, vol. 146, pp. 115-20, 1999.

Figure 2-9 compares the distribution of the ratio of residual currents ($I_R = I_A + I_B + I_C$) measured at the substation bus with residuals measured at the feeder level for the same event. This data is from Utility F, which has monitors at the feeder level and bus level. The ratio of bus-level to feeder-level residual currents is quite consistent. About 70% of events fall within a ratio of 0.89 and 0.93. This means that using bus-level currents will only add a small percent error for 70% of faults. The 0.9 ratio also matches the fault location results at some of utilities with bus level monitors. See especially the results for Utility A in Chapter 4—the results tended to overestimate the impedance to faults by a factor of $1/0.9 \approx 1.1$. This is expected if the bus currents are 90% of the feeder currents.

The residual current worked out best for comparing bus-level currents to feeder-level currents. Compare the residual-current comparison in Figure 2-9 to the phase-current comparison in Figure 2-10. The phase currents had a much wider range of ratios between the bus-level measurements and the feeder-level measurements.
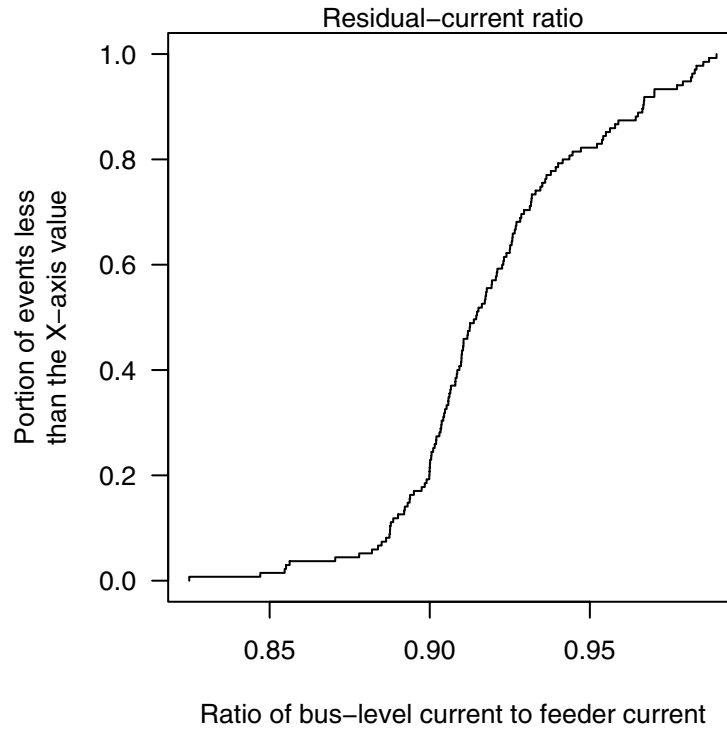
**Figure 2-9**
**Ratio of the Current Measured at the Substation Bus to the Current Measured at the Feeder for Line-to-Ground Faults (Using Residual Currents)**
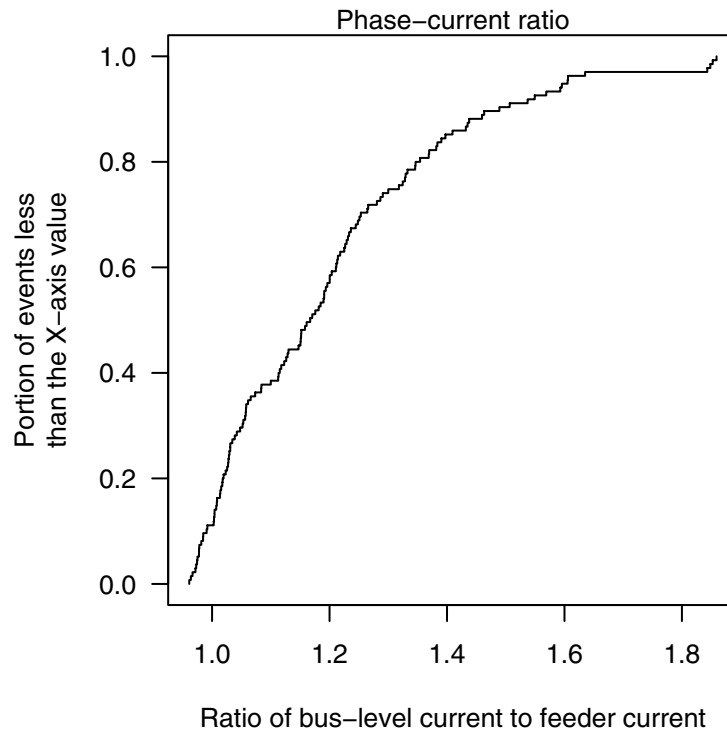


**Figure 2-10**
**Ratio of the Current Measured at the Substation Bus to the Current Measured at the Feeder for Line-to-Ground Faults (Using Phase Currents)**

For the analysis in this report, we accounted for load currents in the following two ways:

- *Line-to-ground faults*—Use the residual current instead of the phase current.

- *Multi-phase faults*—Use a constant-impedance model to factor out the load impedance using the prefault voltage and current.

## Line-to-Line Voltages

If potential transformers are connected phase to phase, we can still estimate locations for ground faults if we know the zero-sequence source impedance. Schweitzer [32] shows that the phase-to-ground voltage is:

$$V_a = 1/3(V_{ab} - V_{ca}) - Z_{0,src}I_0$$

where,

$Z_{0,src}$ = zero-sequence impedance of the source, ohms

$I_0$ = zero-sequence current measured during the fault = $I_a/3$ for a single line-to-ground fault on phase A

## Using the Fault-Location Built into Relays

Digital relays have long had built-in fault location capability. Most algorithms are impedance-based methods. See Schweitzer [32] and Zimmerman and Costello [41] for more background on the use of relays for fault location. Relays typically sample at 16 or 32 points per cycle. This is sufficient for good fault location accuracy.

The advantages of using the fault-location ability in a relay are:

- *Simpler data transmission*—The relay does the calculations and boils down the results into one estimate of the distance. This result can be tied into SCADA for direct transmission to system operators.

- *No need for a system model*—The relay does not use a system model, so there is no need to interface a Cyme or other system model with the fault location setup.

The disadvantages of using the fault-location ability in a relay are:

- *Constant wire size*—The relay does not have a system model. It assumes one constant wire size. This can make the location inaccurate for systems with changing wire size.

- *Limited algorithm*—The location algorithm in a typical relay does not handle the impacts of arc voltage, pre-fault load, infeeds, and some other issues that may require more sophisticated processing.

- *No pole or manhole location number*—The output is a distance. Further interfacing is necessary to translate this distance into a pole or manhole location or physical map location for better use by operators and field crews.

- *Voltage inputs needed*—The relay needs voltage inputs as well as current inputs to estimate a distance to the fault.

Overall, if a utility's circuits are well represented by a constant wire size, then using the built-in fault location capability can give reasonable results.

For the common Schweitzer distribution relays, setting up a relay to do fault location requires input variables set to enable fault location, parameters for the line impedances, possibly source impedances, and the length of the line. For the SEL-251, the parameters are:

**R1, X1, R0, X0** – Positive- and zero-sequence total line resistances and reactances in ohms (not ohms per some length) on the primary.

**RS, XS** – Zero-sequence source resistance and reactance in ohms. This is only needed if the measured voltages are line-to-line instead of line-to-neutral.

**LL** – Line length. This can be in any units, including miles, km, or 100 for 100% of the line length.

The relay inputs for the SEL-351 or SEL-651 series are somewhat different:

**EFLOC** – Set to "Y" to enable fault location.

**Z1MAG, Z1ANG, Z0MAG, and Z0ANG** – Positive- and zero-sequence total line impedance magnitudes (in ohms) and phase angles (in degrees) *on the secondary*.

**Z0SMAG and Z0SANG** – Zero-sequence source impedance magnitude (in ohms) and phase angle (in degrees). This is only needed if the measured voltages are line-to-line instead of line-to-neutral.

**PTR and CTR** – The PT and CT ratios—these are needed because the line impedance parameters are specified on the secondary of the PT and CT.

**LL** – Line length. This can be in any units, including miles, km, or 100 for 100% of the line length.

An important difference between the 251 and 351 is that the 351 and 651 impedance parameters are represented on the secondary side of the CT's and PT's, so this conversion factor needs to be accounted for:

$$Z_{secondary} = \frac{CTR}{PTR} Z_{primary}$$

To convert from resistance and reactance to magnitude and angle (resistances and reactances are normally more readily available for distribution lines), use:

$$Z1MAG = \sqrt{R1^2 + X1^2}\;\frac{CTR}{PTR}$$

$$Z1ANG = \tan^{-1}\!\left(\frac{X1}{R1}\right)$$

The SEL relays are set up to use the total length of a line. This may be fine for subtransmission or transmission lines, but is difficult for distribution lines. The line length may change as the circuit grows or is reconfigured. It also may have taps and have multiple "ends." Therefore, to make setting relays easier, consider the following approach:

- Enter a length of 100 miles for the line length.

- For the distribution line impedance parameters (R1, X1, R0, X0 or Z1MAG, Z1ANG, Z0MAG, and Z0ANG), enter impedance values for the mainline configuration in ohms per 100 miles. On the 351 and 651 relays, multiply the Z1MAG and Z0MAG magnitudes by the CTR/PTR ratio.

- For the line parameters, use the line-configuration impedance of the mainline wire size most commonly used on the line. If wire size decreases with distance from the substation, use the largest wire size unless a smaller size has significantly more mainline coverage. By using the largest wire size, the location estimate will tend to err on the source side: crews should generally start near the estimated location and look outward.

With this approach, results on the relay reports will be given in miles from the substation. To have location results reported in other units (kfeet or km), specify the impedances in ohms per 100 kfeet or ohms per 100 km.

Because impedances are given in ohms per unit length (in this case 100 miles), the relay settings are the same for feeders with the same mainline conductor. This eases entry of relay parameters because many can be standardized.

Consider the case of a 12.5-kV circuit as follows:

First 5 miles: 350-kcmil AAC overhead construction with 4/0 neutral[3]

$R_1 = 0.294$ ohms/mile    $X_1 = 0.656$ ohms/mile

$R_0 = 0.714$ ohms/mile    $X_0 = 1.898$ ohms/mile

Last 3 miles: 4/0 AAC overhead construction with 2/0 neutral

---

[3] Values found using the online line-impedance calculator at http://www.rpad.org/Rpad/Impedances.Rpad

Ignore the impedances of the last three miles. Just consider the 336.4-kcmil mainline at the start of the circuit. Multiply the impedance values above by 100 to get the relay inputs. For a SEL-251, the values are:

R1 = 29.4    X1 = 65.6    R0 = 71.4    X0 = 189.8    LL = 100

For the SEL-351 with a PT ratio of 120 and a CT ratio of 240, the values are:

Z1MAG = 144    Z1ANG = 65.9    Z0MAG = 406    Z0ANG = 69.4
EFLOC = Y    LL = 100

For the zero-sequence line parameters, note that the neutral conductor size and placement impacts the parameters. Use tables of impedances or a line-impedance solver (available in most distribution modeling packages) to find the impedances per unit length.

Because line wire sizes often change on a distribution circuit, the built-in relay algorithm will have errors for faults farther out on the smaller wire size. One way to account for this is to develop a *nomograph*, a translation graph that maps the estimate from the relay to a more realistic estimate using the circuit characteristics [31]. Consider the translation graph in Figure 2-11 for the circuit with a tap and a conductor size reduction. Such a translation could be a graph as shown, developed for each circuit, or the same translation could be done by computer and displayed for operators.
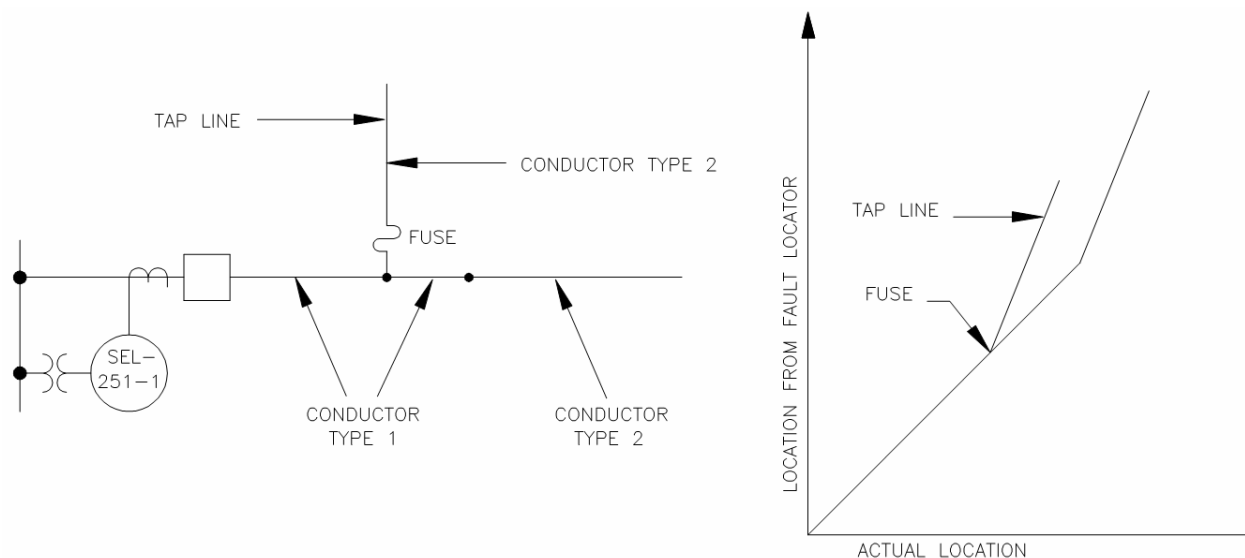


**Figure 2-11**
**Example Translation Graph for a Circuit With Multiple Conductor Sizes**

Schweitzer Engineering Laboratories, "SEL-251-1 Instruction Manual," 2002.

The Schweitzer relays use the Takagi algorithm for fault location [31, 41]. This uses the prefault current to attempt to account for load and fault resistance. If prefault current is unavailable, the relay uses a straight reactance-to-the-fault algorithm. General Electric relays use a similar looking phasor-based impedance estimation method [12].

The default SEL command to download waveshape data (the EVE command) defaults to downloading four samples per cycle in a filtered format. The relay stores 16 samples per cycle (or 32 in case of the 651) but only 4 samples per cycle are downloaded. Whether for fault locating or for identifying coordination issues or for other uses, it is better to download 16 samples per cycle. Four samples per cycle can give useable fault locations, but 16 samples per cycle is better. Figure 2-12 compares 4 samples per cycle to 16 samples per cycle.
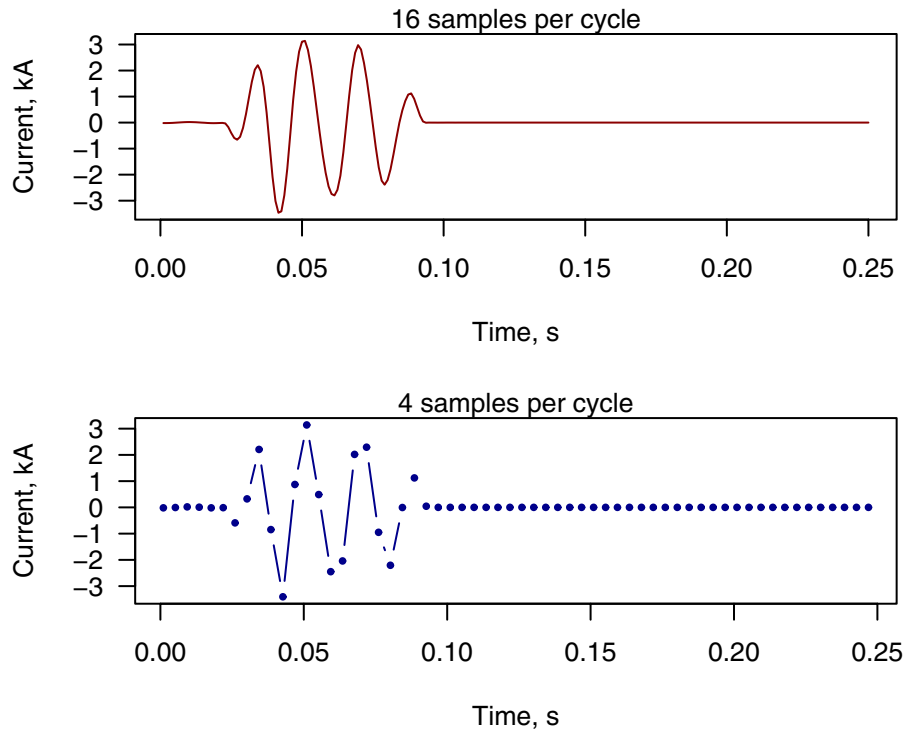


**Figure 2-12**
**Comparison of 4 and 16 Samples Per Cycle**

The default SEL download is also filtered with a cosine filter. This will be analyzed in more detail in the next chapter. Figure 2-13 compares a raw signal with the filtered version of that signal. Filtering can disrupt fault location, especially for short-duration events where the edge effects on the front end and tail end of the filter disrupt the waveform.
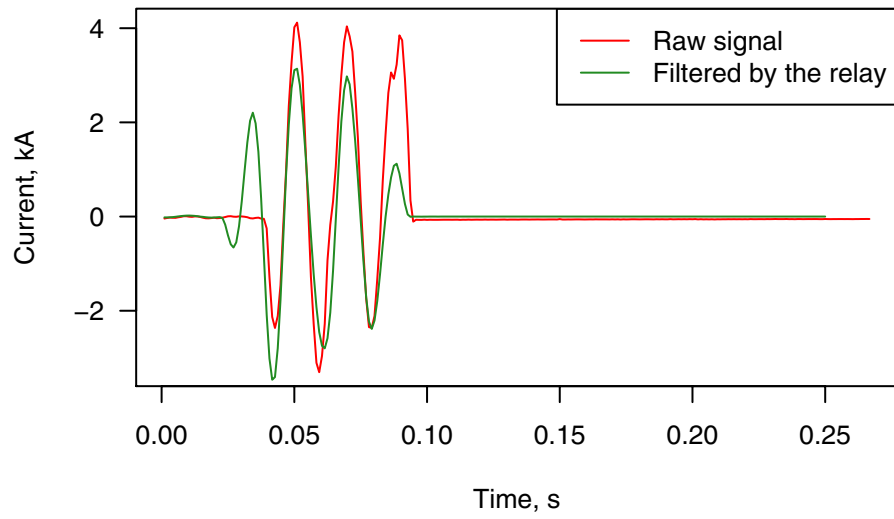
**Figure 2-13**
**A "Raw" Signal Compared to a "Filtered" Signal from an SEL-351S Relay**

# 3
# WAVEFORM ANALYSIS

## Introduction

In this chapter, we evaluate some waveform processing and manipulation that can be done to help avoid problems from waveform abnormalities that may cause problems with fault locating. Some problem areas evaluated include:

- Clipping

- Inrush

- Transients

- DC decay

- Evolving faults

- Intermittent faults

## Filtering

The most common way to identify the magnitude and phase angle from a waveshape is to perform an FFT (Fast-Fourier Transform) on a portion of the signal. Normally, one fundamental-frequency cycle is used for the FFT. Figure 3-1 shows an example of a current wave processed by a rolling FFT. In a rolling FFT, the FFT for one cycle is done repeatedly for a one-cycle-long window sweeping across the entire waveshape. Only the fundamental-frequency result (magnitude and phase angle) from the FFT is kept; the harmonics are discarded.

Figure 3-1 has a relatively large decaying dc offset. The FFT operation filters most of the offset out but not all of it.

Several other ways of filtering waves to synthesize a waveshape into a magnitude and phase angle are possible. Schweitzer and Hou [33] provides an analysis of a number of filtering approaches, including IIR, FIR, FFT, correlation filters, cosine filtering, and Kalman filters.

One effective way to eliminate all but the fundamental frequency is to apply a cosine filter. A one-cycle cosine filter is an FIR filter where the coefficients of the filter are a one-cycle cosine wave. The cosine filter passes the fundamental frequency component but filters out all integer harmonics (see Figure 3-2).
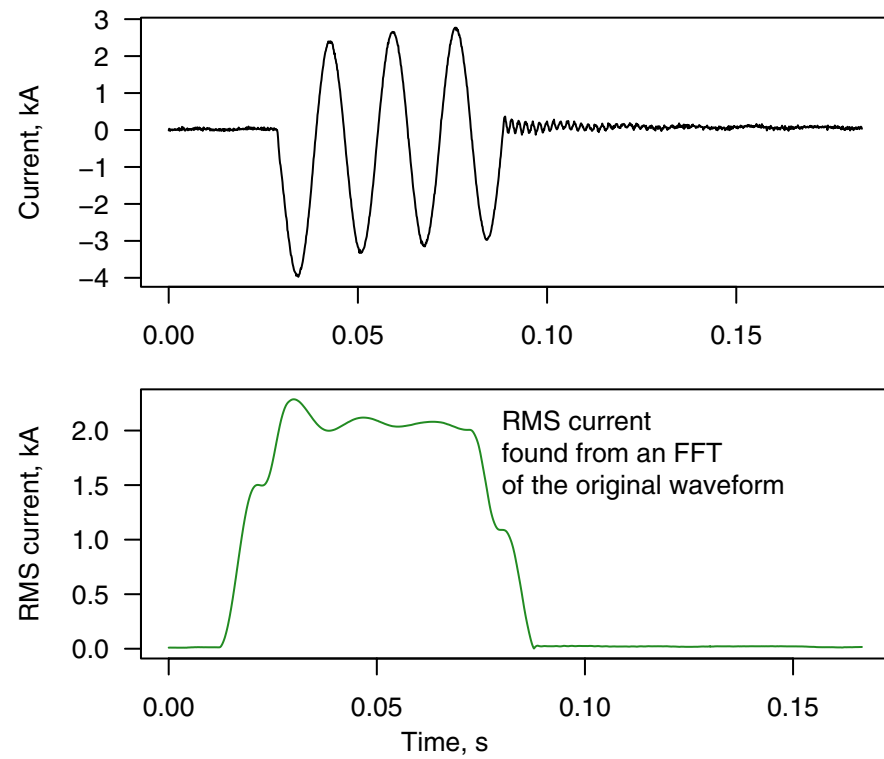
**Figure 3-1**
**A Fault Waveform and the RMS Derived from it Using an FFT**
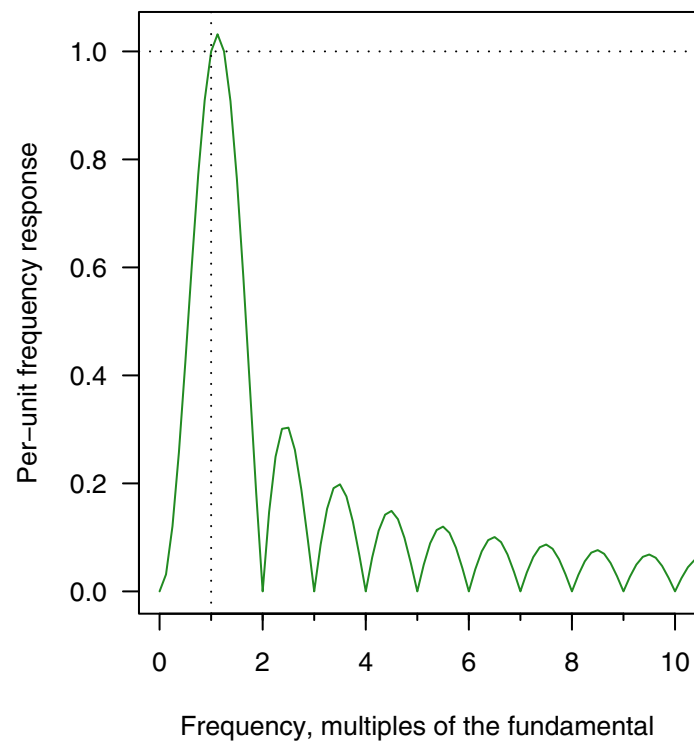


**Figure 3-2**
**Frequency Response of a One-Cycle Cosine Filter**

Figure 3-3 shows an example of a signal filtered by a cosine filter. Note that the cosine filter does a better job of eliminating the dc offset than does the unfiltered signal passed to an FFT. The downside of cosine filtering is that edge effects distort the filter on the front and tail of the signal, a problem for short-duration events or those with abrupt changes.

With a cosine filter, it is also possible to obtain the phase angle by taking the magnitude of the filtered wave at one point on the cycle relative to the magnitude a quarter cycle earlier as:

$$\text{Phase angle} = \tan^{-1} \frac{V_t}{V_{t-1/4 \text{ cycle}}}$$

Schweitzer relays use cosine filtering to derive magnitudes and for use in fault locating algorithms.
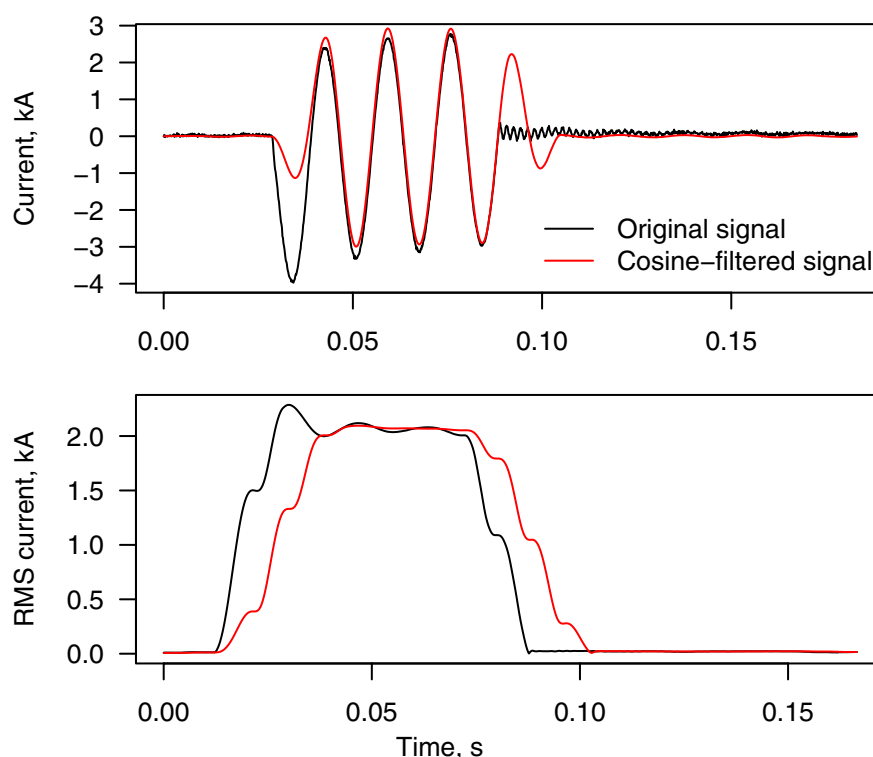


**Figure 3-3**
**A Waveform With DC-Offset Filtered by a Cosine Filter**

Mimic filtering is another type of filter that has been used for relay signals. Benmouyal [2] found that the mimic filter compared well with cosine filters, FFT filtering, and Kalman filters. A mimic filter is a high-pass filter tuned to pass one per unit for the fundamental frequency. Because it is a high-pass filter, it lets through a lot of noise that must be filtered by another filter. Figure 3-4 shows an example of a mimic filter applied to a signal. The mimic filter also does a very good job of removing the dc offset. The disadvantages of the mimic filter are the noise introduced and the phase shift added.

In this report, all of the analysis was done using the classical FFT approach to finding magnitudes and phase angles. For most events there was not any need for better filtering.
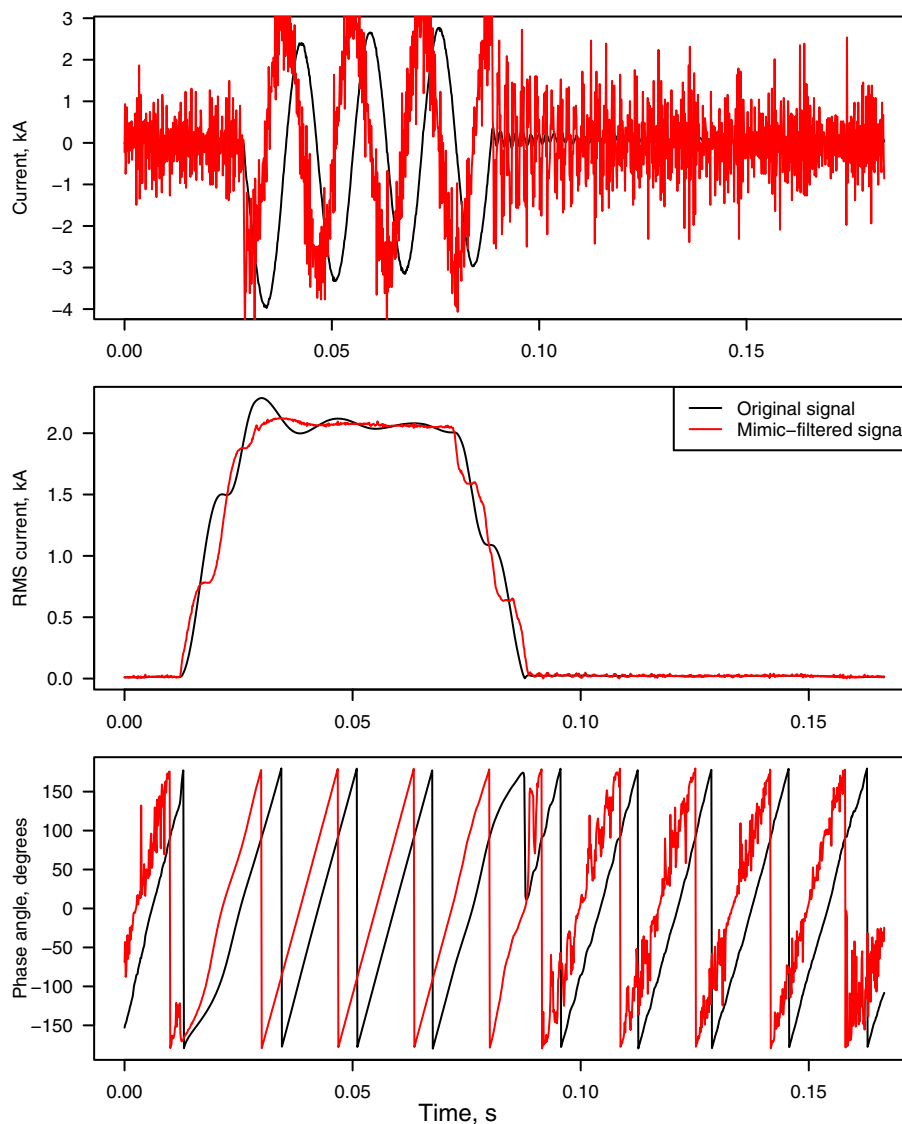


**Figure 3-4**
**A Waveform With DC-Offset Filtered by a Mimic Filter**

## Waveform Clipping and CT Saturation

Especially for high-current faults, current waveforms clipped by monitors and CT's saturated by high currents and/or dc offsets are a concern. Both of these will add error to fault locations. Of course, both are best accounted for by specifying CT's and setting recorder thresholds appropriately to avoid clipping and saturation over the range of fault currents expected. That cannot always be done, especially when adding monitoring to locations with equipment already in place. This section explores ways to recover information when clipping or saturation are present.

## *Declipping*

One way to handle clipping is to identify the clipped portion and replace the clipped part with a spline fit. This can provide good "declipping" in many cases as shown by Figure 3-5.
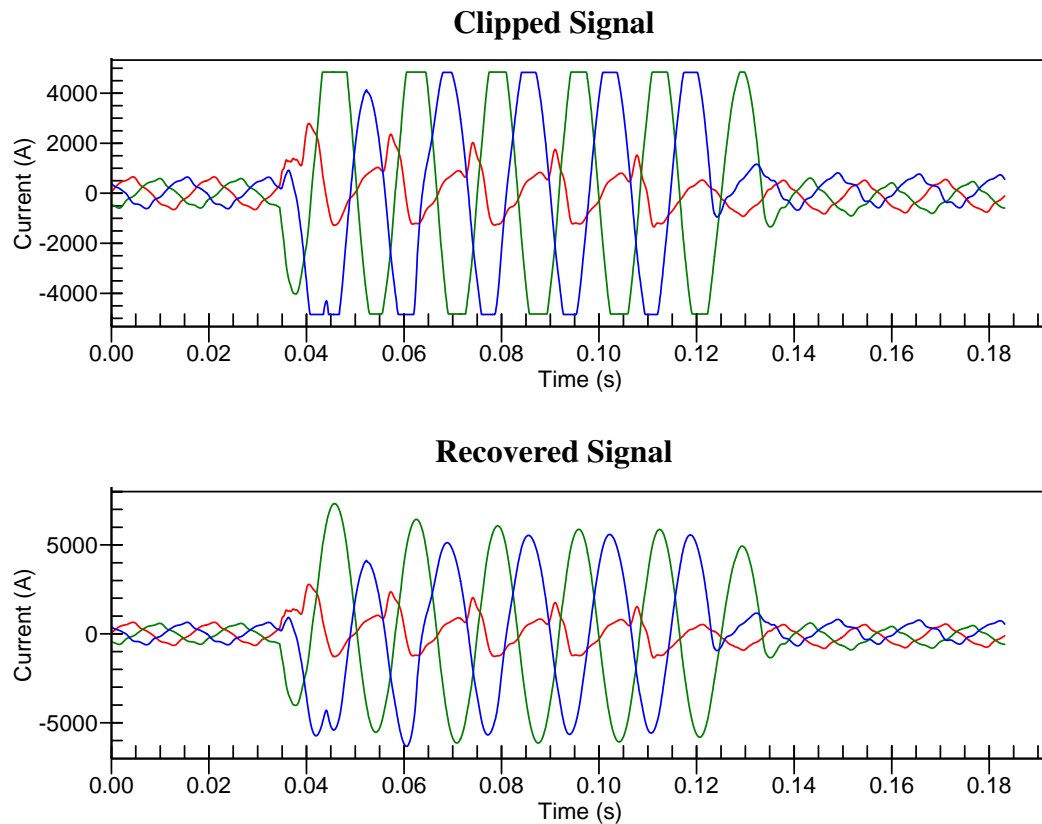


**Figure 3-5**
**Example of a Clipped Waveform and Recovery With Spline Fitting**

Declipping with spline fits falls apart when waves are clipped below about 40%, depending on how noisy the signal is. The example below shows a severely clipped wave fitted with splines. The noise in the waveshape makes the spline fits go crazy.
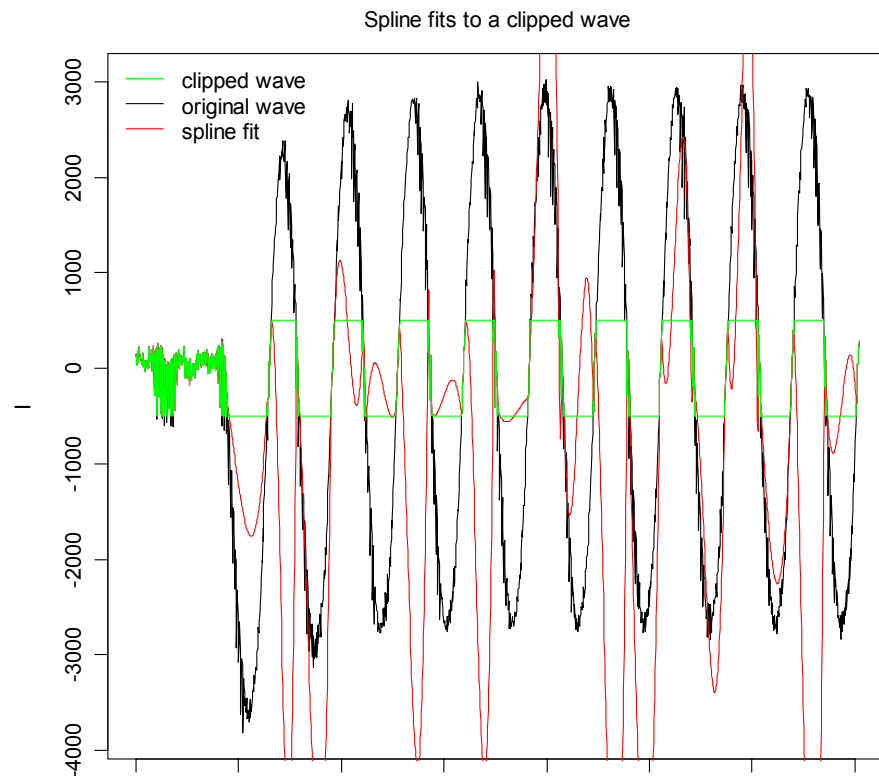
**Figure 3-6**
**Example of a Severely Clipped Waveform and Spline Fitting**

Using sinusoidal fits allows reasonable reconstruction of severely clipped waves. The figure below shows the same severely clipped wave reconstructed with sine wave fits over the first few cycles. The sine-wave fits are redone every cycle. Unlike spline fits, the original data is not reconstructed exactly, but the optimization forces the known points to overlap very closely. The optimization is done by minimizing an objective function, in this case, $x = A \cdot \sin(2 \cdot pi \cdot f \cdot t + B)$ is minimized by adjusting the magnitude (A) and phase angle (B). For this example, the minimization was done with a quasi-Newton method known as BFGS [11].

Cycle-by-cycle sine-wave fits
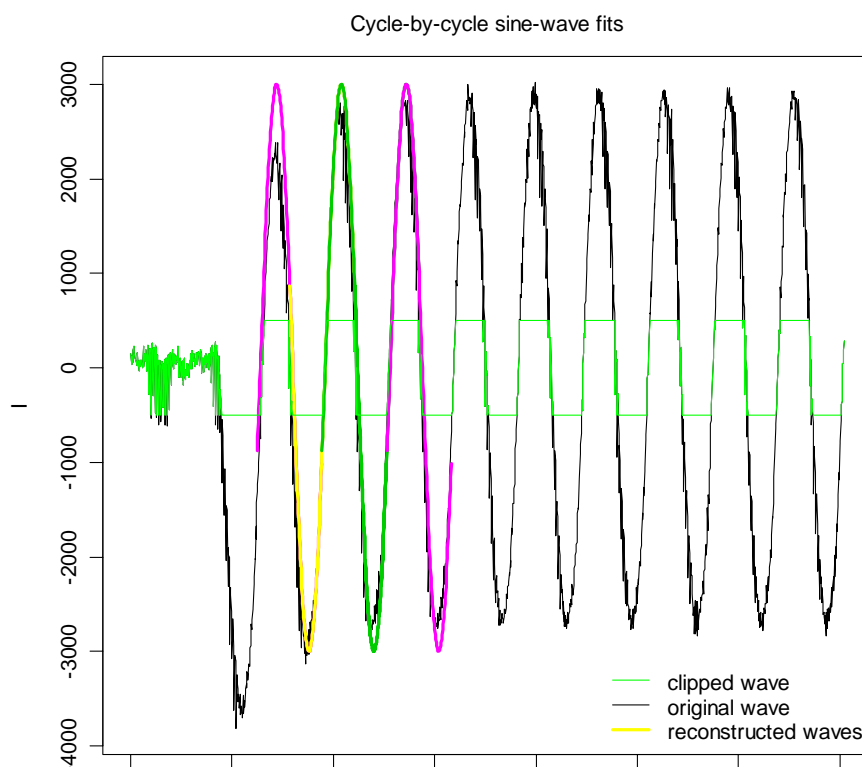


**Figure 3-7**
**Example of a Sine-Wave Reconstruction of a Clipped Wave**

## Accounting for Saturation

Methods for handling saturation include:

- *Use voltage-only fault location*—If the current is heavily distorted from saturation, an easy approach to fault location is to throw out the current and just use the voltage in the fault location.

- *Warn the user*—If it is impossible to account for saturation another way, the user should at least be warned that the location is suspect because of saturation.

- *Wait until the dc offset decays*—Often, CT saturation is caused by fault currents with large dc offsets. The dc offset is largest at the start of the fault and decays with time. The offset is often small after two cycles. As the offset decays, the CT may stop saturating. If the event lasts long enough, saturation errors can be avoided by waiting for the decay to die down. Saturated current waves are high in harmonics, especially the even harmonics. Using the harmonic characteristics or the flux estimate, it is easy to implement an algorithm to identify saturation.

- *Use the unsaturated portion*—Even during heavy saturation, most current waves still contain an unsaturated part. If a point-by-point fault estimate is used (like the algorithms for fault arc detection in Chapter 5), only the "good" points should be used in the point-by-point algorithm.

- *Estimate the unsaturated current*—Using the part of the wave that still contains unsaturated data, the rest of the wave can be filled in by suitable interpolation. This is discussed in more detail following.

Current transformer (CT) saturation can be detected, and it is possible in most cases to reconstruct a reasonable representation of the unsaturated waveshape. Saturation can be detected in a number of ways [references here] as it is important for a number of relaying systems. We use a simplified approach to detect saturation. The current measured equals the rate of change of flux in the measuring CT. The CT saturates when the flux exceeds some value. We can plot the flux by integrating the measured current signal. An example of this is shown below.
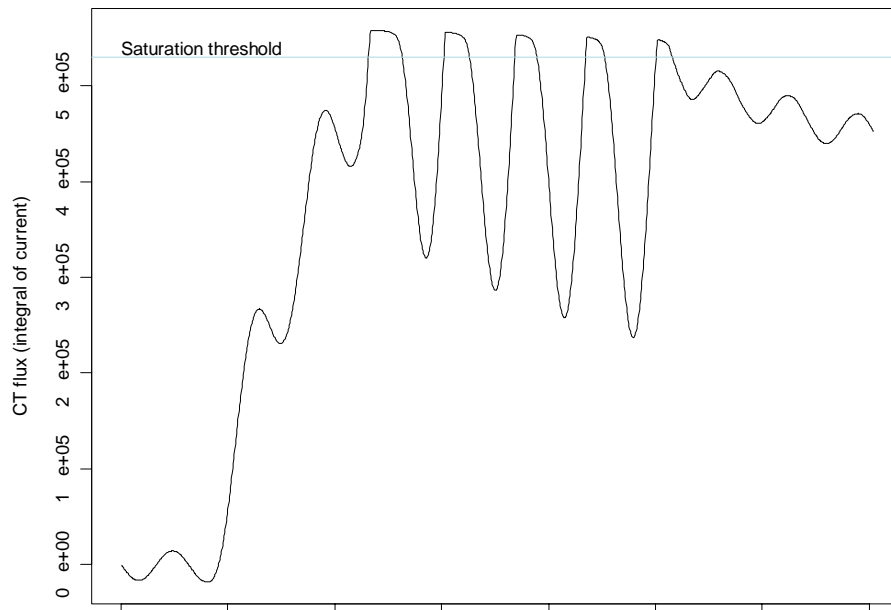


**Figure 3-8**
**Estimate of CT Flux Based on Integrating the Current**

We consider points "good" where the derived flux is less than 95% of the peak flux. We can use these "good" points to reconstruct an estimate of the unsaturated wave by fitting them with a spline fit as shown in the example below. The unsaturated points often include the peaks of the reconstructed wave. In this example, the first two cycles probably underestimate the true peak magnitude; but overall, the spline fit is a reasonable reproduction that will produce a more accurate magnitude and phase angle for fault location.

Saturation is detected by looking for current holding near zero for a significant portion of a cycle. Saturation is indicated if during the fault, the portion of the wave near zero is less than five percent of the peak magnitude for more than eight percent of the duration. An unsaturated wave should be less than five percent of the peak for less than four percent of the duration.
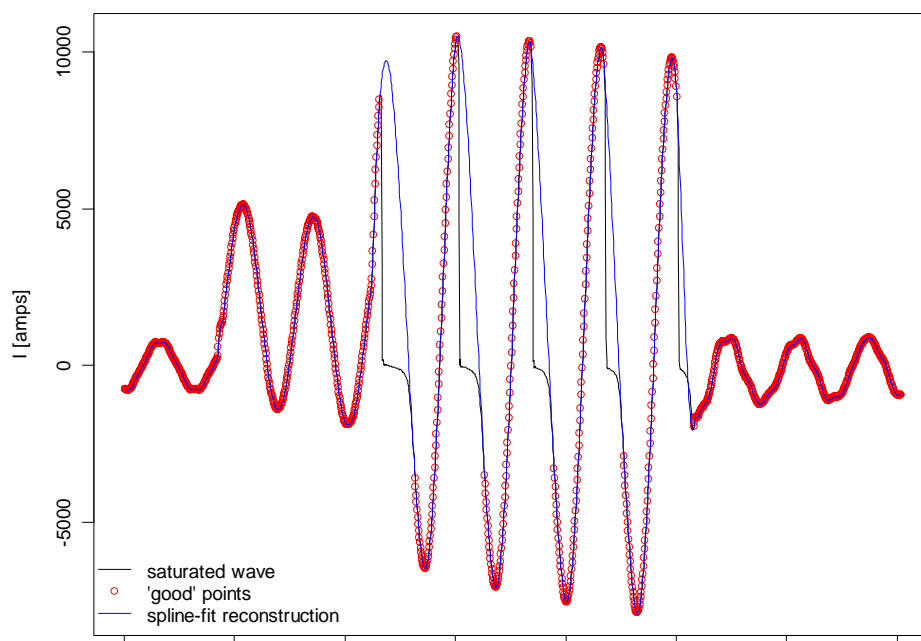
**Figure 3-9**
**Identification of Unsaturated Current Values and Spline-Fit Reconstruction**

## Fault Identification

One of the important parts of a fault location algorithm is identifying the type of the fault and choosing the best part of the fault waveform for further processing. The first step is to try and filter out those events that are not faults. The two most common types of events that could fool a fault location routine are voltage sags and inrush. Both inrush and voltage sags can occur in close time proximity to an outage, so it is important to identify them (inrush from reclosing and voltage sags from adjacent circuit or transmission faults). Voltage sags can cause a rise in the current that may be interpreted as a fault. The direction of power flow is a good indicator of a voltage sag. Inrush normally is high in harmonics, including a dc offset and second harmonics, so these parameters can be used to identify inrush events. Setting parameters for identifying faults is much like setting a relay—you want settings that pick up as many faults as is reasonably possible, but you don't want settings that falsely identify faults from inrush, heavy loads, or voltage sags. Some faults can shift modes or evolve; multiple phases can become involved or phases can extinguish. In these cases, multiple fault types can be tagged to one event.

The sequence currents can also help identify fault type. Table 3-1 shows the phase and sequence currents for different fault types. The negative- and zero-sequence quantities are less susceptible to load (but inrush and voltage sags can cause these sequence currents).

**Table 3-1**
**Phase and Sequence Currents for Different Fault Types**

| Fault Type | Phase A | Phase B | Phase C | Positive Sequence | Negative Sequence | Zero Sequence |
|---|---|---|---|---|---|---|
| Line to ground | $I_F$ | 0 | 0 | $\dfrac{I_F}{3}$ | $\dfrac{I_F}{3}$ | $\dfrac{I_F}{3}$ |
| Line to line | $I_F$ | $-I_F$ | 0 | $\dfrac{I_F}{\sqrt{3}}$ | $-\dfrac{I_F}{\sqrt{3}}$ | 0 |
| Line to line to ground | $I_A$ | $I_B$ | 0 | $\dfrac{I_A + aI_B}{3}$ | $\dfrac{I_A + a^2 I_B}{3}$ | $\dfrac{I_A + I_B}{3}$ |
| Three phase | $I_F$ | $I_F$ | $I_F$ | $I_F$ | 0 | 0 |

Picking the best part of a fault waveform is easy to do by eye, but somewhat harder to program for automatic identification. Initially, a dc offset may cause the current to appear higher than normal as discussed in the previous section. Once it settles down, the fault current stays bolted at close to that level. Occasionally, the fault current(s) will change due to several reasons:

- Current extinguishes on one phase either due to the operation of a downstream device like a fuse or because the fault self extinguished

- Fault current extinguishes and reignites intermittently

- Faults evolve to include more phases or even more circuits

- Arc characteristics change enough to cause the fault current to vary

The most common way to find voltage and current phasors is to pick one fundamental-frequency cycle and apply an FFT to find the magnitude and phase angle of all parameters. It is also possible to pick several cycles at multiple points in time and perform multiple locations to test for variation. Deriving magnitude and phase angle from more than one cycle is also a possibility. For the analysis in this report, just one cycle was used. Some experimentation was done with taking multiple locations at different points in time, and it was found that in most cases tested that it did not change significantly.

The default fault-classification parameters used for most of the analysis in this report is shown in Table 3-2. This set of criteria worked relatively well, but more tweaking is needed. We also need to determine which (if any) of the parameters in Table 3-2 could be set be the user. The three-phase classification system is the most difficult because it only involves positive-sequence parameters, so if load is heavy, it may be difficult to distinguish between a load step and a small three-phase fault.

For all fault types but three-phase faults, the point on the waveshape is taken as the point where the negative-sequence current ($I_2$) is the highest. For three-phase faults, the point on the waveshape is taken as the point where the positive-sequence current ($I_1$) is the highest.

**Table 3-2**
**Initial Criteria for Fault Classification**

| Fault Type | Fault Classification Criteria |
|---|---|
| Line to ground | $\|I_2\| > 150 \text{ A}$ AND<br>$\|I_0\| > 100 \text{ A}$ AND<br>$\|I_2\| < 1.5 \cdot \|I_0\|$ AND<br>$\|I_2\| > 0.1 \cdot \|I_1\|$ |
| Line to line | $\|I_2\| > 300 \text{ A}$ AND<br>$\|I_0\| < 100 \text{ A}$ AND<br>$\|I_2\| > 0.3 \cdot \|I_1\|$ |
| Line to line to ground | $\|I_2\| > 100 \text{ A}$ AND<br>$\|I_0\| > 100 \text{ A}$ AND<br>$\|I_2\| > 1.8 \cdot \|I_0\|$ AND<br>$\|I_2\| > 0.3 \cdot \|I_1\|$ |
| Three phase | ( $\|I_1\| > 2000 \text{ A}$ OR<br>$\|I_1\| > 1.5 \cdot \|I_{1,prefault}\|$ ) AND<br>$\|I_2\| < 500 \text{ A}$ AND<br>not another fault type |

Before picking the maximum current, the following criteria using the second harmonic and the dc component can eliminate bad cycles on the waveshape due to distortion from incomplete cycles, half-cycle blips, inrush, dc offset, and saturation:

$$\frac{\left|I_{\text{2nd harmonic}}\right|}{\left|I_{\text{fundamental frequency}}\right|} < 0.05$$

$$\frac{\left|I_{\text{dc component}}\right|}{\left|I_{\text{fundamental frequency}}\right|} < 0.1$$

This criteria was not used in most of the analysis in this report, but later processing found that it helps eliminate problems with picking a bad cycle from the waveshape.

## Difficult Events

The library of events collected from utilities will help refine fault-location and identification algorithms. As the data has come in, we have identified several events that have characteristics that may make fault location difficult. Several examples of these are shown in this section. Consider Figure 3-10, a short-duration evolving fault cleared by a recloser. The fault started on phase B and evolved to a double-line-to-ground fault also involving phase C. In this case, the fault-identification algorithm correctly picked out one cycle from the wave for the line-to-ground fault and another complete cycle where the event was a line-to-line-to-ground fault. The cycles chosen by the algorithm are shown with the green dots marked "LG" and "LLG" in the fourth panel from the top in Figure 3-10.
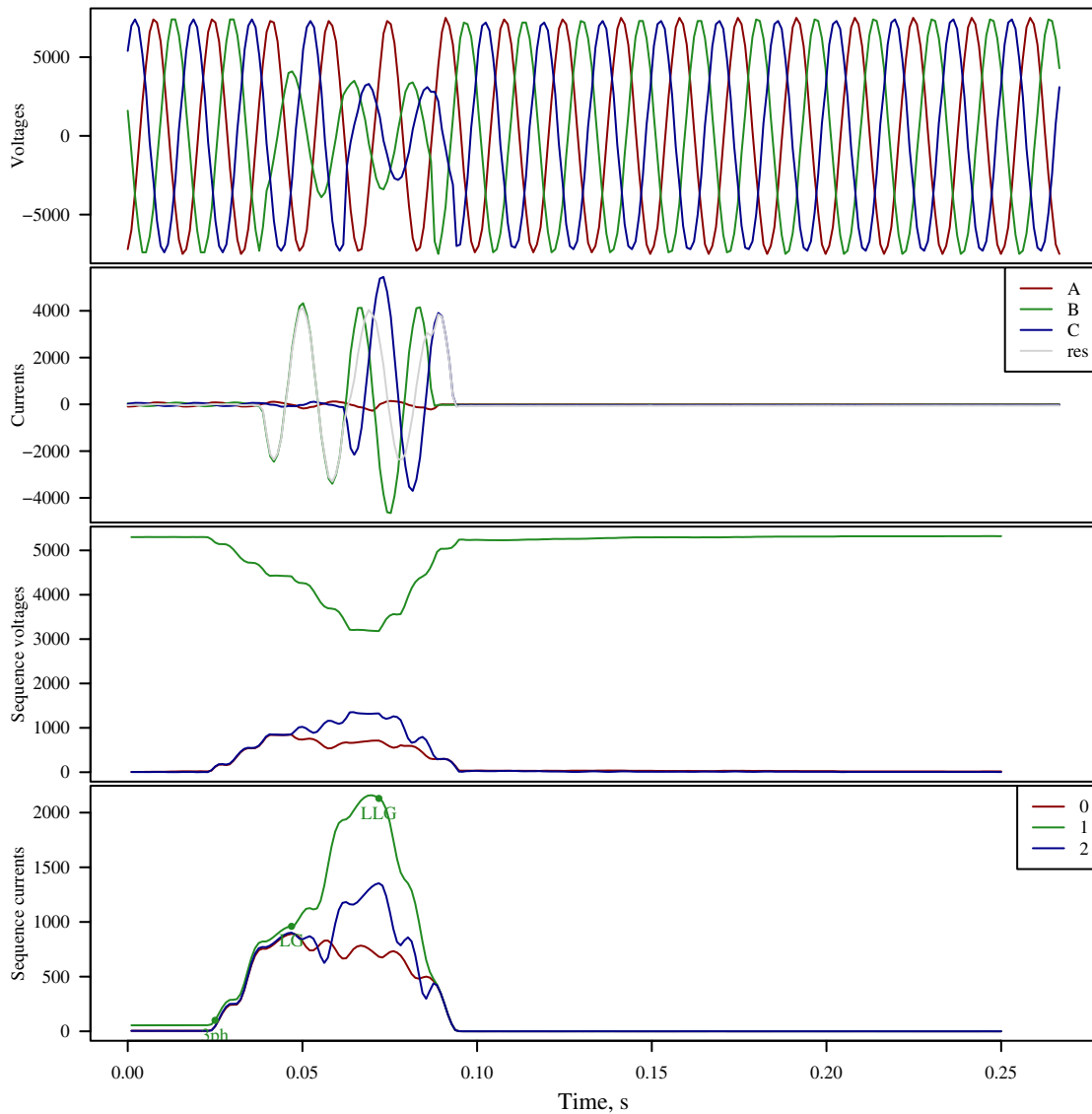
| | | prefault | | LG | | LLG | | LLL |
|---|---|---|---|---|---|---|---|---|
| Va | 5295.84 *an( | -164.16 ) | 5247.34 *an( | 105.90 ) | 5186.97 *an( | -74.48 ) | 5302.19 *an( | -6.42 ) |
| Vb | 5295.50 *an( | 75.82 ) | 2784.68 *an( | -24.18 ) | 2399.54 *an( | 142.34 ) | 4956.42 *an( | -124.45 ) |
| Vc | 5289.60 *an( | -44.07 ) | 5245.70 *an( | -133.91 ) | 2117.51 *an( | 48.59 ) | 5277.49 *an( | 113.91 ) |
| Ia | 65.68 *an( | 166.27 ) | 97.07 *an( | -74.39 ) | 116.40 *an( | -115.92 ) | 63.28 *an( | -29.84 ) |
| Ib | 53.15 *an( | 52.05 ) | 2752.69 *an( | -85.11 ) | 3148.04 *an( | 100.19 ) | 190.39 *an( | -152.21 ) |
| Ic | 43.40 *an( | -69.63 ) | 66.86 *an( | -167.02 ) | 3254.54 *an( | -40.82 ) | 48.65 *an( | 87.54 ) |
| V0 | 3.50 *an( | 72.41 ) | 846.16 *an( | 177.14 ) | 712.44 *an( | -65.42 ) | 118.81 *an( | 23.87 ) |
| V1 | 5293.65 *an( | -164.14 ) | 4414.34 *an( | 103.87 ) | 3181.17 *an( | -79.48 ) | 5178.13 *an( | -5.68 ) |
| V2 | 4.15 *an( | -157.41 ) | 856.21 *an( | 57.08 ) | 1324.65 *an( | -67.33 ) | 128.97 *an( | -86.64 ) |
| I0 | 7.74 *an( | 133.61 ) | 890.46 *an( | -85.80 ) | 682.38 *an( | 25.03 ) | 44.16 *an( | -147.27 ) |
| I1 | 54.03 *an( | 169.26 ) | 960.68 *an( | 36.94 ) | 2130.47 *an( | -149.90 ) | 100.76 *an( | -31.75 ) |
| I2 | 5.39 *an( | -179.14 ) | 902.54 *an( | 153.39 ) | 1354.26 *an( | 29.90 ) | 45.86 *an( | 82.02 ) |
| Ir | 23.22 *an( | 133.61 ) | 2671.37 *an( | -85.80 ) | 2047.13 *an( | 25.03 ) | 132.49 *an( | -147.27 ) |
| Zfault | | NA | | 0.496+0.917i | | 0.254+0.502i | | 37.684+5.981i |
| zfault3 | | NA | | NA | | 0.256+0.487i | | 59.622-1.642i |

**Figure 3-10**
**Short-Duration Fault that Started as a Single-Line-to-Ground Fault and Evolved to a Double-Line-to-Ground Fault**

Figure 3-11 and Figure 3-12 shows more evolving faults, each with peculiarities that make location more difficult (noise or intermittent action).

**Figure 3-11**
**Evolving Fault that also has a Short-Duration Blip in the Middle**
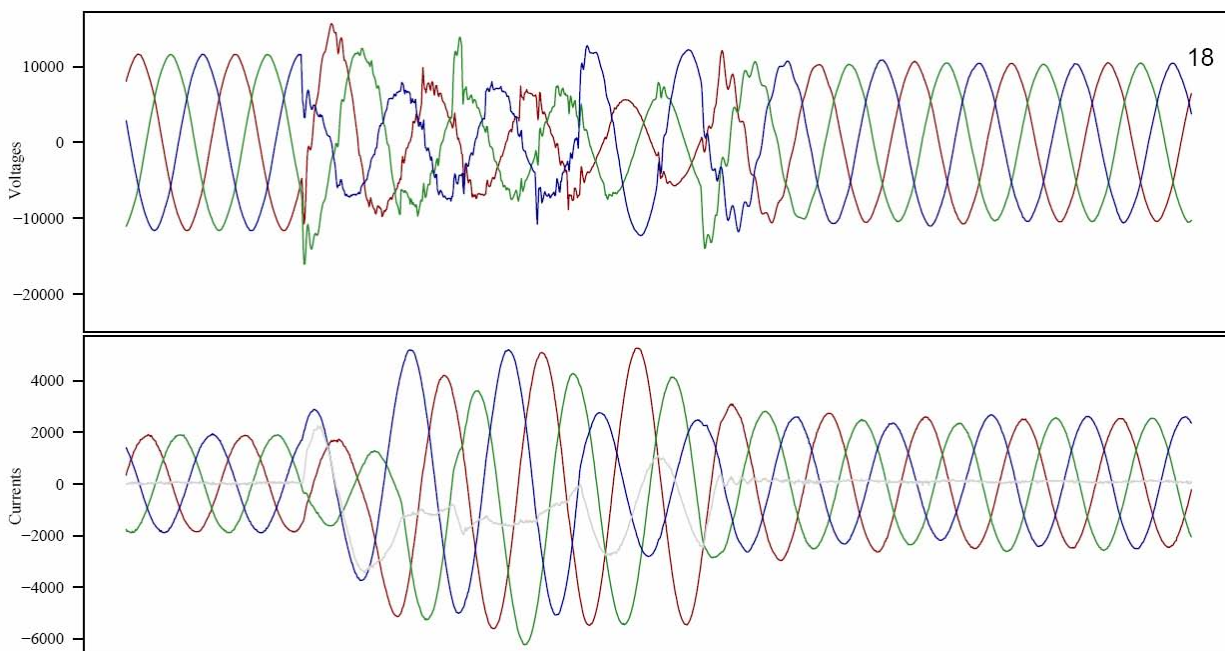
**Figure 3-12**
**Changing Fault With Heavy Noise and Distortion in Voltage Measurements**

Another common problem is when recorders do not capture a prefault period. One example is shown in Figure 3-13 where the recorder didn't start recording fast enough. Some fault events naturally will not have a prefault value. Upon reclose of a circuit breaker or recloser into a permanent fault, there is no load current because the circuit is open until the device closes in. Missing the start can happen with both relays and power quality monitors. Better trigger settings can help avoid this. For algorithms that rely on prefault values, this is a problem.

Figure 3-14 shows another example where the prefault period was missed. This was an unusual event that appeared to jump from phase A to phase B. We do not know why this occurred, and we are not sure how this type of event should be reported to an operator. Fortunately, this type of event is rare.

Figure 3-15 shows an example of a low-level line-to-ground fault. Lower-magnitude fault currents can be difficult to separate from load current, so we need events like this to test the fault identification and fault location algorithms.

**Figure 3-13**
**Evolving Fault With No Prefault Data**

Figure 3-16 to Figure 3-20 show examples of events which we normally want excluded by the fault identification algorithm. These include a current-limiting fuse operation, inrush, a capacitor switching, and half-cycle blips. Although they should normally be excluded, these types of events may include important information, so having a separate routine that can classify each of these types of events might be beneficial in helping engineers track down problems on their systems.
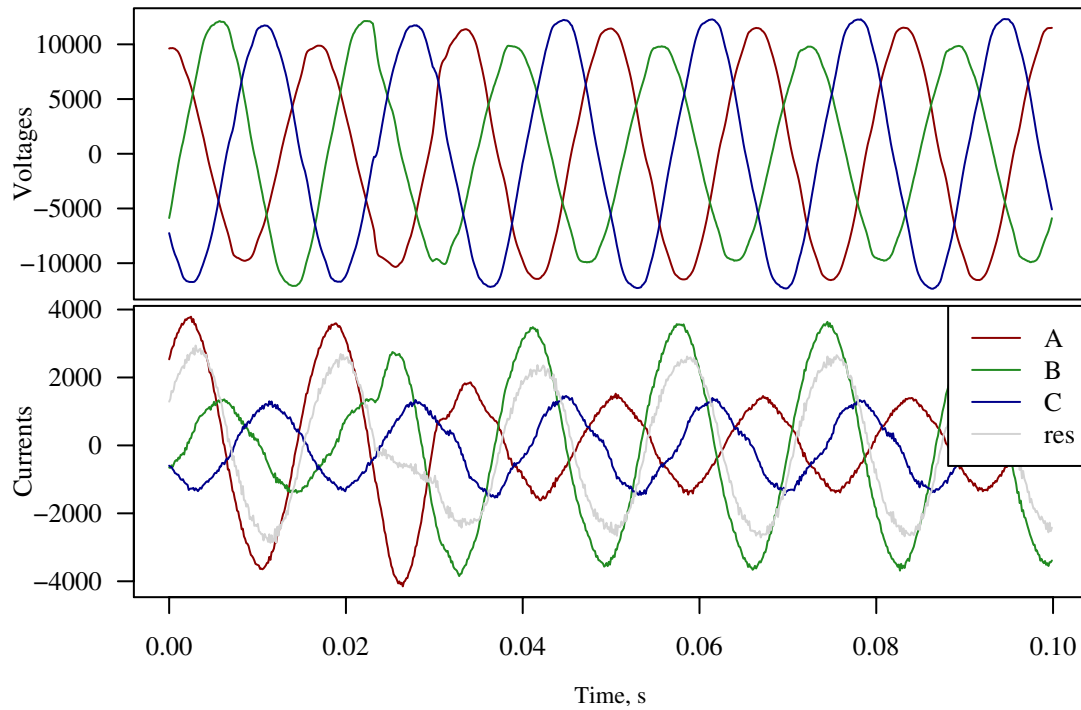
**Figure 3-14**
**Unusual Fault that Shifted from Phase A to Phase B**
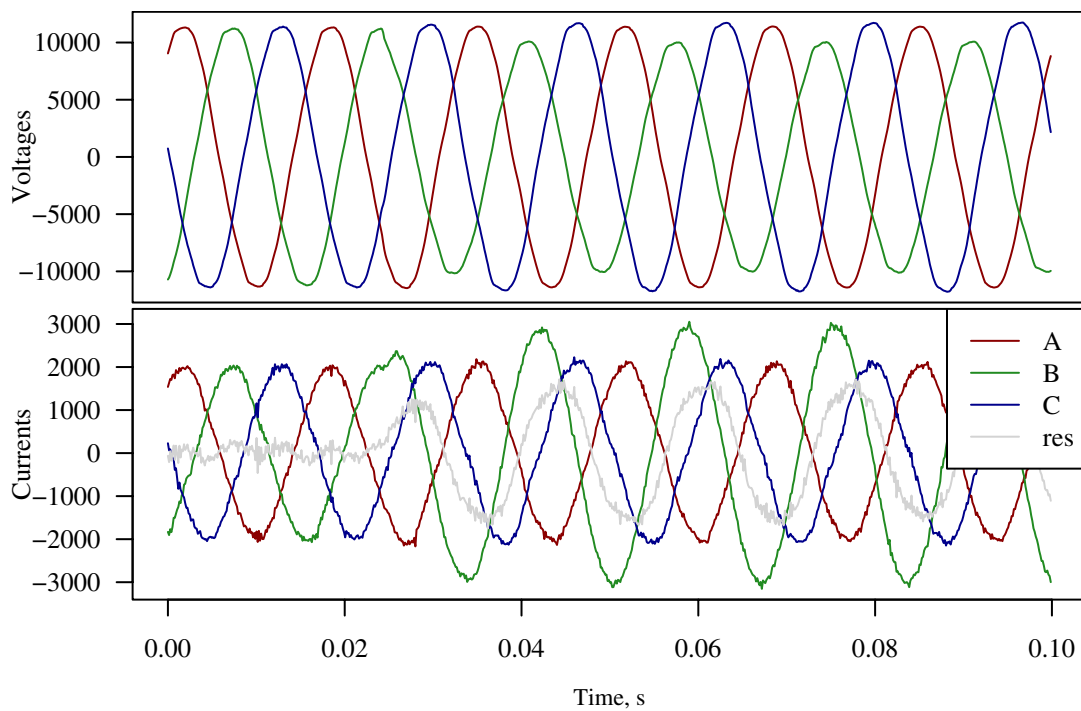


**Figure 3-15**
**Lower-Level Line-to-Ground Fault**
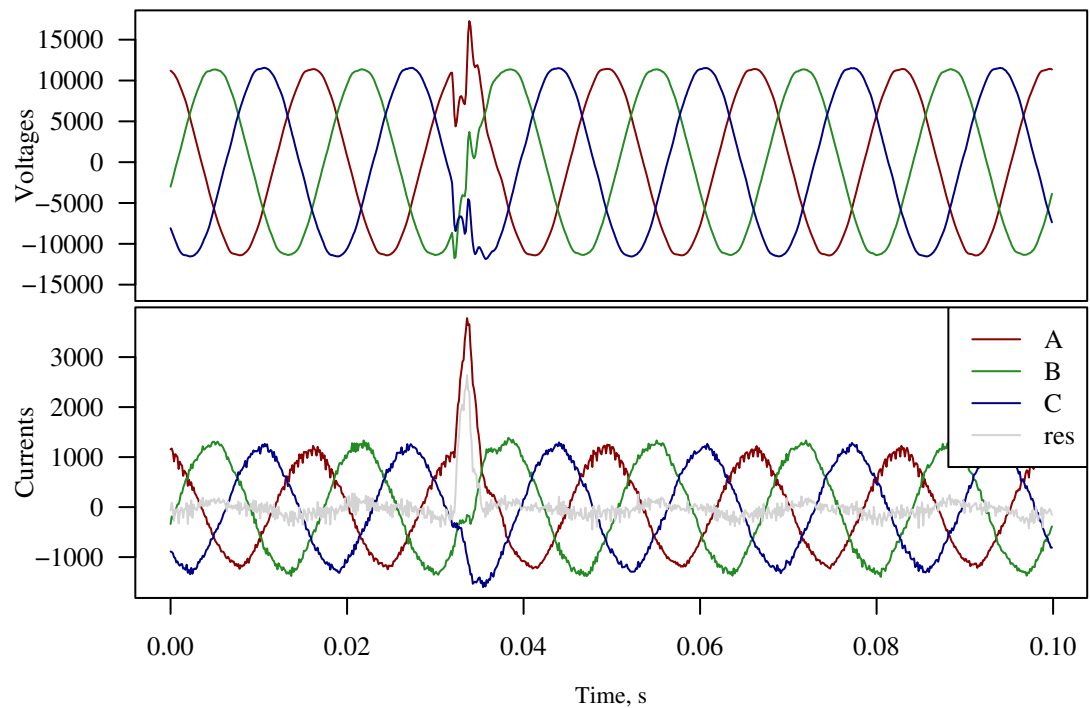
**Figure 3-16**
**Current-Limiting Fuse Operation**
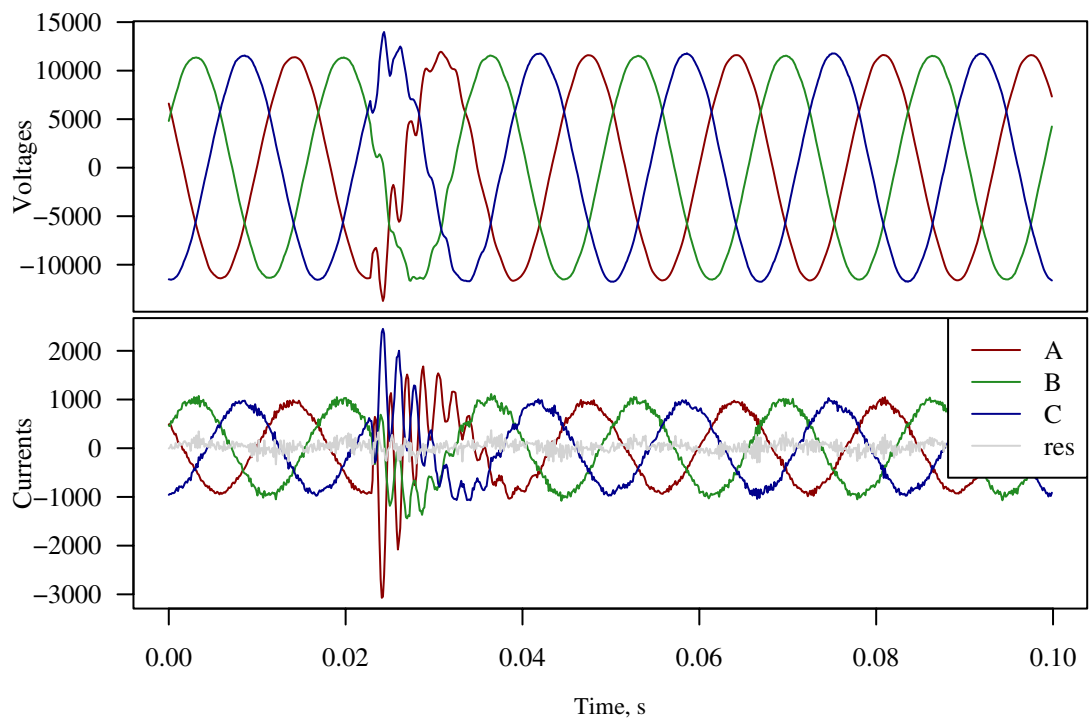


**Figure 3-17**
**Capacitor Switching Transient**
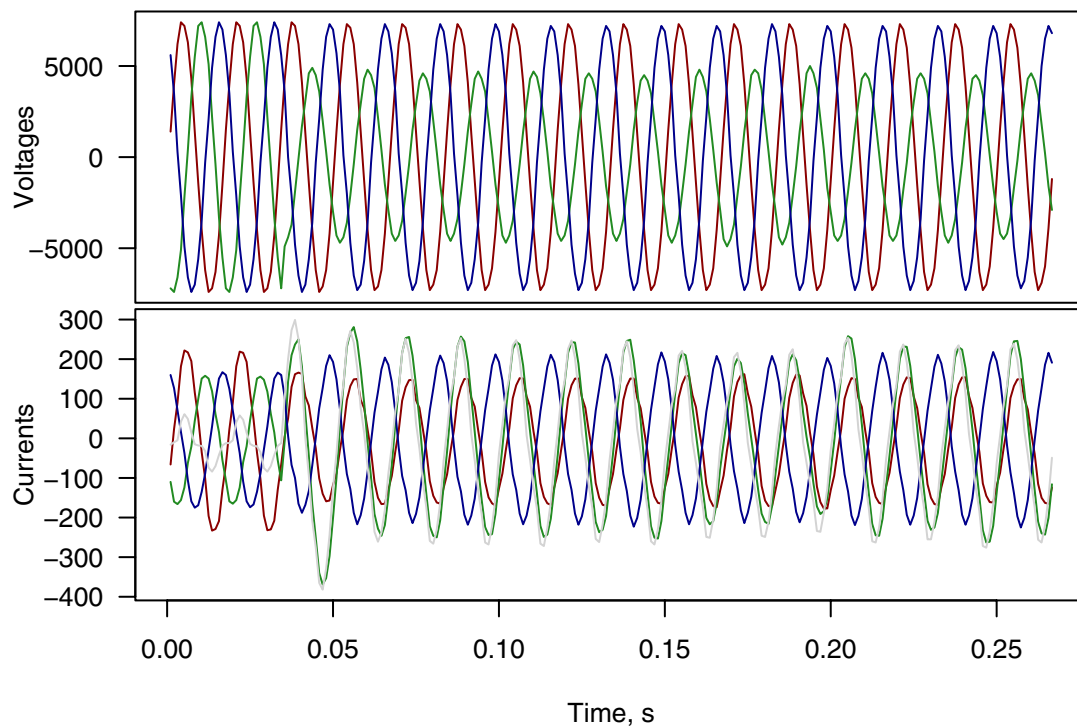
**Figure 3-18**
**Voltage Sag that might be Interpreted as a Fault**
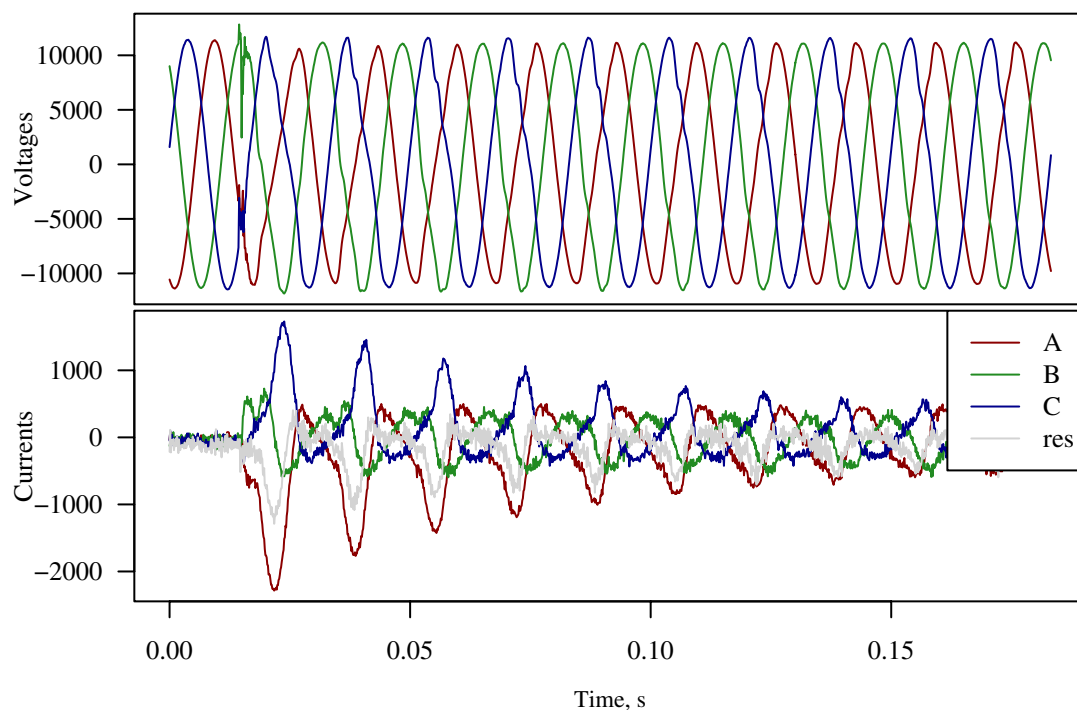


**Figure 3-19**
**Inrush Example**
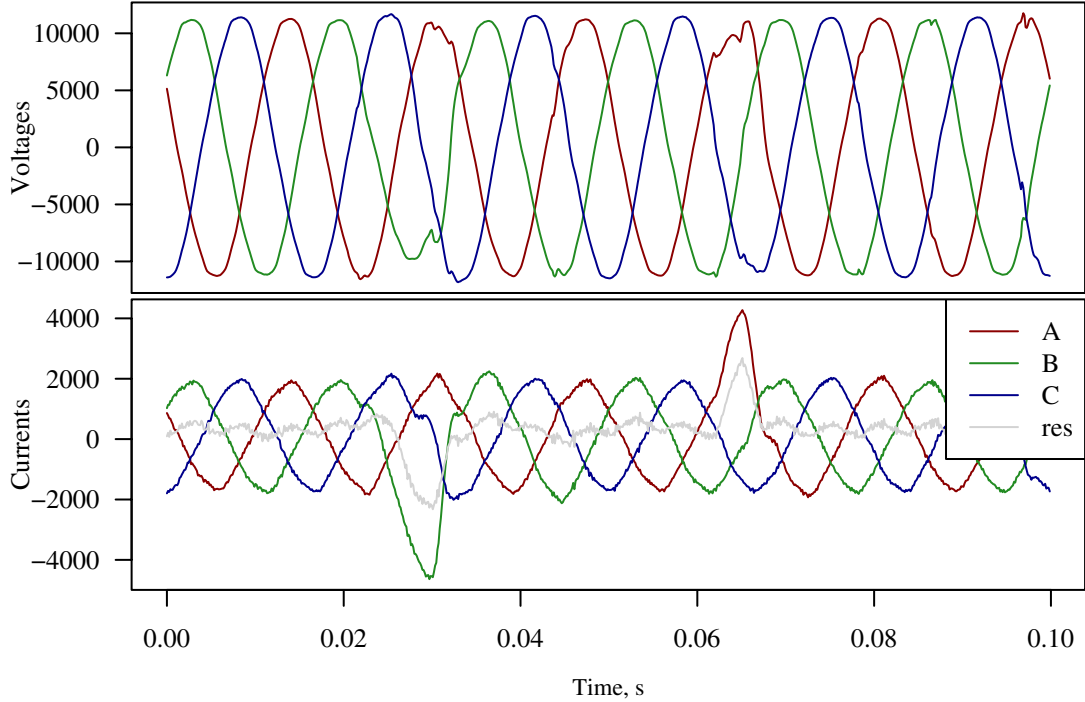
**Figure 3-20**
**Two Half-Cycle Blips on Different Phases**

# *4*
# ANALYSIS OF DATA SETS

## Introduction

This chapter summarizes the fault and outage data collected from several utilities. The fault waveshapes were processed through several fault identification and location algorithms. The default algorithm used is the basic absolute value of the line impedance to the fault. Table 4-1 summarizes the data collected. Not all of this data has been fully analyzed yet (data from F and G came in too late), but it provides an excellent set of data. The data includes the most common types of data recorders that might be used for fault locating, both urban and rural circuits are represented, a wide range of voltages are present, and a number of different circuit models were provided. Such a wide range of data will help in developing a more widely useable implementation.

**Table 4-1**
**Fault Data Set Summary**

| Utility | Number of Events | Monitor | Samples Per Cycle | Voltage | System Type | Circuit Data |
|---------|------------------|---------|-------------------|---------|-------------|--------------|
| A | 211 | Bus PQ monitors | 128 | 13.8 kV | Suburban | Cyme/ArcGIS |
| B | 401 | Bus PQ monitors<br>GE feeder relays<br>SEL feeder relays | 128<br>32<br>16 | 13.8 and 27 kV | Urban | Custom format |
| C | 23 | Bus PQ monitors | 128 | 12 kV | Urban | SynerGEE |
| D | 10 | SEL feeder relays | 4 & 16 | 13 and 25 kV | Suburban/rural | FeederAll |
| E | 32 | SEL feeder relays<br>SEL recloser relay<br>DFA | 16<br>32<br>256 | 12 and 34 kV | Suburban/rural | Cyme |
| F | 1124 | Feeder and bus-level RTU | 16 | 12 and 23 kV | Suburban/rural | Cyme |
| G | 12 | SEL feeder relays | 4 | 12 kV | Suburban | PSS/Adept |

## Utility A

Utility A provided many useful events with fault data correlated with location. The main parameters of this dataset include:

- 211 fault events

- Bus-level power-quality monitors

  – 128 samples per cycle

- Mainly suburban

- 13.8 kV

- Circuit data model available from an Arcview GIS or from Cymdist

This dataset included events from several substations during one year. The initial set of matches between the monitors and the outage database narrowed the list of events. Outages and monitor events were matched if their times were within 30 minutes, they were at the same substation, and the outage had a pole number or other location indicated in the database. Then, each monitor event was manually reviewed to see if it matched the utility outage database records. With such a large number of events, the dataset from utility A provided several opportunities to evaluate fault-location approaches in detail for various different types of faults.

Figure 4-1 shows estimates of impedance to the fault from the Cyme data and known fault location compared to the estimate of the same impedance estimated from the fault waveshape. For perfect fault location, these would be equal and fall on top of the straight line shown (the line is not a linear fit to the data). Figure 4-1 is for line-to-ground faults, so the loop impedance is the parameter of interest $(2 \cdot Z_1 + Z_0)/3$. The waveshape estimate is the estimate that will lead to the predicted fault location. In general, the locations are relatively accurate.

Generally, the impedance from the fault waveshape overestimates the distance to the fault. This can be corrected with a linear adjust multiplier (we will evaluate this). The more important parameter is the spread around a linear fit. Except for a few outliers, all of the data is within plus or minus one ohm. Ohms are not what we want for a final answer on accuracy—we want an estimate of the distance accuracy. For this, we can use the fact that overhead lines have an impedance of about one ohm per mile for the loop impedance. Therefore, Figure 4-1 can be interpreted as having the x and y axis scales in miles. So, we see that almost all of the estimates are within plus and minus one mile.

Each of the colors in Figure 4-1 represents a different location at utility A. There is no strong difference from site to site in this data.

There are some outliers in the data. These were investigated, but it is uncertain as to what caused the differences. Possibilities could include: the monitoring waveshape did not match with the fault that caused the outage, the pole number was recorded wrong on the outage report, the Cyme data had connectivity errors, or the fault-location algorithm malfunctioned for some unknown reason.
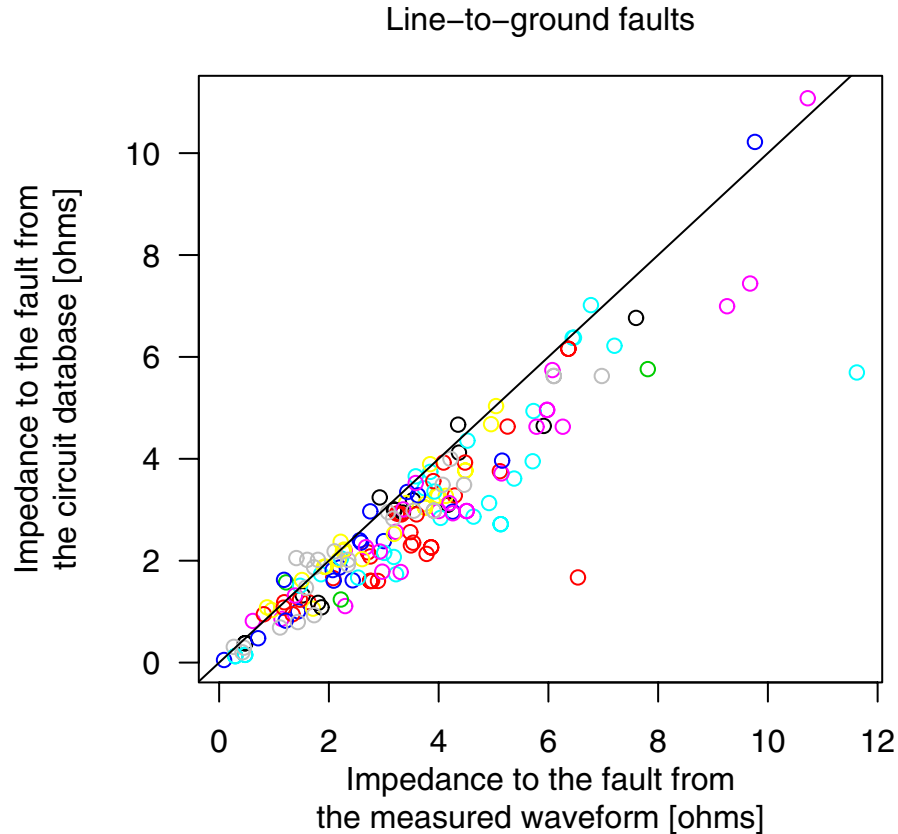
**Figure 4-1**
**Utility A: Impedance Estimated from the Waveform Versus Impedance to the Fault from the Circuit Database**

Figure 4-2 shows a similar comparison but for double line-to-ground faults. The correlation between the circuit database impedances and the impedances from the waveform appears to be even better than for line-to-ground faults. This is surprising because the monitors at utility A are bus-level monitors with significant loading. For line-to-ground faults, loading interferes less with fault location, because the residual current can be used $(I_A + I_B + I_C)$. For multiphase faults, the load current on each phase makes it more difficult to separate the fault current from the load current. Figure 4-3 shows this same data for double line-to-ground faults segmented by load. There is no noticeable impact on whether the total loading on the circuit was high or low when the fault happened.

Line–to–line–to–ground faults
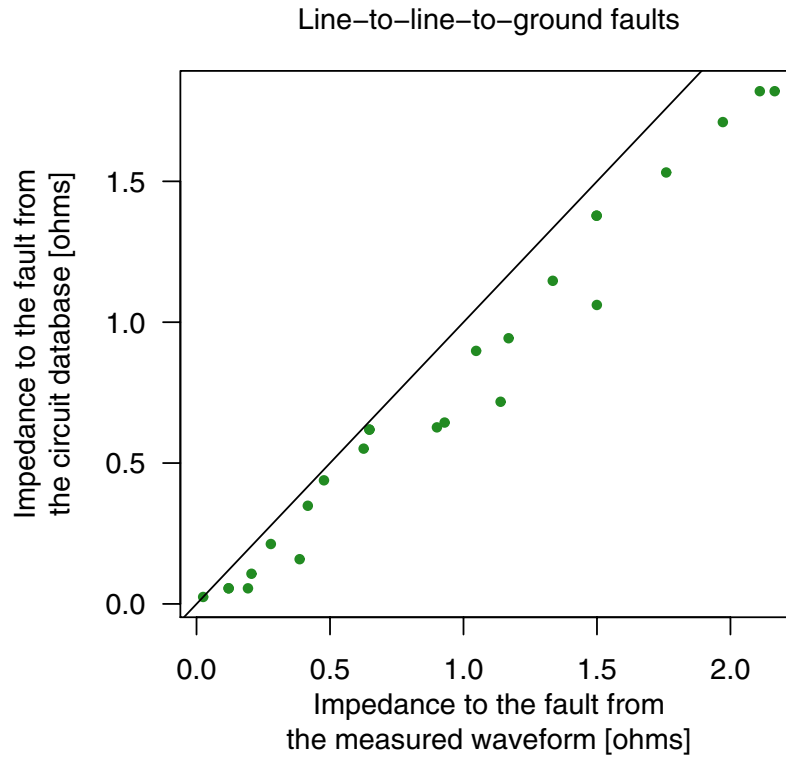


**Figure 4-2**
**Utility A: Impedance Estimated from the Waveform Versus Impedance to the Fault from the Circuit Database**

Line–to–line–to–ground faults
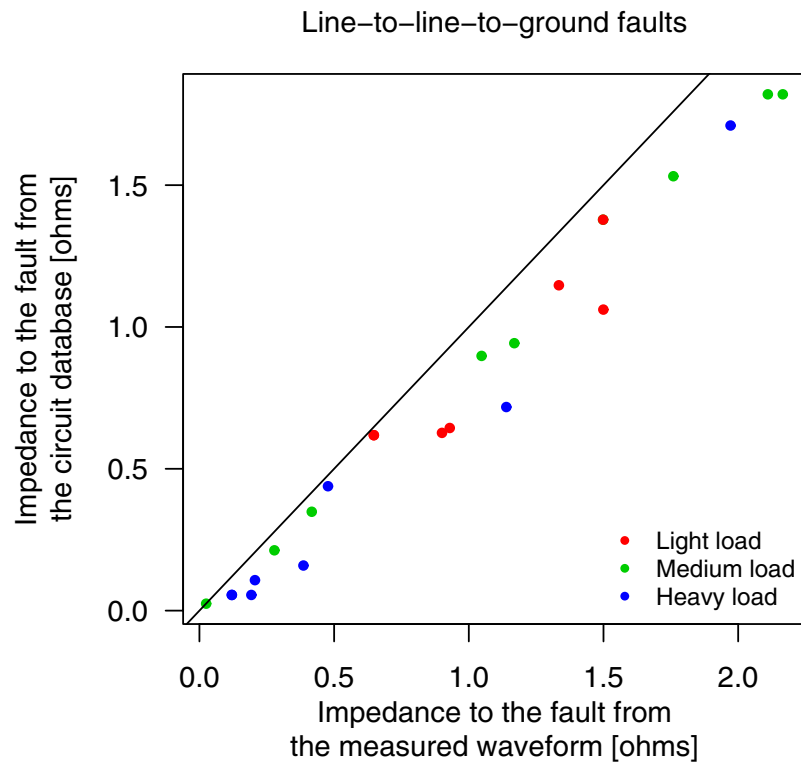


**Figure 4-3**
**Utility A: Impact of Load on Impedance Estimated from the Waveform Versus Impedance to the Fault from the Circuit Database**

Figure 4-4 shows an example of a line-to-ground fault measured at utility A. This fault was cleared by the substation breaker. Figure 4-5 shows the circuit that was faulted with the known fault location. Location estimates from the waveform are also shown. Multiple locations are estimated because the radial circuit has a number of branches. Because the circuit breaker locked out, an operator could narrow the choices just to those on the mainline—assuming coordination of downstream protective devices. As with many of the faults at utility A, this prediction is an overestimate. The overestimate can be factored out of the model by including a multiplying factor.



```
                        prefault                    LG
      Va    8149.6 *an(   -18.2 )   6534.3 *an(  -151.0 )
      Vb    8101.9 *an(  -138.2 )   8598.4 *an(    94.7 )
      Vc    8203.5 *an(   101.4 )   8158.5 *an(   -19.0 )
      Ia    1181.7 *an(   -26.5 )   3711.9 *an(   169.9 )
      Ib    1281.5 *an(  -145.6 )   1282.3 *an(    73.6 )
      Ic    1312.1 *an(    93.3 )   1545.7 *an(   -35.2 )
      V0      45.0 *an(    49.1 )   1013.2 *an(    64.8 )
      V1    8151.6 *an(   -18.3 )   7736.8 *an(  -144.7 )
      V2      25.8 *an(  -156.8 )    422.2 *an(    66.9 )
      I0      31.8 *an(   142.6 )    752.7 *an(   154.0 )
      I1    1258.4 *an(   -26.3 )   2103.6 *an(  -177.3 )
      I2      47.0 *an(   167.9 )    972.4 *an(   154.4 )
      Ir      95.3 *an(   142.6 )   2258.0 *an(   154.0 )
   Zfault                   NA                 1.66+2.37i
   Zfault3                  NA                        NA
```
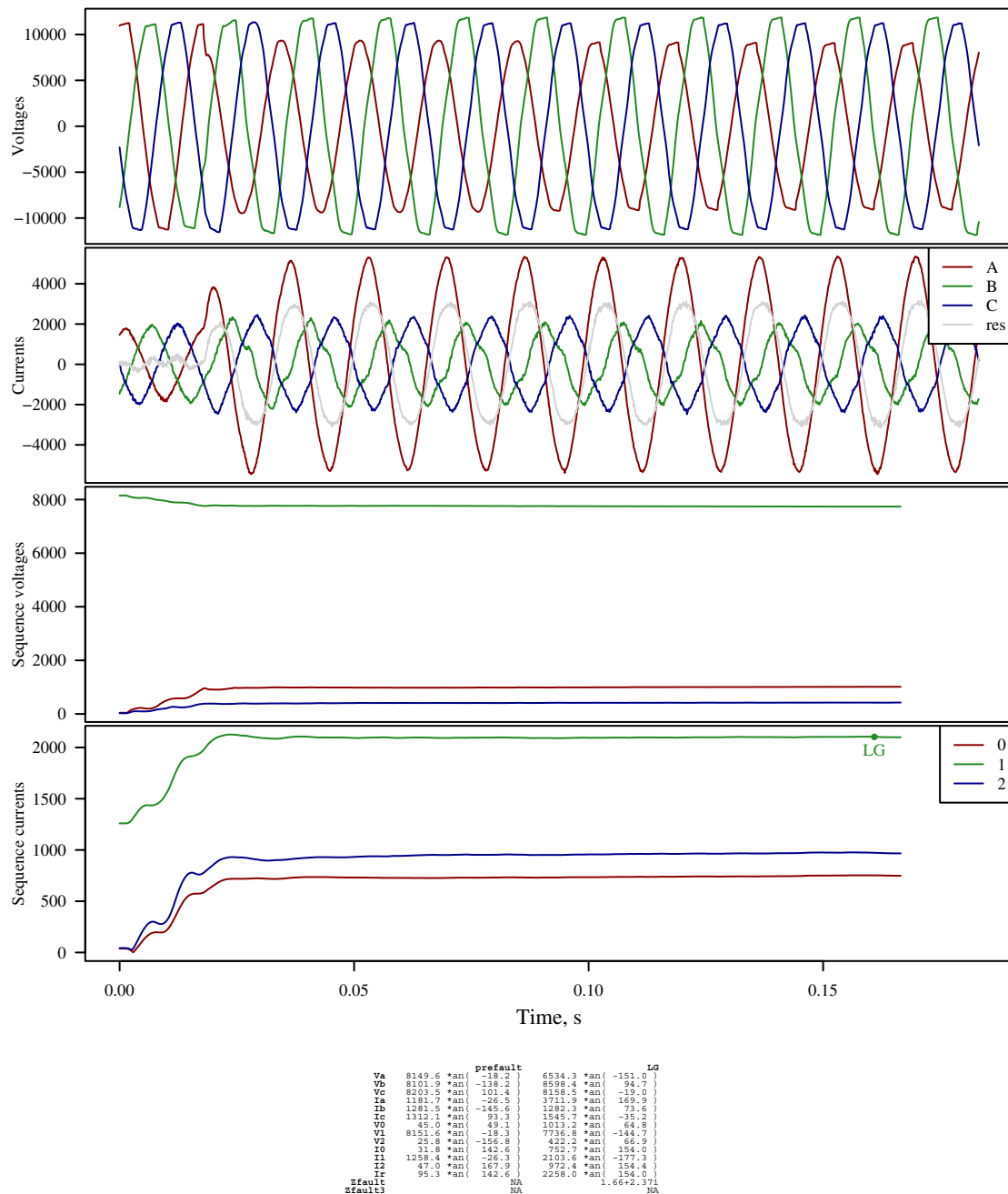
**Figure 4-4**
**Example Line-to-Ground Fault**

z1 = 0.493+0.53i  z0 = 2.64+2.16i  zs = 1.21+1.07i



**Figure 4-5**
**Fault Estimates Relative to a Known Location (for the Event Plotted in Figure 4-4)**

Solid red: Known fault location

Purple circles: Location estimates

Figure 4-6 and Figure 4-7 give another example of a measured waveshape along with the estimated fault location. This case is for a line-to-ground fault cleared by a fuse. Normally, a fault-location system would not be used in a situation like this (the outage-management system and customer calls would narrow the search location sufficiently). Nevertheless, these waveforms are still useful in evaluating fault-location algorithms. This example also overshot on the location estimate.

As discussed in Chapter 2, several different variations of impedance-based fault location are available. Table 4-2 compares the results of several algorithms for line-to-ground faults. The basic absolute value of impedance (Z) algorithm is what we've shown for most of the estimates of impedance to the fault (in Figure 4-1 and Figure 4-2 for example). The Takagi algorithm is used in SEL relays. Con Edison uses the reactance to fault method, and Progress Carolina uses the fault current magnitude approach. The model with a nonlinear arc is a newer model that handles the arc voltage more accurately.

All of these methods work reasonably well. The K factor in the table is a multiplier than can be applied to distance estimates. This can correct for the over-reaching for example. For this dataset, the best models are the fault current magnitude and the nonlinear arc model. These have the lowest $R^2$. The $R^2$ is a measure of the dispersion in the data.

Table 4-3 shows a similar comparison, but instead of using a linear model, quantile modeling is used. In quantile modeling, instead of estimating the average, a quantile is estimated. For example, the 50% quantile is the midpoint or median prediction. This is useful for examining the range and dispersity of a model. In the better models, 50% of the data falls roughly between 10% high and slightly more than 10% low.
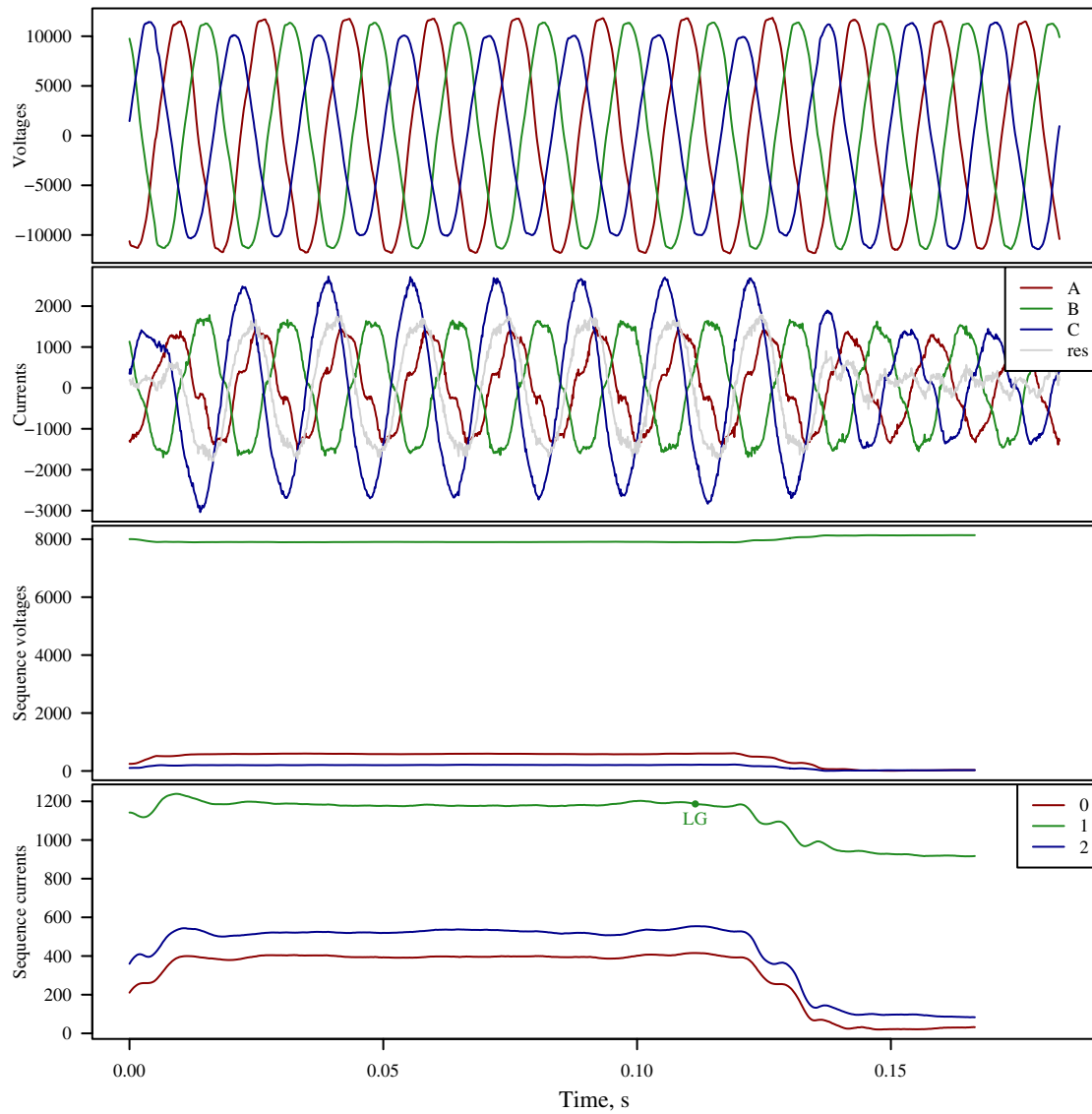
|          | prefault                    | LG                          |
|----------|-----------------------------|-----------------------------|
| Va       | 8097.6 *an( 154.92 )        | 8413.6 *an(  41.17 )        |
| Vb       | 8184.2 *an(  35.05 )        | 8156.6 *an( -74.54 )        |
| Vc       | 7981.3 *an( -82.75 )        | 7138.9 *an( 159.98 )        |
| Ia       | 873.3 *an( 174.73 )         | 885.5 *an(  54.91 )         |
| Ib       | 1109.0 *an(  45.92 )        | 1132.2 *an( -66.28 )        |
| Ic       | 1024.1 *an( -88.15 )        | 1896.2 *an( 125.06 )        |
| V0       | 143.3 *an( -29.85 )         | 601.1 *an(   3.86 )         |
| V1       | 8086.3 *an( 155.73 )        | 7896.4 *an(  42.29 )        |
| V2       | 94.5 *an( 157.11 )          | 214.8 *an( 120.25 )         |
| I0       | 53.5 *an( -113.92 )         | 415.5 *an(  95.74 )         |
| I1       | 989.2 *an( 163.70 )         | 1186.4 *an(  30.46 )        |
| I2       | 179.9 *an( -55.67 )         | 554.1 *an( -148.41 )        |
| Ir       | 160.4 *an( -113.92 )        | 1246.5 *an(  95.74 )        |
| Zfault   | NA                          | 2.49+5.161                  |
| Zfault3  | NA                          | NA                          |

**Figure 4-6**
**Example Line-to-Ground Fault**

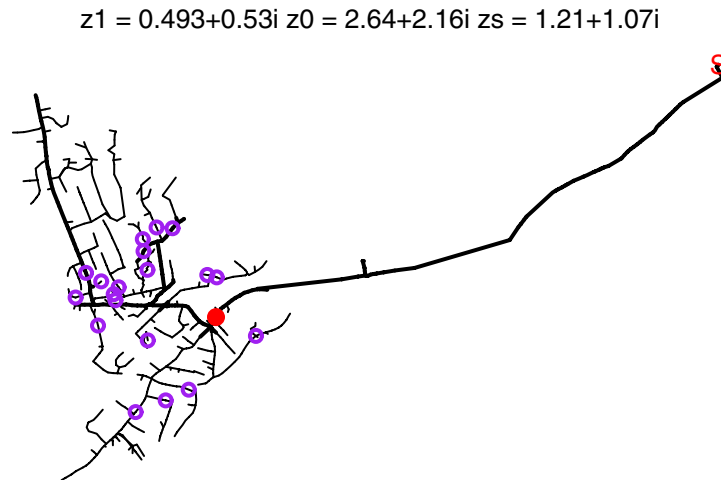z1 = 1.52+2.27i z0 = 5.28+7.72i zs = 2.77+4.09i
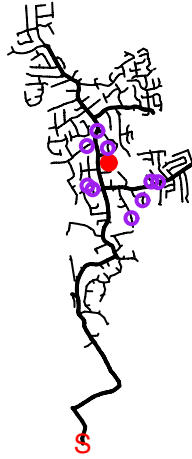


**Figure 4-7**
**Fault Estimates Relative to a Known Location (for the Event Plotted in Figure 4-6)**

Solid red: Known fault location

Purple circles: Location estimates

**Table 4-2**
**Linear Model of Several Fault-Location Algorithms**

| Fault Location Algorithm | Percent Failed | K | R$^2$ |
|---|---|---|---|
| Absolute value of impedance (Z) | 0 | 0.814 | 0.958 |
| Reactance to the fault (X) | 0 | 0.759 | 0.957 |
| Fault current magnitude | 0 | 0.848 | 0.969 |
| Voltage sag | 7.5 | 0.801 | 0.934 |
| Takagi | 0 | 1.242 | 0.947 |
| Impedance with a nonlinear arc | 0.6 | 0.895 | 0.966 |

**Table 4-3**
**Median and Quantile Models of Several Fault-Location Algorithms**

| Fault Location Algorithm | Median | Lower 10% | Upper 10% | Lower 25% | Upper 25% |
|---|---|---|---|---|---|
| Absolute value of impedance (Z) | 0.829 | 0.702 | 1.23 | 0.881 | 1.14 |
| Reactance to the fault (X) | 0.789 | 0.649 | 1.21 | 0.882 | 1.10 |
| Fault current magnitude | 0.873 | 0.747 | 1.18 | 0.889 | 1.10 |
| Voltage sag | 0.817 | 0.721 | 1.32 | 0.831 | 1.16 |
| Takagi | 1.289 | 0.679 | 1.25 | 0.859 | 1.11 |
| Impedance with a nonlinear arc | 0.902 | 0.733 | 1.19 | 0.862 | 1.09 |

Figure 4-8 further compares these models by showing predicted quantities versus those estimated from the circuit database. The median prediction line is shown in dark blue, and the gray lines show the upper and lower 25% prediction lines as well as the upper and lower 10% prediction lines. Each of the parameters in Figure 4-8 is scaled to an "impedance-like" quantity for easier comparison. For example, instead of showing fault current ($I$), an equivalent impedance is found as $Z_{eq} = V/I$. In all cases, parameters closer to zero are faults closer to the substation.

Based on the results of Table 4-2, Table 4-3, and Figure 4-8, the fault current magnitude algorithm and the nonlinear arc model perform the best (lowest $R^2$ and tightest error bands). The voltage sag and Takagi methods perform the worst. More examination and comparisons are warranted. For example, some models might work better than others in some situations. For example, the nonlinear arc model may work better for those faults with significant arc voltage, but perform worse for faults without significant arc voltage.
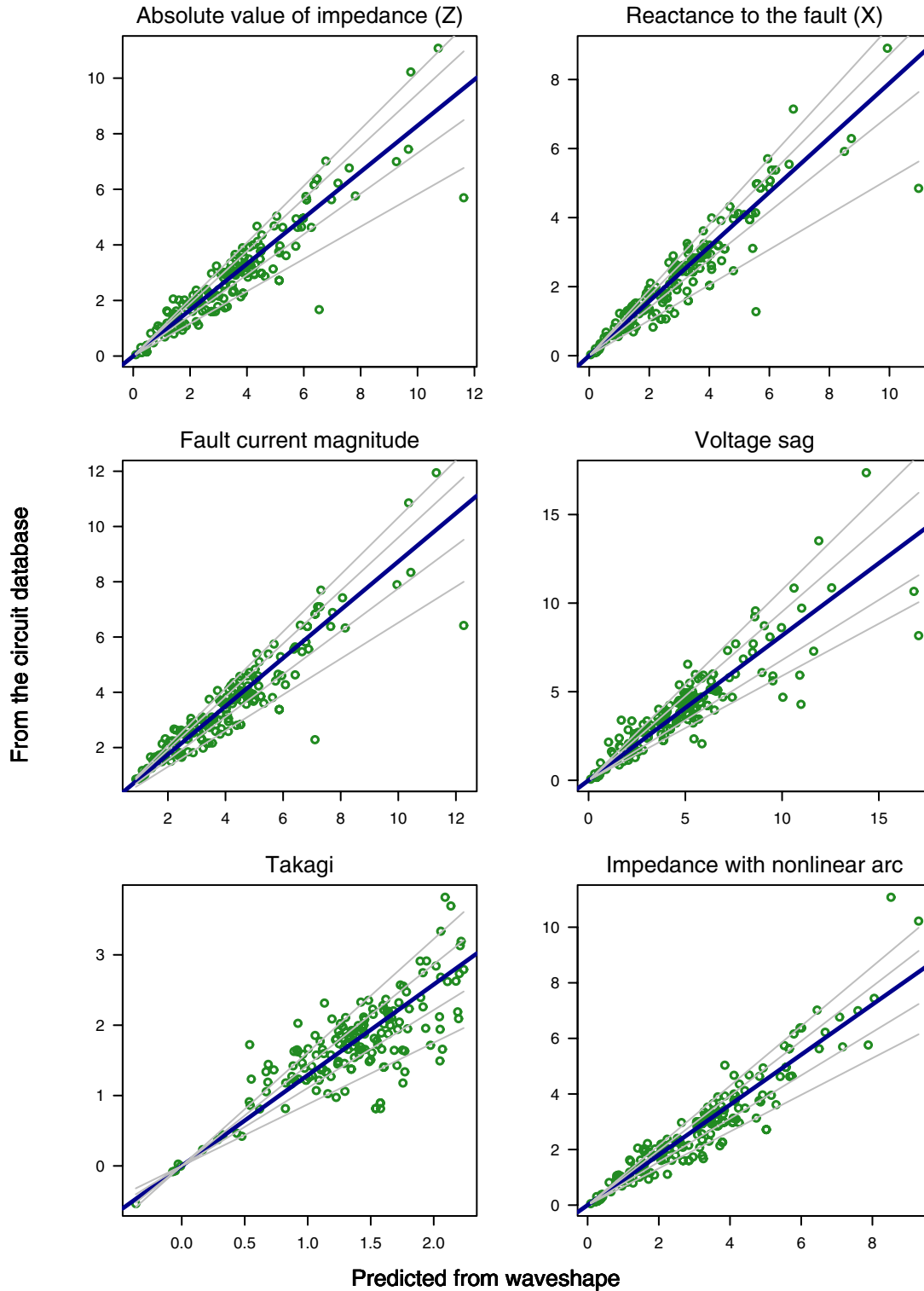
**Figure 4-8**
**Predicted Versus Parameters from the Circuit Database for Several Fault-Location Algorithms**

## Utility B

Utility B provided a large dataset for evaluation with over 400 fault events correlated with known locations. The dataset had the following parameters:

- 401 fault events in the dataset

- Bus-level power-quality monitors

  - 128 samples per cycle

- Mainly urban circuits feeding secondary networks

- 13.8 kV and 27 kV

- Custom internal circuit data model

This dataset was from a one-year time period at many substations. Utility B's standard transformer connection to the secondary network load is a delta – wye transformer. From a fault-location perspective, this makes it easier to find line-to-ground faults. Since the load is connected phase to phase, load currents do not disrupt line-to-ground faults (the most common fault type).

One disadvantage of this dataset is that utility B's circuit data only includes positive-sequence impedances. This makes line-to-ground fault locating more challenging. All calculations are done by treating the loop impedance as being equal to the positive-sequence impedance. Then, an adjustment factor can hopefully account for the ratio of positive-sequence to loop impedances.

Utility B also provided digital relay files at one substation. These include GE and Schweitzer digital relays with either 16 or 32 samples per cycle. While these proved helpful in evaluating relays as fault-locating instruments, the actual data was not evaluated in much detail. The substation had mixed network and non-network load, and had grounding transformers. The infeeds from feeder grounding transformers could interfere with fault location.

Figure 4-9 shows the loop impedance estimated from monitoring waveshapes compared with the positive-sequence impedance from the circuit database. As expected, the ratio is not near unity. However, there is a relatively linear relationship between the two parameters. As long as the relationship is predictable, a linear adjustment multiplier can be used.

In Figure 4-9, each color represents a different location. Unlike utility A, utility B has significant differences between sites. This is helpful, because with enough good data, different adjustment factors can be applied to different locations to account for differences in the ratio of the positive-sequence impedance to the loop impedance.
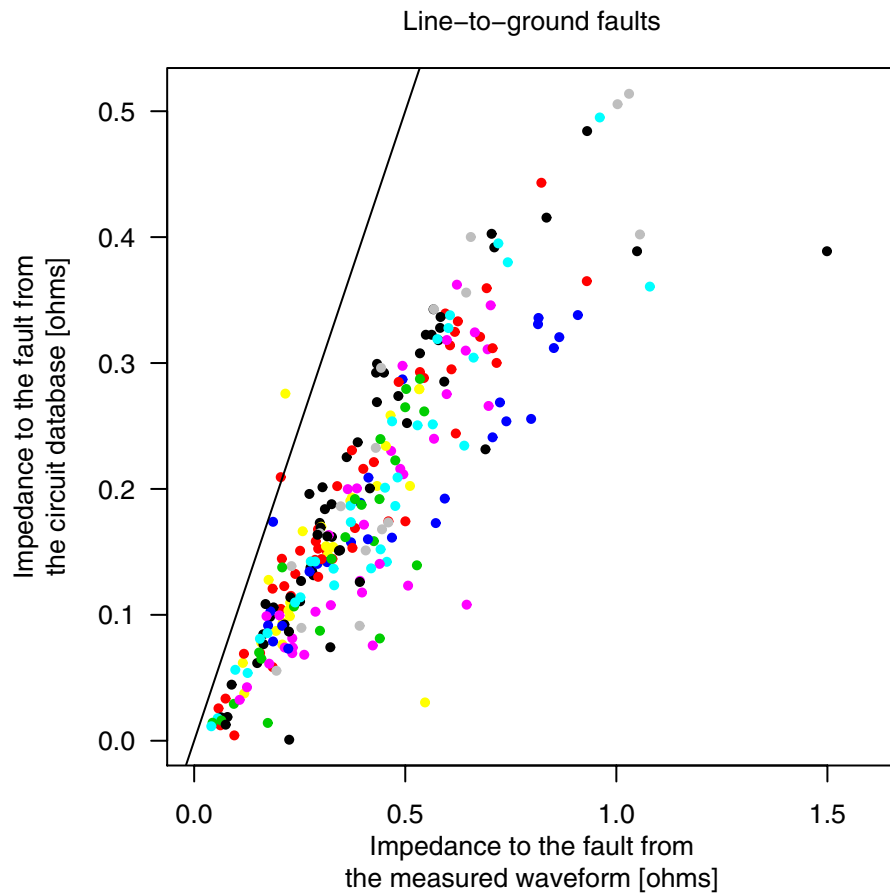
**Figure 4-9**
**Utility B: Impedance Estimated from the Waveform Versus Impedance to the Fault from the Circuit Database**

Figure 4-10 shows a similar graph for double line-to-ground faults. The dispersion is wider, but that is not unexpected given the difficulty of separating the high load current from the fault current.
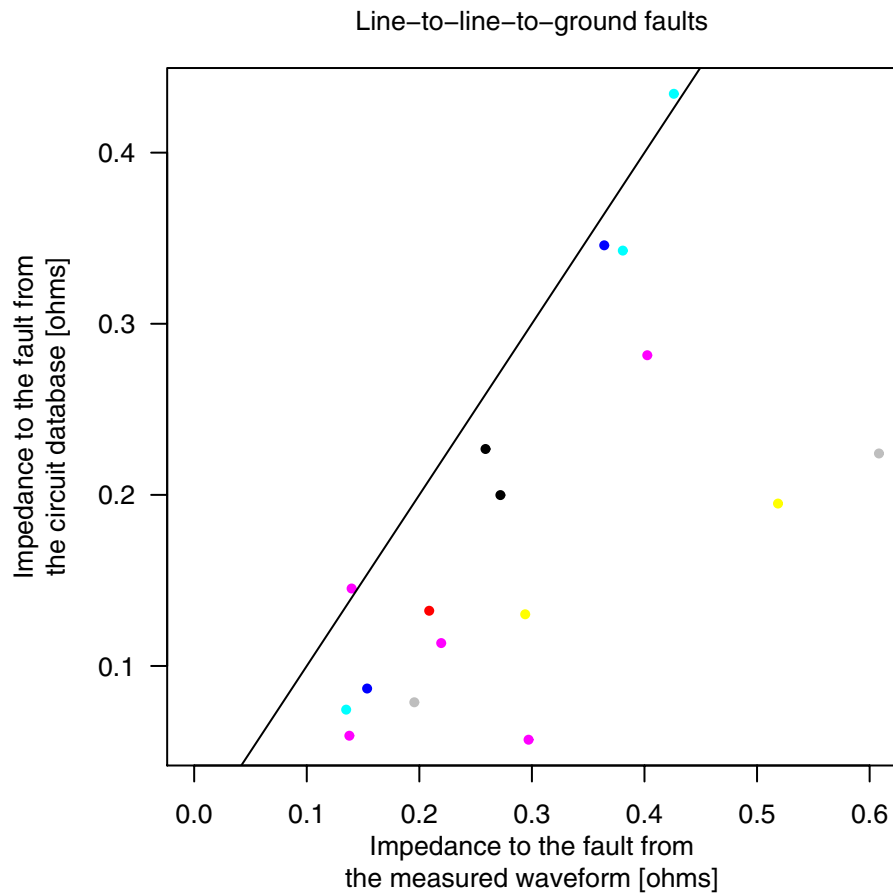
**Figure 4-10**
**Utility B: Impedance Estimated from the Waveform Versus Impedance to the Fault from the Circuit Database**

A further evaluation was done to try and improve the location. Figure 4-11 shows the reactance to the fault as used by Stergiou [36, 37]. This shows a more linear relationship. Also, the fault type is shown by different colors. Many of the outliers are transformer faults (labeled "TRAN").

Measured fault impedance versus impedance from the circuit database
Line–to–line–to–ground faults
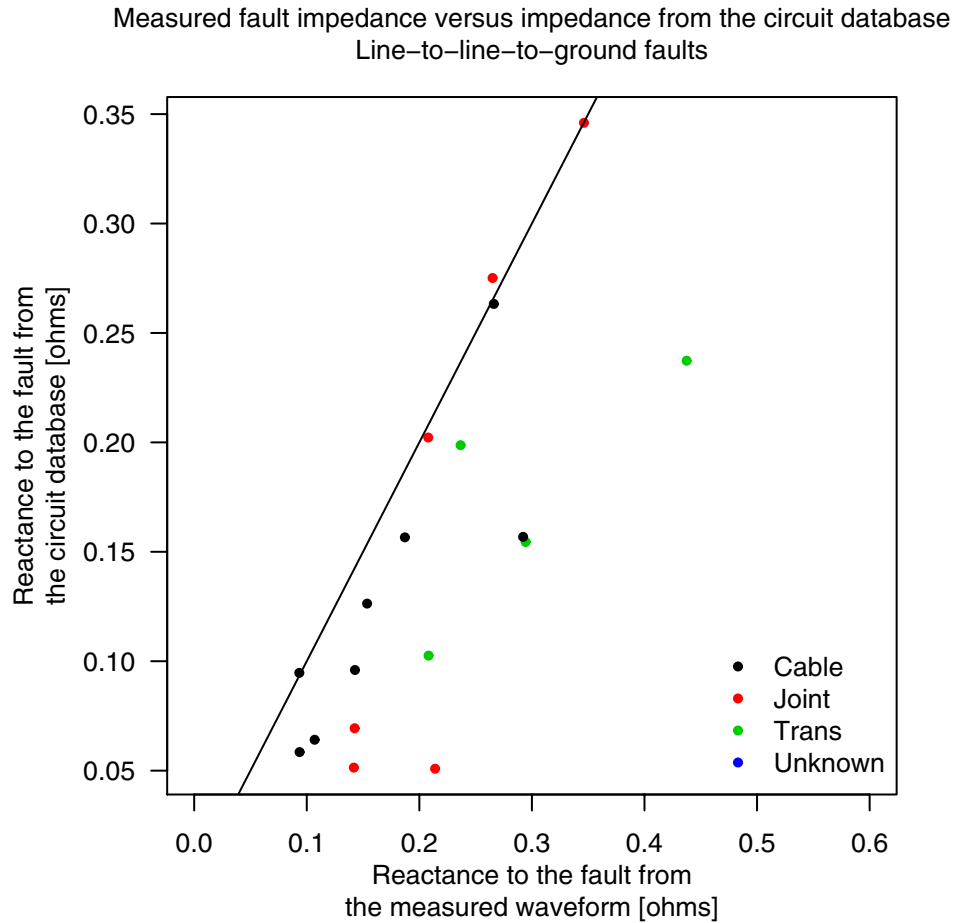
**Figure 4-11**
**Utility B: Reactance Estimated from the Waveform Versus Reactance to the Fault from the Circuit Database**

Figure 4-12 shows another comparison for three-phase faults. With three-phase faults, the impedances compared are both the positive-sequence impedance. Separating load and fault current is again a difficulty. Although there are a number of outliers, there is at least significant correlation.
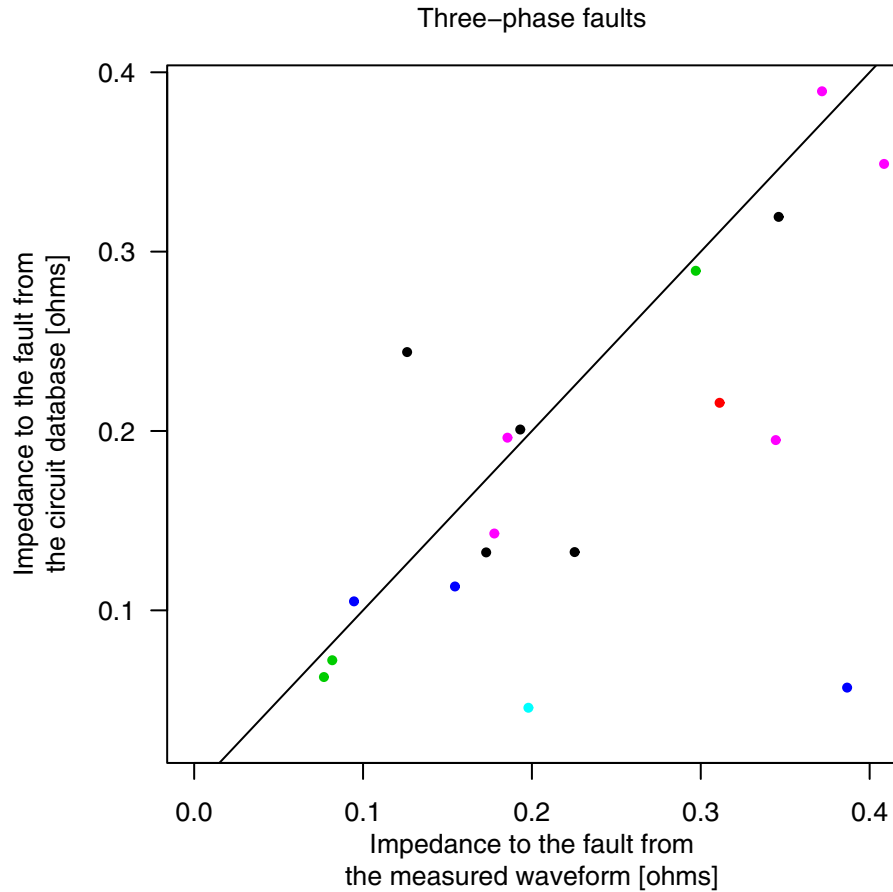
**Figure 4-12**
**Utility B: Impedance Estimated from the Waveform Versus Impedance to the Fault from the Circuit Database**

Table 4-4 and Table 4-5 summarize linear and quantile models applied to several fault location algorithms with line-to-ground faults. As with utility A, all performed relatively well. Because there was significant difference from site to site (presumably because the ratio of the positive-sequence to the zero-sequence changes), it is expected that given sites could be tuned to give more consistent results.

**Table 4-4**
**Linear Model of Several Fault-Location Algorithms**

| Fault Location Algorithm | Percent Failed | K | $R^2$ |
|---|---|---|---|
| Absolute value of impedance (Z) | 0 | 0.427 | 0.908 |
| Reactance to the fault (X) | 0 | 0.468 | 0.828 |
| Fault current magnitude | 0 | 0.765 | 0.944 |
| Voltage sag | 0.8 | 0.358 | 0.930 |
| Takagi | 0 | 0.787 | 0.924 |
| Impedance with a nonlinear arc | 0 | 0.499 | 0.947 |

**Table 4-5**
**Median and Quantile Models of Several Fault-Location Algorithms**

| Fault Location Algorithm | Median | Lower 10% | Upper 10% | Lower 25% | Upper 25% |
|---|---|---|---|---|---|
| Absolute value of impedance (Z) | 0.481 | 0.664 | 1.21 | 0.784 | 1.12 |
| Reactance to the fault (X) | 0.576 | 0.668 | 1.30 | 0.807 | 1.15 |
| Fault current magnitude | 0.828 | 0.724 | 1.22 | 0.886 | 1.09 |
| Voltage sag | 0.383 | 0.590 | 1.25 | 0.804 | 1.14 |
| Takagi | 0.766 | 0.636 | 1.36 | 0.823 | 1.21 |
| Impedance with a nonlinear arc | 0.522 | 0.694 | 1.24 | 0.852 | 1.11 |

Figure 4-13 shows results graphically for several fault-location algorithms. Based on the fitted models and the graphical results, the nonlinear arc model and the absolute value of impedance appear to be the most reliable models.
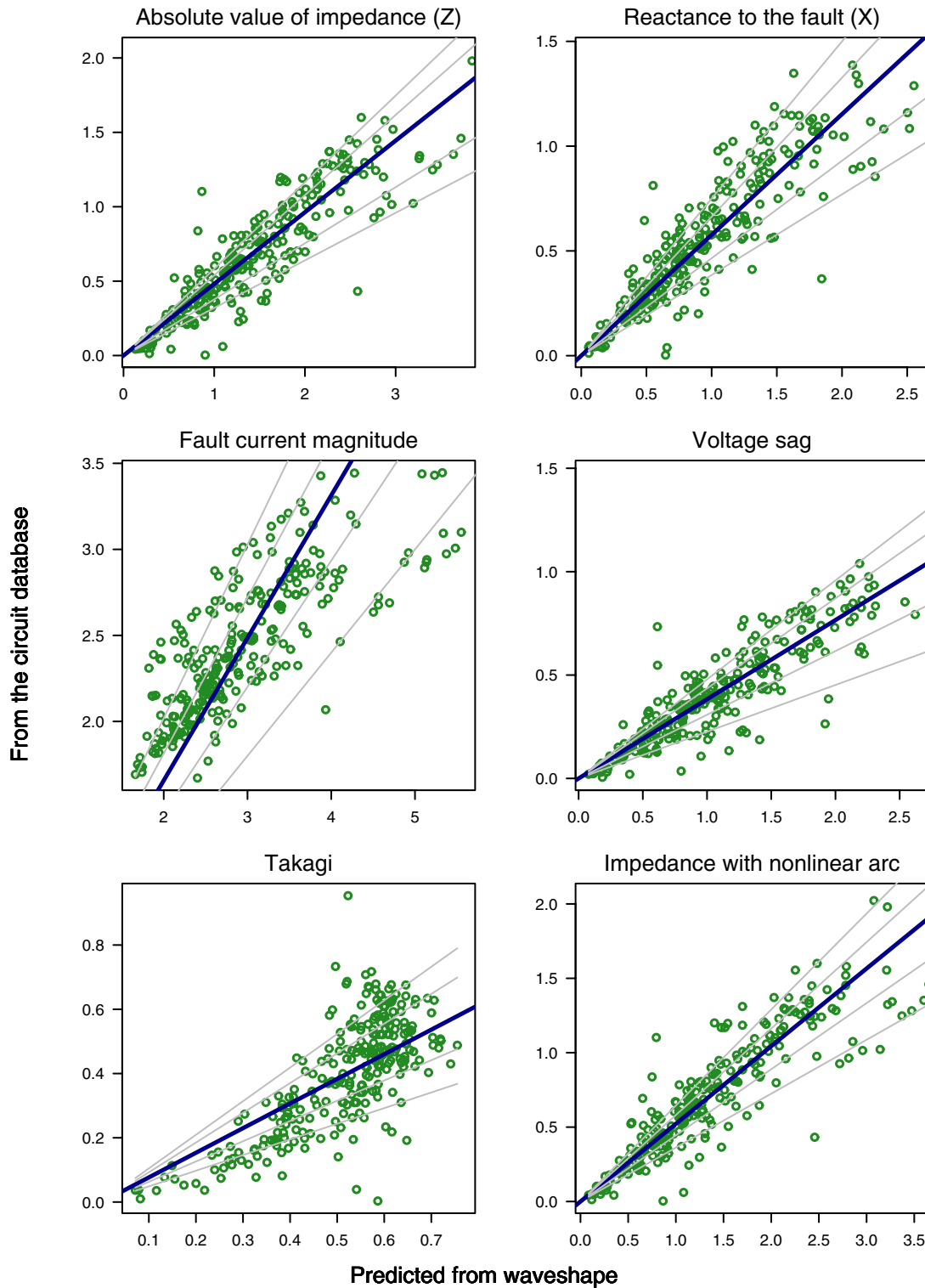
**Figure 4-13**
**Actual Versus Measured Parameters for Several Fault-Location Algorithms**

## Utility C

Utility C provided several outage and fault events on circuits at two substations. The details of the model include:

- 23 fault events in the dataset

- Bus-level power-quality monitors

  - 128 samples per cycle

- Urban

- 12.5 kV

- Stoner SynerGEE circuit data model

Figure 4-14 shows impedance to the fault versus impedance from the circuit database from the events in the dataset for utility C. This graph includes line-to-ground as well as multi-phase faults. For line-to-ground faults, the loop impedance is compared ($Z_s$), and for multi-phase faults, the positive-sequence impedance is compared ($Z_1$). The data has a good 1:1 fit. Most of the outliers have logical reasons for the "misses":

- Event #3 & 4: This is an unusual event that started on phase C, decayed, reignited on phase B, decayed, and again reignited and decayed on phase B (see Figure 4-15). This fault was caused by cables failing from a contractor dig-in.

- Event #7: Unknown.

- Event #17: The impedance on this one matches well, but the phase angle is way off for some unknown reason.

- Event #18: The outage is listed as being on one circuit, but the faulted portion is now connected to another circuit in the SynerGEE database.

- Event #20: This was only a 1.5-cycle event that started as two phases and jumped to three phases. It is difficult to get a full cycle for this event.

The monitor at substation B had only phase-to-phase voltage measurements. The neutral voltage was derived using the zero-sequence source impedance as discussed in Chapter 2. The location estimates at substation B seemed to be as accurate as those out of substation A which had line-to-neutral voltage monitoring.
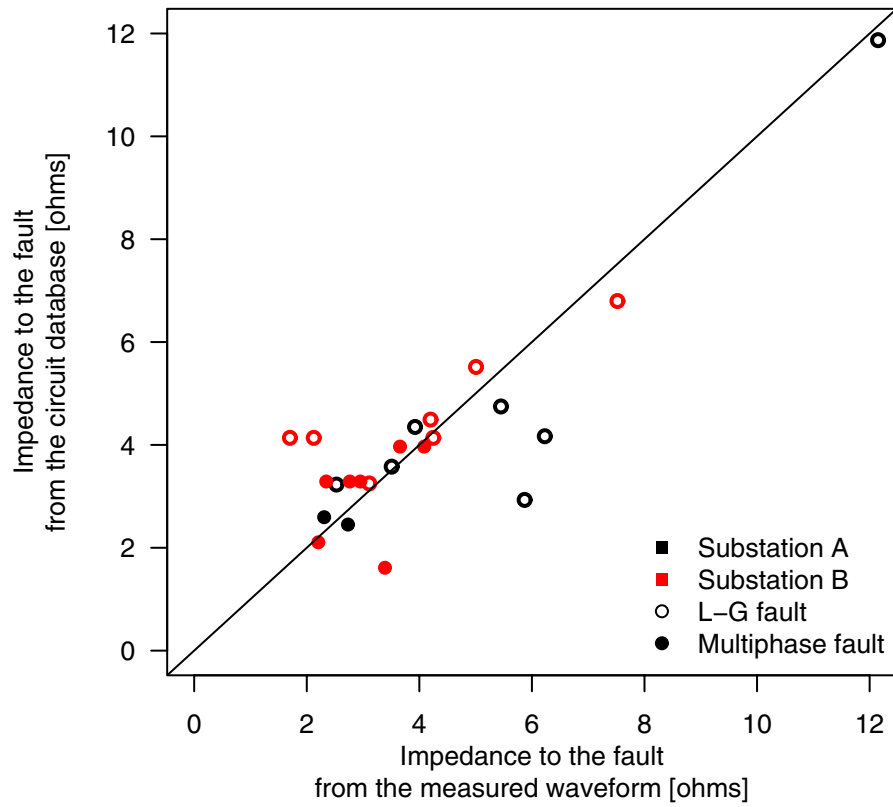
**Figure 4-14**
**Utility C: Impedance Estimated from the Waveform Versus Impedance to the Fault from the Circuit Database**

**Figure 4-15**
**Unusual Event Caused by a Dig-in**

## Utility D

Utility D provided data on several outages with waveforms recorded by SEL-251 and SEL-351 relays. All of the data was provided in four-samples per cycle filtered format, and some of the events were also available in 16-samples per cycle unfiltered format. The main characteristics of this dataset include:

- 10 fault events in the dataset
- Feeder-level SEL relays
  - 4 or 16 samples per cycle
- Mainly suburban/rural
- 13.2 and 25 kV
- ABB FeederAll circuit data model

Figure 4-16 shows comparisons of the impedance to the fault from the waveshape and from the circuit database to the known fault location. Line-to-ground faults and multiphase faults are shown. Both correspond well to a 1:1 ratio. Even most of the short-duration faults were identified reasonably well.



**Figure 4-16**
**Utility D: Impedance Estimated from the Waveform Versus Impedance to the Fault from the Circuit Database**

Utility D's relay data gives us a good chance to evaluate the internal fault location capability in the SEL relays as several of the relays had the fault-locating capability enabled. Figure 4-17 compares the impedance from the built-in location algorithm to that from the circuit database. The X-axis value in Figure 4-17 was obtained by taking the impedance settings of the relay (R1, X1, R0, and X0) and multiplying by the relay's estimate of distance and dividing by the line length setting in the relay (LL). At the five locations where fault locating was enabled, the built-in locating algorithm worked well.
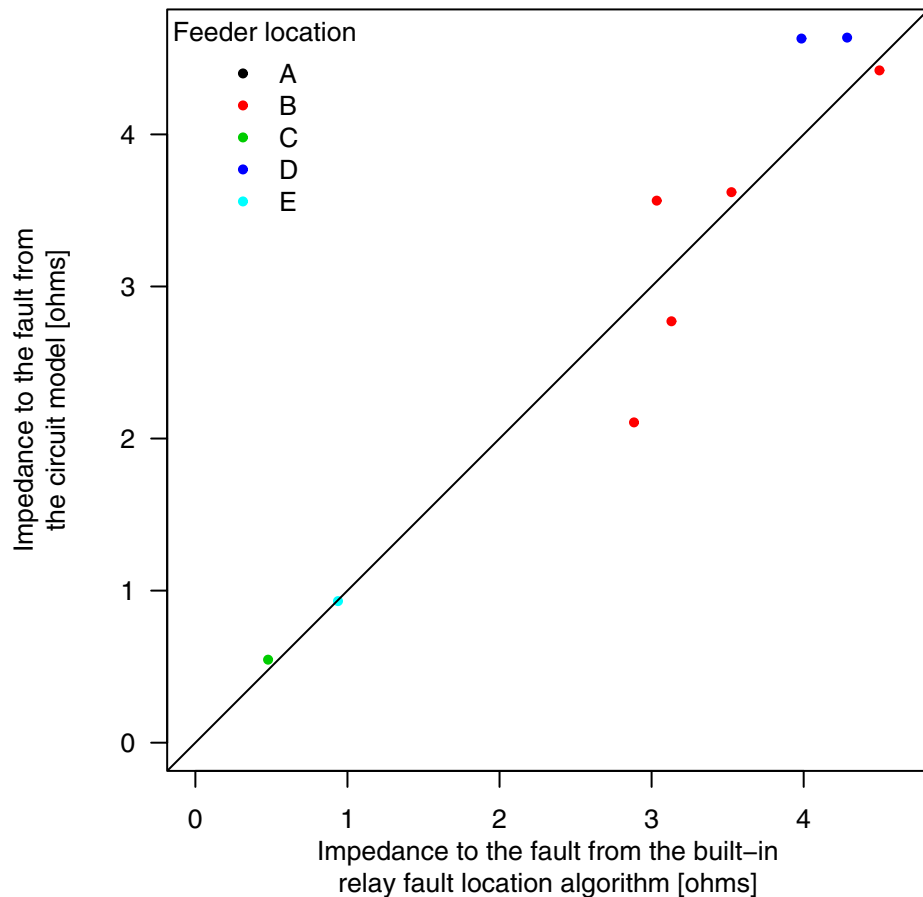


**Figure 4-17**
**Utility D: Impedance Estimated from the SEL Relay's Built-in Location Estimate Versus Impedance to the Fault from the Circuit Database**

## Utility E

Utility E provided several outages along with the corresponding fault event data. The main parameters of this dataset are:

- 32 fault events in the dataset

- Feeder-level substation SEL 251 and 351 relays

  – 16 samples per cycle

- SEL 651 recloser control

    – 32 samples per cycle

- DFA substation monitor

    – 256 samples per cycle

- Mainly suburban/rural

- 12.5 and 34.5 kV

- Cyme circuit data model

Figure 4-18 shows a comparison of the impedance to the fault from the circuit database to the impedance from the circuit model. Both line-to-ground faults and multiphase faults are included. Correlation was good except for a handful of short-duration events. On these events, the downloaded data had filtering enabled. The filtering can reduce the magnitude of the fault current and increase the apparent impedance (because *Z = V/I*).



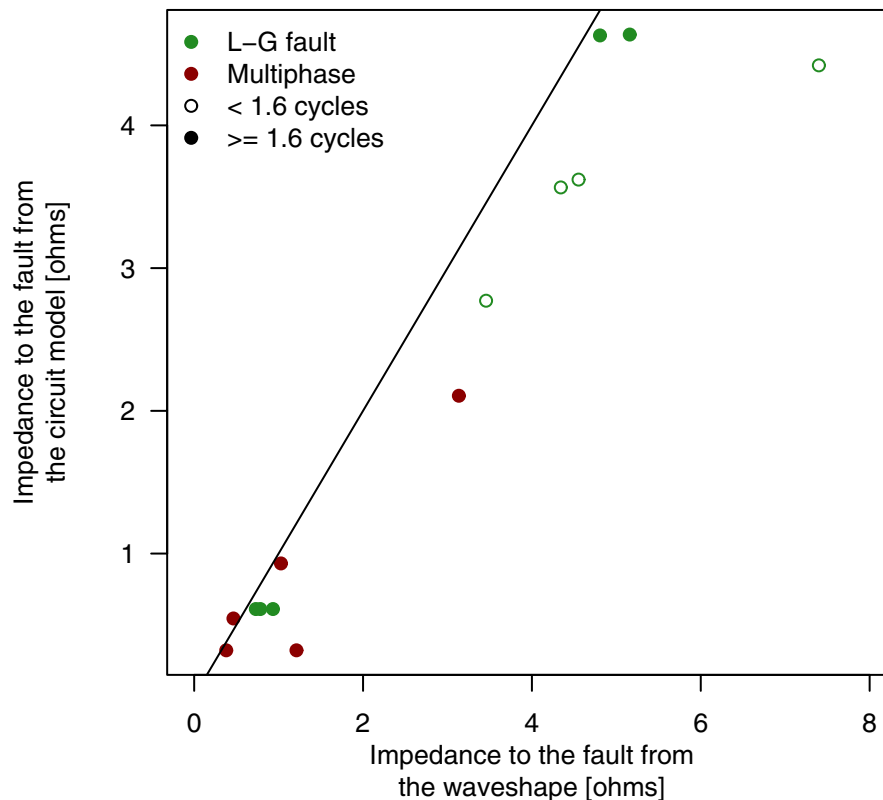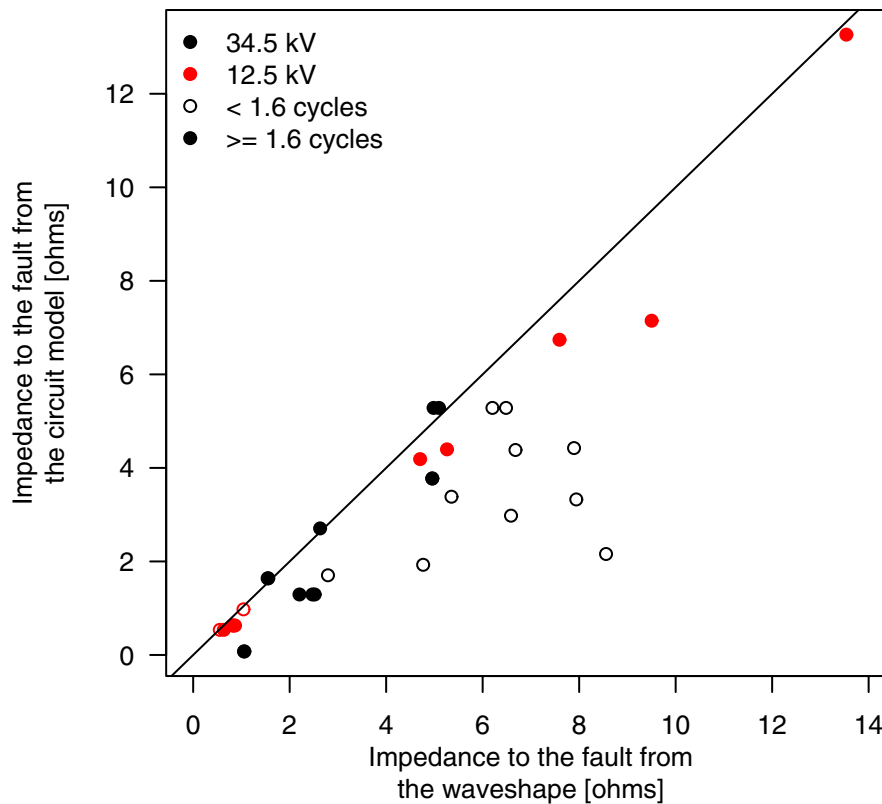**Figure 4-18**
**Utility E: Impedance Estimated from the Waveform Versus Impedance to the Fault from the Circuit Database**

## Utility F

Utility F provided a huge data set for analysis at all of their substations in one of their operating region. The main characteristics of the dataset for Utility F are:

- 1124 outage events in the dataset

- Feeder-level and bus-level substation RTU data acquisition units

  - 16 samples per cycle

- Mainly suburban/rural

- 12.5 and 23 kV

- Cyme circuit data model

This dataset arrived too late to do significant analysis on. Because it is such a large data set and because it contains both feeder monitors and bus-level monitors, it could provide additional insight on fault-location algorithms. This data will be analyzed in more detail in the 2007 project. Some subset of the 1124 outage events will be identified to make analysis easier. Each of these 1124 outages had a monitoring event associated (meaning it was on the same feeder within thirty minutes), but none have been manually reviewed to make sure that they matched.

## Utility G

Utility G provided a small set of data for analysis. The main characteristics of the dataset for Utility G are:

- 12 fault events in the dataset

- SEL-251 and SEL-351 relays

  - 4 samples per cycle

- Mainly suburban/rural

- 12.5 kV

- PTI PSS/Adept circuit data model

This dataset arrived too late to do any significant analysis on and some key part of the data were missing. This data will be updated and analyzed in more detail in the 2007 project. This data set helps increase the number of relay events we have plus, it is the first data we have in the PSS/Adept format.

# 5
# IMPACT OF FAULT ARC VOLTAGE

## Background

One of the surprising and important outcomes of this project is that it is possible to use monitoring waveforms to predict the arc voltage during an arc. Knowing the arc voltage may help improve fault location estimates and has the potential to help in other ways.

Good fault location can be done by assuming a bolted fault—no fault arc resistance. The reactance-to-fault method used by Con Edison and the fault-current method used by Progress Carolina assume a bolted fault (but the reactance-to-fault method attempts to bypass the fault resistance by only considering the reactive part). Results from the EPRI fault study published in the early 1980s showed that actual fault currents were close to the calculated value [3, 7]. The EPRI report found that calculated fault currents were approximately 2% higher than the measured value. Therefore, we assume that fault resistance cannot play a drastic role, but some faults may have enough arc voltage to make the bolted-fault assumption less accurate than desired.
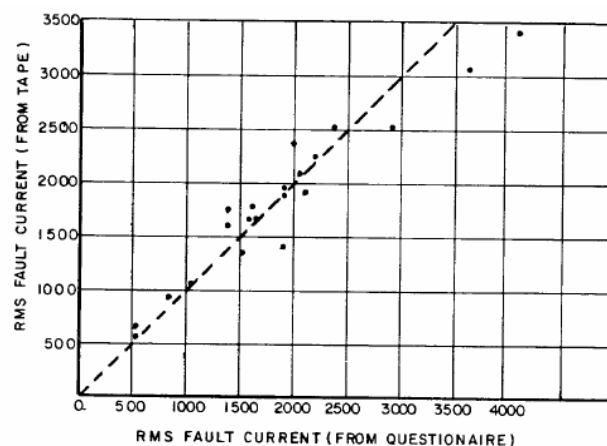


**Figure 5-1**
**Calculated Versus Measured Fault Currents from the EPRI Distribution Fault Study**

**Source**: EPRI 1209-1, *Distribution Fault Current Analysis*. Electric Power Research Institute, Palo Alto, CA: 1983.

Figure 5-2 shows various arcs recorded during the EPRI Distribution Power Quality (DPQ) study. Arcs are generally resistive (the short-circuit current is in phase with the arc voltage), but it is a nonlinear resistance. Arcs tend to be a square wave because the voltage tends to be constant regardless of current.

It is generally more convenient to talk about arc voltage rather than arc resistance. In air, arcs have about 400 V per foot of arc length.
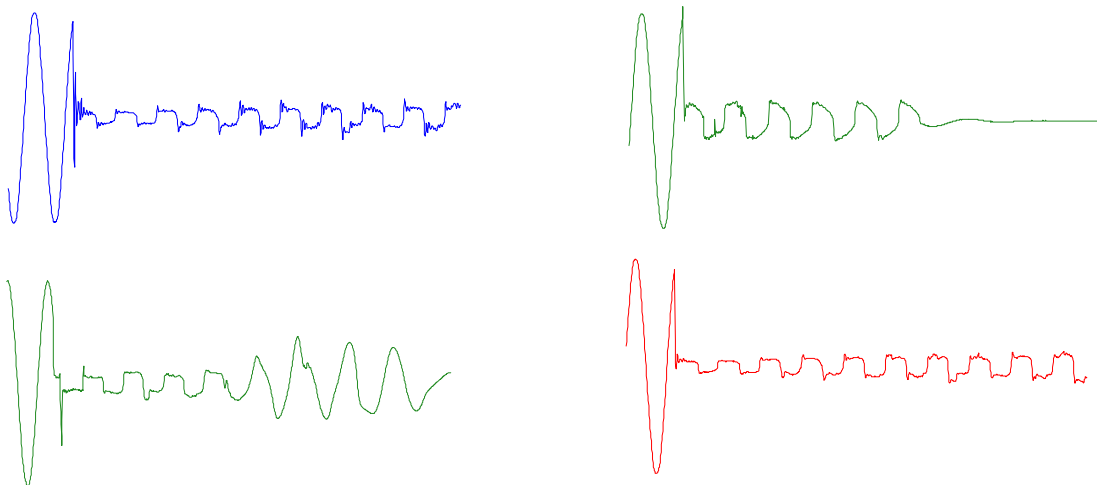


**Figure 5-2**
**Arc Voltages Measured by Feeder Monitors in the EPRI DPQ Study**

Being able to estimate the arc voltage could help utilities in several ways:

* *Improving fault location algorithms*—Of most interest for this report, accounting for the impact of arc voltages can possibly improve the accuracy of fault locations.

* *Estimating arc power and energy*—Equipment explosions, manhole explosions, and arc flash are fundamentally a function of the power and energy in an arc. Monitoring can provide better knowledge of arc energies in these situations. Monitoring to estimate arc energies can be used to develop better estimates of safety hazards, design arc flash boundaries or clothing requirements, or help perform failure forensics.

* *Fault type estimation*—It may be possible to use the arc voltage to help differentiate between different types of faults. Preliminary data shows a marked difference between splice failures and cable failures. It may also help to differentiate between tree faults and lightning for example. Such knowledge can help field crews when searching for faults.

## Arc Theory

Many distribution faults involve arcs through the air, either directly through the air or across the surface of hardware. Although a relatively good conductor, the arc is a very hot, explosive fireball that can cause further damage at the fault location (including fires, wire burndowns, and equipment damage). This section discusses some of the physical properties of arcs along with how arcs can cause damage.

Normally, the air is a relatively good insulator, but when heavily ionized, the air becomes a low-resistance conductor. An arc stream in the air consists of highly ionized gas particles. The arc ionization is due to *thermal* ionization caused by collisions from the random velocities of particles (between electrons, photons, atoms, or molecules). Thermal ionization increases with increasing temperature and with increasing pressure. The heat produced by the current flow ($I^2R$) maintains the ionization. The arc stream has very low resistance because there is an abundance of free, charged particles, so current flow can be maintained with little electric field. Another type, ionization caused by acceleration of electrons from the electric field, may initially start the ionization during the electric-field breakdown; but once the arc is created, electric-field ionization plays a less significant role than thermal ionization.

One of the characteristics that is useful for estimating arc-related phenomenon is the arc voltage. The voltage across an arc remains constant over a wide range of currents and arc lengths, so the arc resistance decreases as the current increases. The voltage across an arc ranges between 25 and 40 V/in (10 to 16 V/cm) over the current range of 100 A to 80 kA [15, 38]. The arc voltage is somewhat chaotic and varies as the arc length changes. More variation exists at lower currents. As an illustration of the energy in an arc, consider a 3-in (7.6-cm) arc that has a voltage of about 100 V. If the fault current is 10 kA, the power in the arc is P = V ˙ I = 100 V ˙ 10 kA = 1 MW. Yes, 1 MW! Arcs are explosive and as hot as the surface of the sun.

An upper bound of roughly 10,000 to 20,000 K on the temperature of the arc maintains the relatively constant arc voltage per unit length. For larger currents, the arc responds by increasing the volume of gas ionized (the arc expands rather than increasing the arc-stream temperature). Higher currents increase the cross-sectional area of the arc, which reduces the resistance of the arc column—the current density is the same, but the area is larger. So, the voltage drop along the arc stream remains roughly constant. The arc voltage depends on the type of gas and the pressure. One of the reasons an arc voltage under oil has a higher voltage gradient than an arc in air is because the ionizing gas is mainly Hydrogen, which has a high heat conductivity. A high heat conductivity causes the arc to restrict and creates a higher-density current flow (and more resistance). The arc voltage gradient is also a function of pressure. For arcs in Nitrogen (the main ionizing gas of arcs in air), the arc voltage increases with pressure as $V \propto P^k$ where *k* is approximately 0.3 [4].

Another parameter of interest is the arc resistance. A 3-ft (1-m) arc has a voltage of about 1400 V. If the fault current at that point in the line was 1000 A, then the arc resistance is about 1.4 Ω. A 1-ft (0.3-m) arc with the same fault current has a resistance of 0.47°Ω. Most fault arcs have resistances of 0 to 2 Ω.

An arc voltage waveform has distinguishing characteristics. Figure 5-2 shows several voltages on several arcing faults measured during the EPRI DPQ project. The voltage on the arc is in phase with the fault current (it is primarily resistive). When the arc current goes to zero, the arc will extinguish. The recovery voltage builds up quickly because of the stored energy in the system inductance—the voltage builds to a point and causes arc reignition. The reason for the blip at the start of the waveform (it is not a straight square wave) is that the arc cools off at the current zero. Cooling lowers the ionization rate and increases the arc resistance. Once it heats up again, the voltage characteristic flattens out. The waveform is high in the odd harmonics and for many purposes can be approximated as a square wave.

The movement and growth of an arc is primarily in the vertical direction. Tests at IREQ in Quebec showed that the primary reason that the arc elongates and moves vertically is the rising hot gases of the arc [6]. The magnetic forces (*J*×*B*) did not dominate the direction or elongation.

The temperature in the arc can be on the order of 10,000 K. This heat creates hazards from burning and from the pressure wave developed during the fault. The longer the arc, the more energy is created. NFPA provides guidelines on safe distances for workers based on arc blasts. Arcs can cause fires: pole fires or fires in oil-filled equipment such transformers.

Although many electrical damage characteristics are a function of $\int I^2 \, dt$, the pressure wave is primarily a function of $\int I \, dt$ (because the voltage along the arc length is constant and relatively independent of the arc current). Where arcs attach to wires, melting weakens wires and can lead to wire burndown. Most tests have shown that the damage is proportional to $\int I^k \, dt$, where *k* is near one but varies depending on the conductor type. For burndowns or other situations where the arc burns the conductor, the total length of the arc is unimportant, the small portion of the arc near the attachment point is important. The voltage drop near the attachment point is also very constant and does not vary significantly with current. The damage to conductors is very much like that of an electrical arc-cutting torch.

Distribution voltages can sustain very long arcs, but self-clearing faults can occur such as when a conductor breaks and falls to the ground (stretching an arc as it falls). The maximum arc length is important because the longer the arc, the more energy is in the arc. For circuits with fault currents on the order of 1000 A and where the transient rise to the open-circuit voltage is about 10 μs, about 50 V may be interrupted per centimeter of arc length (Slepian [35]). For a line-to-ground voltage of 7200 V, a line-to-ground arc can get to a length of about 12 feet (3.7 m) before it clears. As another approximation, the length that an arc can maintain in resistive circuits is (from Rizk and Nguyen [28] with some reformulation):

$$l = V\sqrt{I}$$

where,

    *l*   =   arc length, in (1 in = 2.54 cm)

    *I*   =   rms current in the previous half cycle, A

    *V*   =   system rms voltage, kV (line to ground or line to line depending on fault type)

## Theory Behind Arc Voltage Estimation

European researchers initially developed arc voltage estimation as a way to try and determine if a transmission-line fault was temporary or permanent (Radojevic et al. [24-26]). They assumed that permanent faults would have little arc voltage, and temporary faults have more significant arc voltage. Their approach relied on the approximation that the arc voltage was a square wave (Figure 5-3).
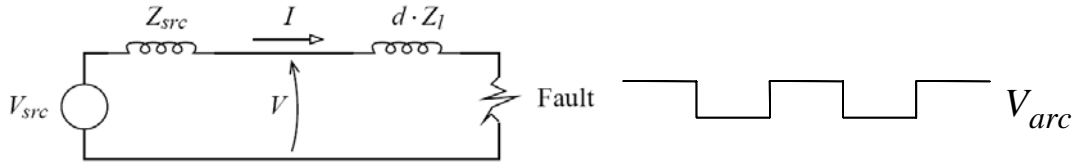
**Figure 5-3**
**Arc Voltage Estimation**

Once the square-wave assumption is made, we can estimate arc voltage from the point-by-point monitoring waveforms as follows:

$$V = R \cdot I + L \cdot \mathrm{d}I/\mathrm{d}t + V_{arc} \cdot \mathrm{sign}(I)$$

This is an overdetermined system. If we use 128 points over one cycle, that gives us 128 equations and three unknowns ($R$, $L$, and $V_{arc}$). It assumes that the arc voltage is a square wave in phase with the line current. This approach follows that developed by Radojevic et al. They developed their methodology for transmission lines, but it applies well to distribution circuits. They developed and tested their methodology mainly using EMTP transient simulations. The large number of fault events collected during this study has given us a significant opportunity to test and develop this approach with real data from distribution monitors.

Two enhancements were needed to make the approach of Radojevic et al work more consistently with monitoring data:

1. The derivative of current ($\mathrm{d}I/\mathrm{d}t$) was estimated with smoothing splines. Just using trapezoidal approximation ($i_{k+1} - i_{k-1}$)/2$\Delta$t resulted in far too much noise that dominated the result.

2. A constrained minimization approach was used to solve the overdetermined system. The error squared was minimized as suggested by Radojevic et al., but the solution parameters ($R$, $L$, and $V_{arc}$) were constrained to be positive using a quadratic programming solution.

## DPQ Verification of Arc Voltage Estimation

EPRI's Distribution Power Quality (DPQ) project recorded power quality in distribution substations and on distribution feeders measured on the primary at voltages from 4.16 to 34.5 kV (EPRI TR-106294-V2 and EPRI TR-106294-V3 [8, 9]). Two hundred seventy seven sites resulted in 5691 monitor-months of data. In most cases three monitors were installed for each randomly selected feeder, one at the substation and two at randomly selected places along the feeder.

The EPRI DPQ study monitored many distribution feeders with three monitors on each circuit. We verified the arc voltage estimation by estimating the arc voltage at the substation monitor with that of a downstream monitor that more directly estimated the voltage across the arc. The following graphs compare the estimated arc voltage to the measured arc voltage.

Figure 5-4 shows a fault measured at substation, and Figure 5-5 shows the same event measured at a downstream feeder location. The downstream feeder location is just barely upstream of the fault. The arc voltage in Figure 5-5 has the classic square wave arc voltage shape. Figure 5-6 compares the estimates of arc voltage based on the substation monitor with the actual measurement of the arc voltage from the downstream feeder site. The estimate is quite close and captures the important aspects of the event: the arc voltage magnitude and the fact that it increases during the event (presumably, the arc is elongating).
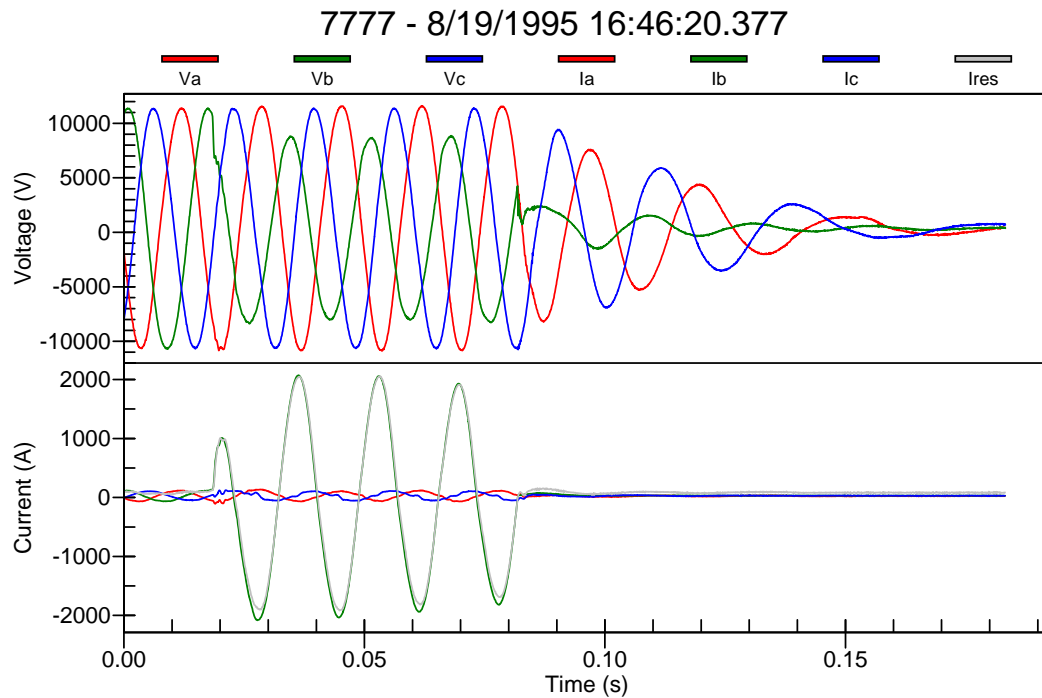


**Figure 5-4**
**Substation Monitoring of an Event from the EPRI DPQ Database**

Figure 5-7 shows similar comparisons with three other faults at different locations in the DPQ study. All show good estimation. The last of the three events does show significant deviation during the first two cycles of the fault. This is due to a saturated current waveform that appears as a transient on the last portion of the square-wave arc waveform. Once the dc offset decayed and the saturation finished, the arc voltage estimate matched well with the downstream measurement.
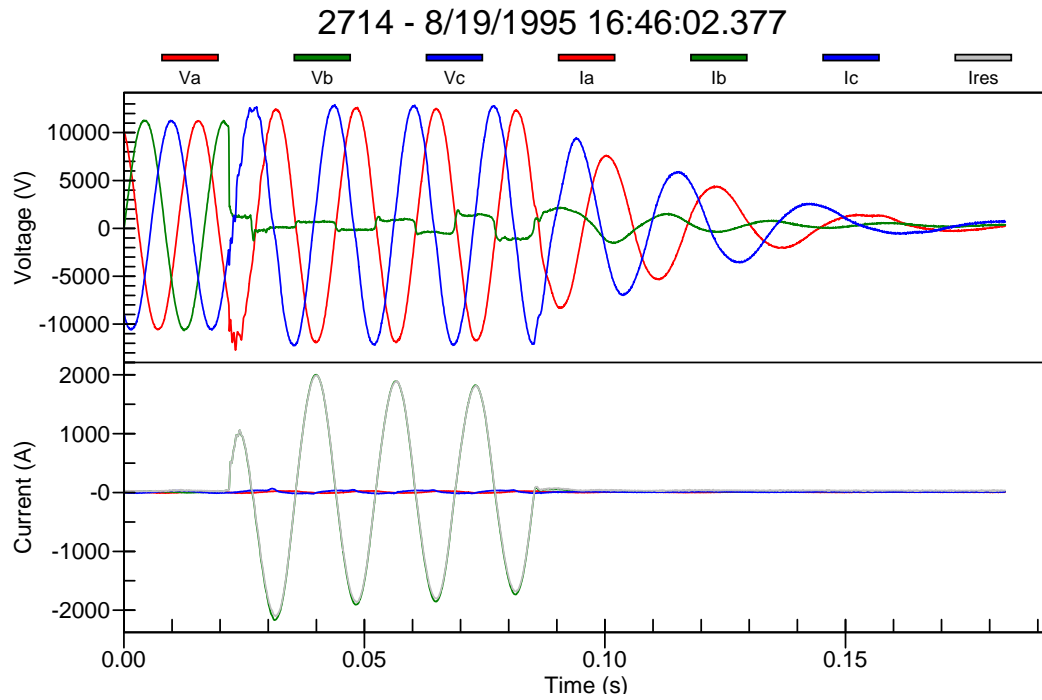
**Figure 5-5
Downstream Feeder Monitor Results for the Same Event**
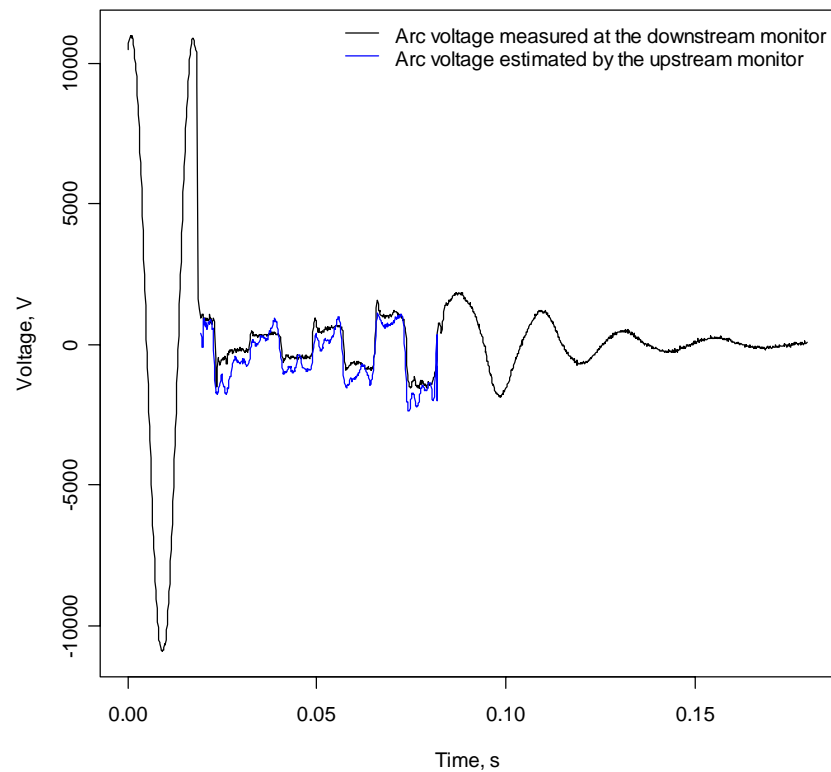


**Figure 5-6
Comparing the Arc Voltage Estimate from the Substation Data With the Measured
Arc Voltage**
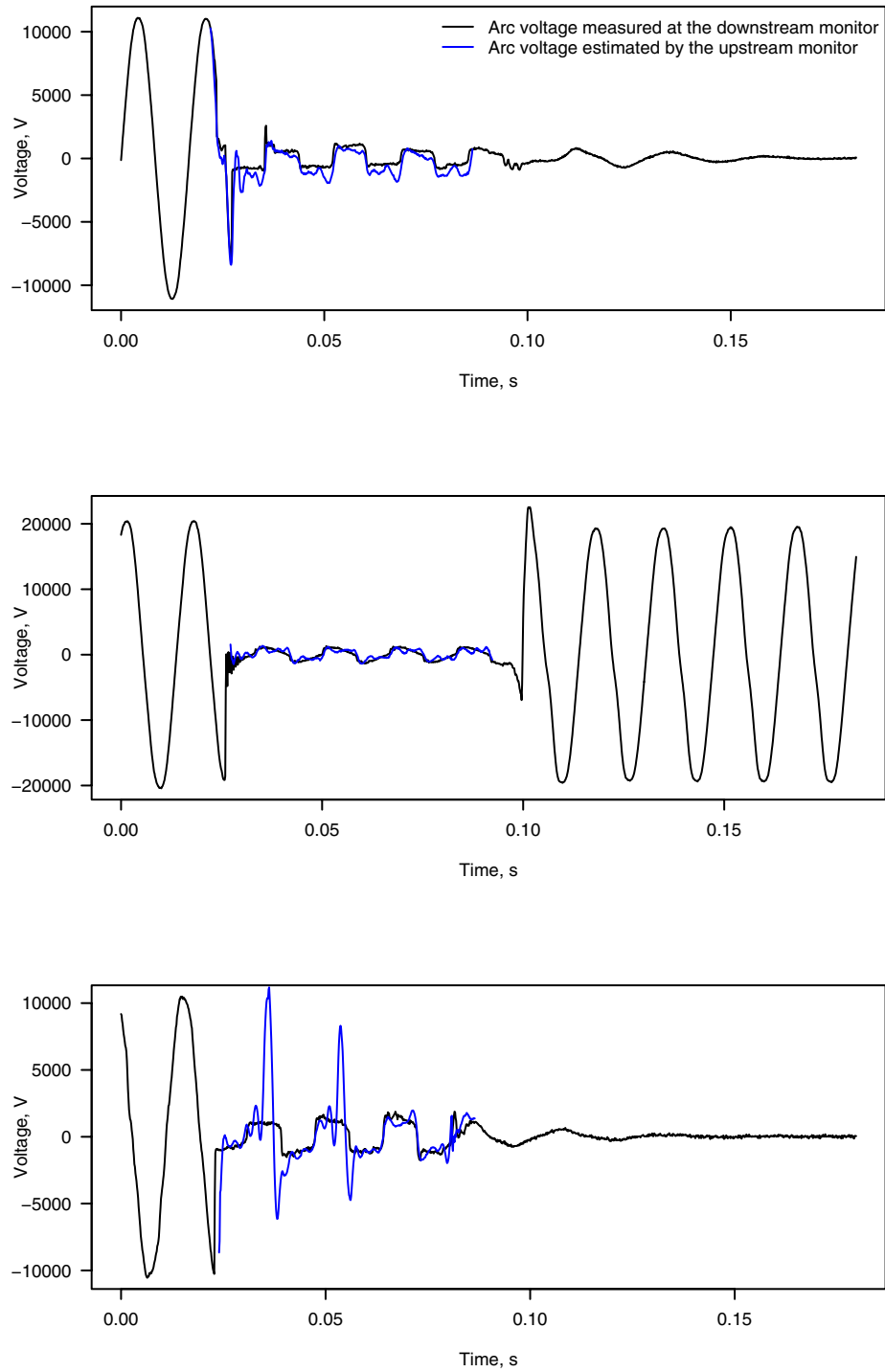
**Figure 5-7**
**Comparing Arc Voltages With Estimates from Feeder Monitors for Three Different Events (EPRI DPQ Study)**

## Impact on Fault-Location Accuracy

As shown in Chapter 4 for both utilities A and B, the fault-location approach assuming a nonlinear arc voltage was one of the better models. It was not dramatically better, but it was one of the best. Further work is needed to evaluate performance on more data and more monitoring types.

## Arc Voltage Estimates

The arc voltage estimate from the nonlinear arc model is useful is several ways. It could help with accident investigations, equipment failure forensics, and developing guidelines for arc flash protection and other hazards related to the power and energy created by the arc. Figure 5-8 shows the distribution of arc voltages for faults at Utility A. The median arc voltage is about 600 V, and about 20% of events have an arc voltage of over 1200 V. In open air, 1200 V corresponds to an arc length of about three feet.
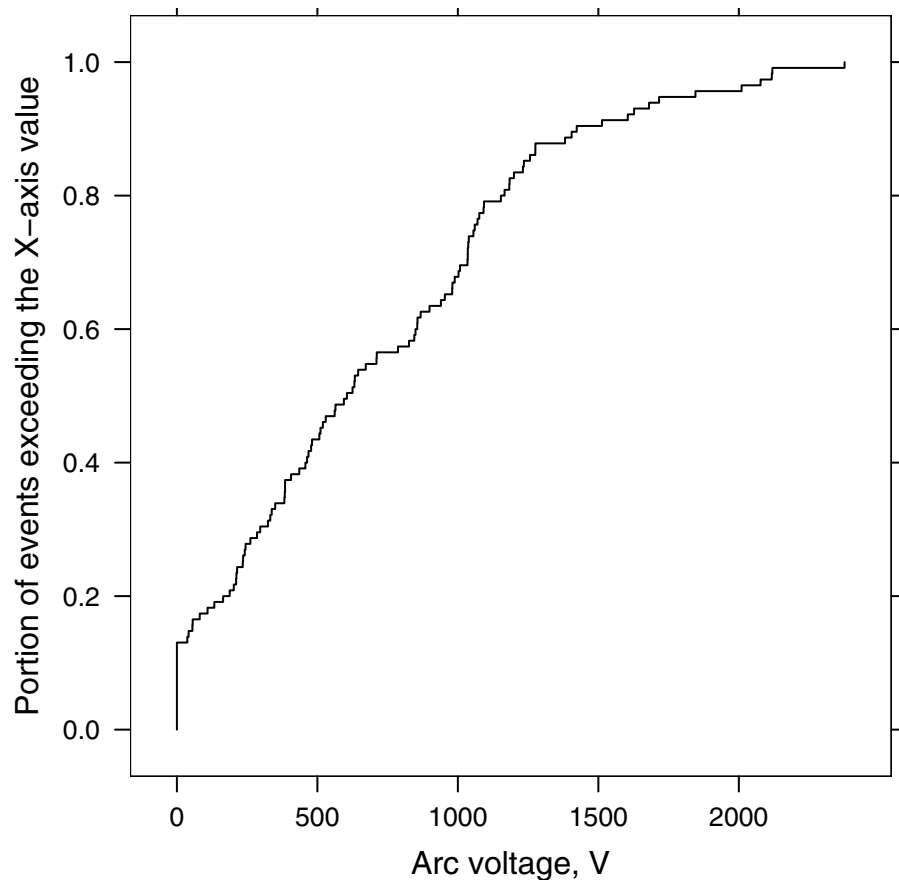


**Figure 5-8**
**Estimates of Arc Voltage (Utility A – a Mainly Overhead Utility)**

Figure 5-9 shows the same arc voltage data broken down by fault cause. Some causes stand out as having a higher-than-normal or lower-than-normal arc voltage. Cables generally have low arc voltage when faulted. Trees, animals, and conductors off the pin—all are scenarios that can lead to a long arc through the air.
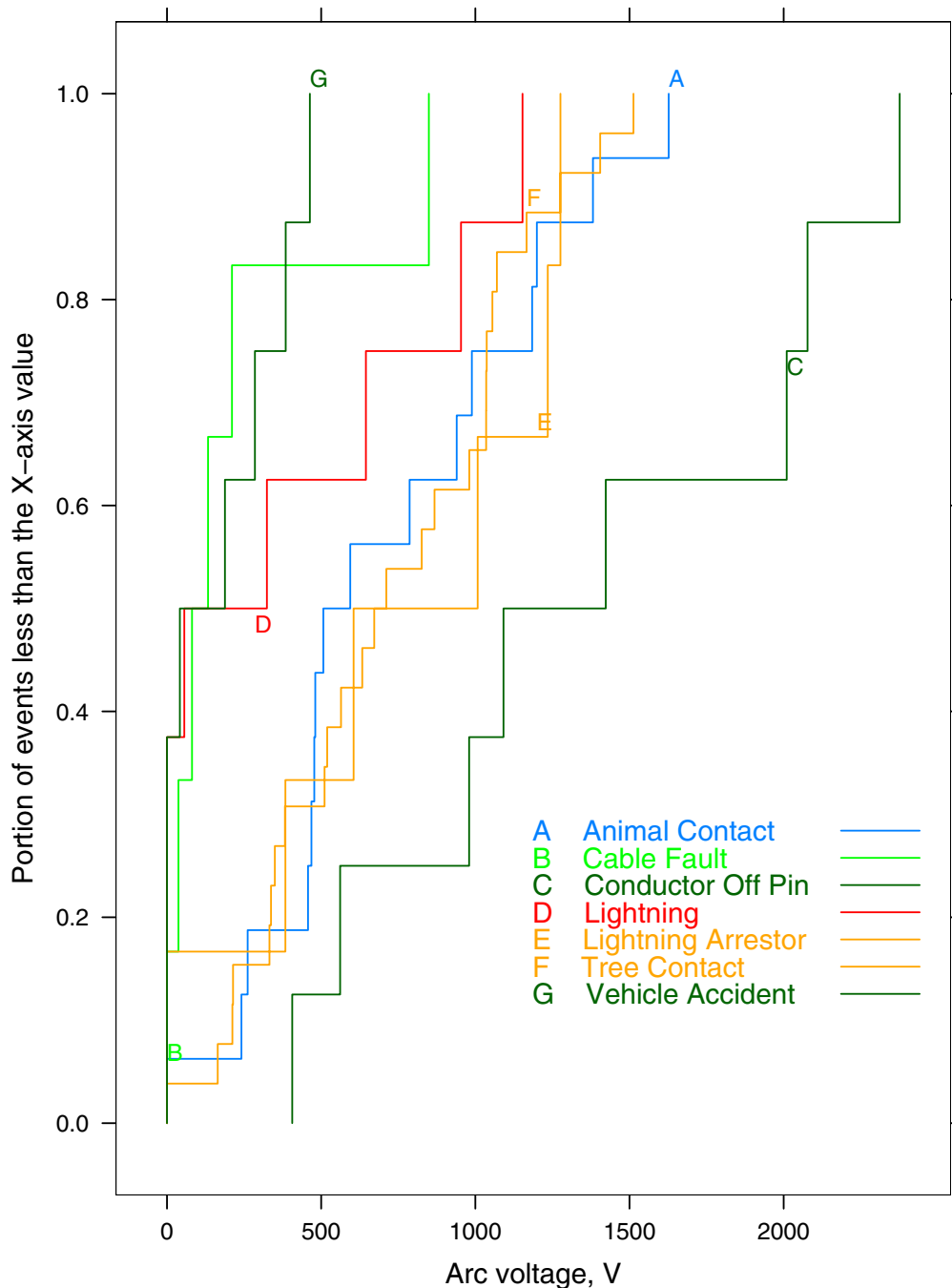


**Figure 5-9**
**Estimates of Arc Voltage by Fault Cause (Utility A)**

Figure 5-10 shows a distribution of arc voltages at a mainly underground utility (Utility B). The shape of the distribution and the range of arc voltages is surprisingly similar to Utility A. The median arc voltage is near 300 V, and 90% of arc voltages are greater than 1200 V.
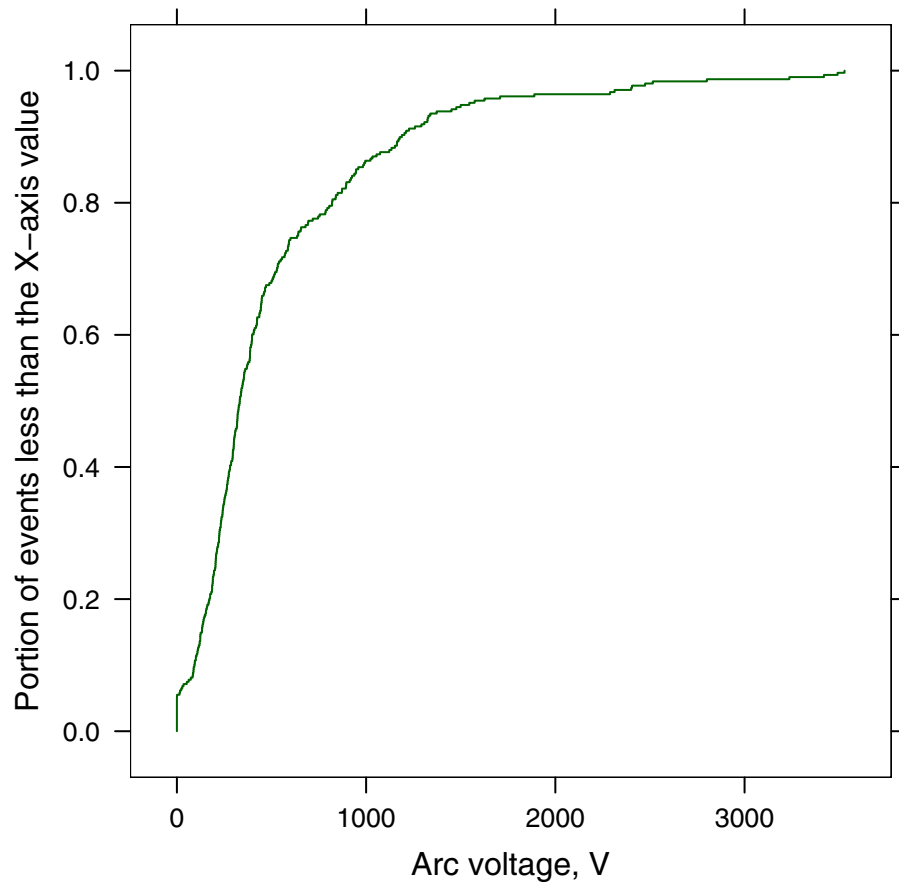
**Figure 5-10**
**Estimates of Arc Voltage (Utility B – a Mainly Underground Utility)**

The arc voltages on the underground primary showed significant differences between joints, cables, and transformers (see Figure 5-11). Figure 5-12 shows that joints have significant difference between solid joints, stop joints, and paper joints. This corresponds well with tests done by Hydro Quebec on cable and splice failures reported by Koch and Christophe [20]. They found low arc voltages on both PILC cables and splices and higher voltages from XLPE cables and premolded splices. The differences in arc voltage probabilities could be used to aid in fault location. Events with high arc voltage could signal joint failures, and this could be quantified using probabilities. This may aid crews in searching for faults.
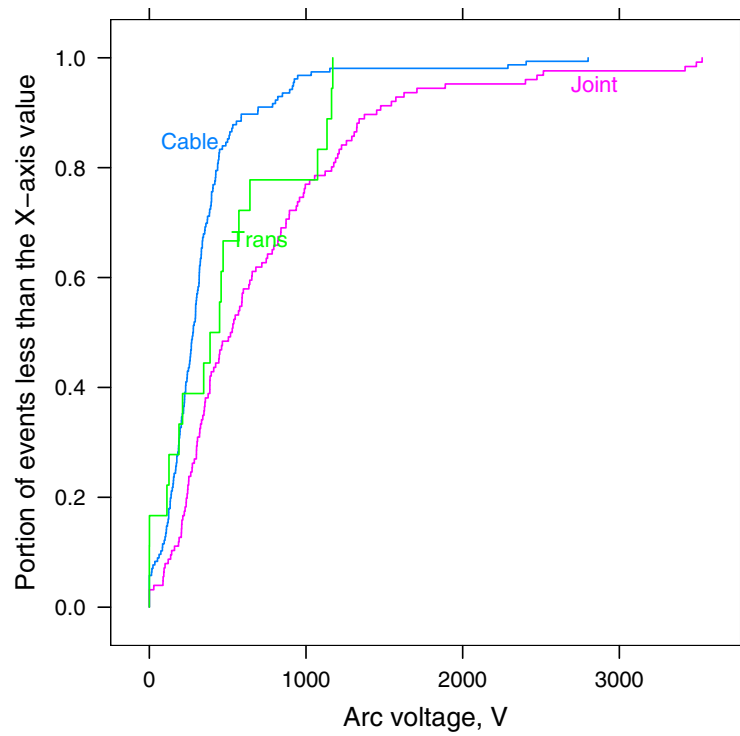
**Figure 5-11**
**Estimates of Arc Voltage by Fault Type (Utility B)**
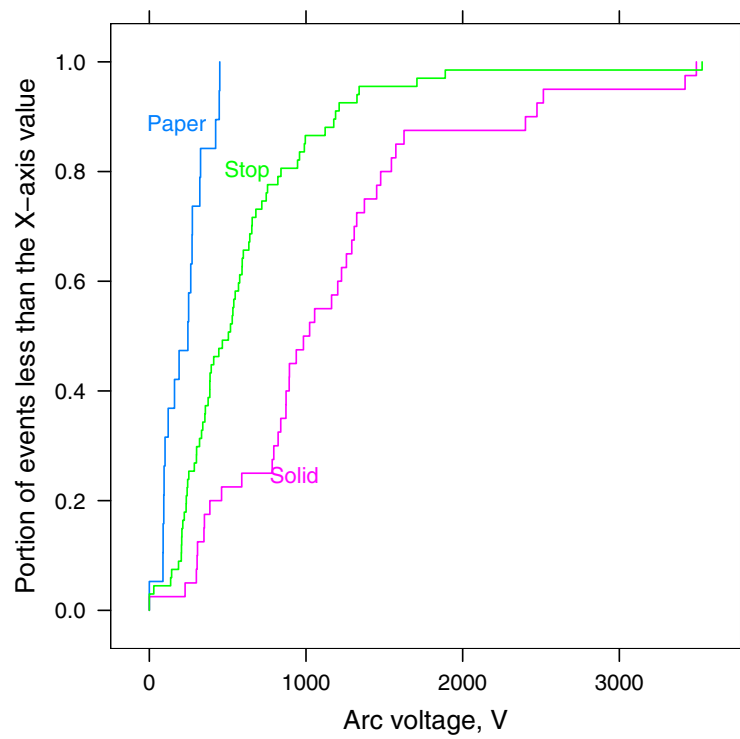


**Figure 5-12**
**Estimates of Arc Voltage by Splice Failure Type (Utility B)**

### *Impact of Sample Rate*

Because the basic assumption of the nonlinear arc model is that the voltage across the arc is a square wave, we might assume that the algorithm is sensitive to sample rate. Figure 5-13 compares arc voltage estimates at the original 128 samples per cycle against an estimate of arc voltage with all signals downsampled to 16 samples per cycle. The downsampled estimate and the original estimate are linearly correlated, but there is significant spread between the two. This suggests that a reduced sample rate makes the algorithm more error prone. More work is need to evaluate different filtering and differentiation approaches at 16 samples per cycle.
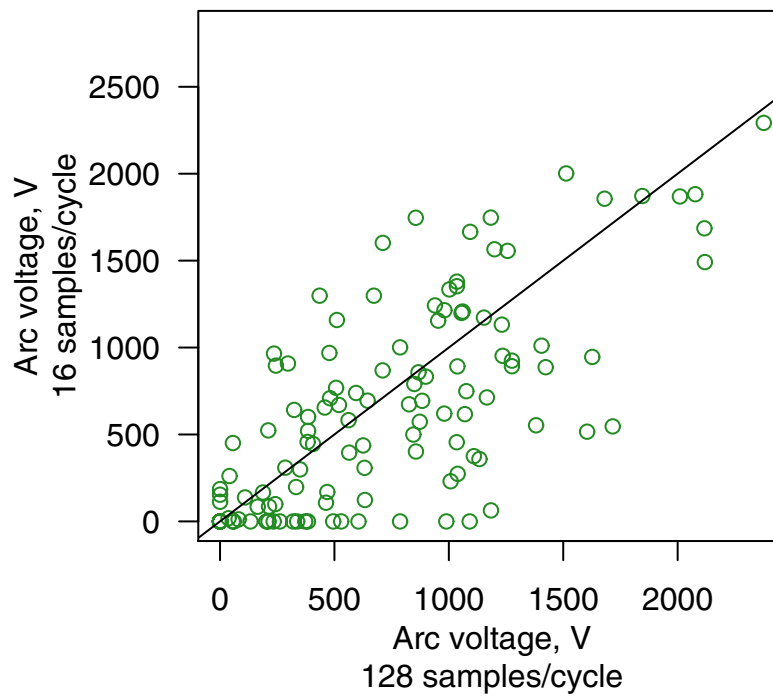


**Figure 5-13**
**Comparison of Arc Voltage Estimates With 16 and 128 Samples Per Cycle (Utility A)**

## Further Work

More work could be done to further apply the nonlinear-arc concept. Some possibilities include:

- *Half-cycle blips*—Is it possible to estimate a location and arc voltage with only a half-cycle event? It may be possible, but we need to test with short-duration events with known locations (fuse operations are likely candidates as are half-cycle self-clearing blips that change to full-blown faults).

- *Fault-cause estimation*—More data sets and more analysis of the existing datasets could lead to ways to estimate the causes of faults (within certain probabilities).

- *Voltage-only estimation*—As shown in Chapter 2, the currents during a fault can be derived from the prefault voltage, the voltage sag during the fault, and the source impedances. Using these derived currents, it may be possible to estimate arc characteristics using only voltage. This may increase the applicability of the algorithm.

In addition to these measures that may help with fault location, further work on arc parameter evaluation could help with arc flash prediction and model development, equipment failure analysis, and forensic investigations of damage and equipment failure.

# *6*
# DISCUSSION OF FAULT LOCATION APPROACHES

## Discussion Questions

One of the main goals of the project in 2006 is to determine the range of possibilities for an impedance-based fault locating system. To do that, a number of discussion questions were identified to help utilities planning for the monitoring capabilities needed for a fault-location system. These questions are discussed in the section following:

1. Do you need to monitor each feeder, or is one monitor per substation bus sufficient?

2. Can you just monitor voltage, or do you need both voltage and current?

3. Can rms data be used in place of waveform data? If so, under what circumstances?

4. Does asymmetry in fault waveforms affect results? If so, how do you correct for that?

5. Does fault impedance skew results? If so, how do you correct for that?

6. Does fault location work well for circuits with significant amounts of underground?

7. Does fault location work in urban as well as rural circuits?

8. What sample rate is sufficient?

9. Do any monitoring data sources have any peculiarities that need to be accounted for?

10. After a certain number of faults have been located, is it possible to provide a correction factor to account for inaccuracies in CTs or PTs or in circuit models?

11. What input data is most significant as far as accuracy?

12. Do circuit capacitors influence results? What about line voltage regulators?

13. Does the circuit X/R ratio change results?

14. Does load current affect results? If so, how do you account for that?

15. Are there faults that are particularly difficult to locate (line-to-line for example)?

16. Can you estimate a range of accuracy (say 4 to 4.5 miles with 80% probability) on the answer rather than just one location?

17. Are the built-in algorithms on relays suitable?

18. Can feeder devices (even simple ones in customer meters) improve fault location accuracy?

## Discussion of Questions Considered

**Question 1.** Do you need to monitor each feeder, or is one monitor per substation bus sufficient?

**Response:** Feeder-level monitors are the best, but good fault location can be achieved with bus-level monitors. For line-to-ground faults, the key to achieving good location accuracy is using the residual current ($I_A + I_B + I_C$). This avoids most of the load current. For line-to-ground faults, the bus-level currents and the feeder-level currents are consistent within a multiplier factor for 70% of events (see Figure 2-9). For multiphase faults, using a constant-impedance load model works reasonably well, but there is room for more research to investigate better load models for fault location.

**Question 2.** Can you just monitor voltage, or do you need both voltage and current?

**Response:** Measuring both voltage and current is the best, but voltage-only fault location is possible. Voltage-only fault location is less predictable because a prefault voltage is needed as a reference to the faulted voltage during the fault. If the prefault voltage is missing or misidentified, it will add error to the location, possibly even giving a nonsense answer. A nonsense answer may actually be better than a severely wrong but reasonable answer. Given that, a voltage-only algorithm can have uses on instrumentation where currents are unavailable.

**Question 3.** Can rms data be used in place of waveform data? If so, under what circumstances?

**Response:** Waveforms are better and allow more sophisticated processing to account for arc impedance or various load models that may be developed. That said, rms data could be used for fault location. The accuracy of the rms calculation is important. One of the key parts of a fault-location algorithm is identifying a good portion of the fault to use in calculations. When using rms data from instrumentation, that estimation is left up to the given piece of equipment. It may work well, but instruments put in widespread use for fault locating should be tested for various fault-type. If possible, try to avoid using rms data, but it could be useful for supplemental monitoring data such as from customer meters.

**Question 4.** Does asymmetry in fault waveforms affect results? If so, how do you correct for that?

**Response:** Asymmetry can cause error in fault-location algorithms. The best way to avoid these errors is to wait until the asymmetry has decayed out. This is normally possible for recloser or feeder breaker lockouts. If that is not possible, Chapter 3 has additional methods for handling asymmetry.

**Question 5.** Does fault impedance skew results? If so, how do you correct for that?

**Response:** Fault impedance is normally low and does not cause dramatic errors in fault locations. One drawback of many published fault-location algorithms is that they attempt to model the arc effect as a linear resistance. That is not a reasonable approximation. The arc impedance is highly nonlinear. The nonlinear arc modeling discussed in Chapter 5 more accurately models arc characteristics and leads to one of the better fault-locating algorithms.

**Question 6.** Does fault location work well for circuits with significant amounts of underground?

**Response:** Yes. Impedance-based fault location works well on urban, underground systems. Both Utility B and Utility C are urban, mainly underground utilities. Accuracy gets better closer to the substation where circuit impedances between the substation and the fault are in the same range as the substation source impedance. In urban areas with high load, multiphase faults are the most difficult to locate because of the difficulty of separating load and fault current.

**Question 7.** Does fault location work in urban as well as rural circuits?

**Response:** Yes. See the answer to question 6. The most difficult faults to identify are distant faults on rural circuits. As the fault current drops, the fault-current profile flattens out. The flat portion is where the location is most difficult (far from the substation).

**Question 8.** What sample rate is sufficient?

**Response:** Even relays that report four samples per cycle can give useful fault locations, but higher is better. More advanced algorithms and filtering are better at higher sample rates. The power quality recorders that have 128 or more samples per cycle are the best. Relay-level sampling of 16 samples per cycle is good but still may not be enough to allow accurate arc voltage modeling.

**Question 9.** Do any monitoring data sources have any peculiarities that need to be accounted for?

**Response:** We have not encountered any significant peculiarities in the data provided by utilities. Some recorders and instrumentation have their quirks, but none are significant enough to need special attention.

**Question 10.** After a certain number of faults have been located, is it possible to provide a correction factor to account for inaccuracies in CTs or PTs or in circuit models?

**Response:** Unknown. While we have a considerable dataset, the data was gathered over a short time horizon, so we do not have any significant history in the dataset. If we can get more data built up, we are hopeful that correction factors can be applied to correct for inaccuracies in line impedances, earth return impedance, and more. More advanced learning algorithms could provide more automatic correction factors.

**Question 11.** What input data is most significant as far as accuracy?

**Response:** The line impedance characteristics are the most important. It is also important that the circuit model actually reflects the connectivity and circuit characteristics that are in the field.

**Question 12.** Do circuit capacitors influence results? What about line voltage regulators?

**Response:** Circuit capacitors do not appear to influence fault-location results. The analysis of the data in this report was done without regard to capacitors—they were ignored, and that did not seem to impact the accuracy. While no rigorous investigations were done, checks on circuits with capacitors did not reveal anything unique about the impacts of capacitors. On circuits with capacitors, a ringing after the circuit faults can be pronounced, but as long as that part of the waveform is not used for fault location, it should not impact location estimates. Likewise, voltage regulators are not expected to significantly upset location estimates. Again, they were ignored in the analysis done in this report. A regulator at its neutral position does not add any impedance to the line.

**Question 13.** Does the circuit X/R ratio change results?

**Response:** It does not seem to impact results. Cable circuits have a much different X/R ratio than overhead circuits and the data has shown similar accuracy with cable faults than with overhead faults.

**Question 14.** Does load current affect results? If so, how do you account for that?

**Response:** Load current can impact results, especially for bus-level monitors. The main ways to account for load current are (1) for line-to-ground faults, use the residual current $(I_A + I_B + I_C)$ to avoid all but the zero-sequence unbalance, and (2) use a constant-impedance (or other suitable load model) to divide out the load for multi-phase faults.

**Question 15.** Are there faults that are particularly difficult to locate (line-to-line for example)?

**Response:** We have not identified any particularly hard-to-find faults of normal faults. It mainly depends on the circuit configuration. If a circuit has heavy branching and multiple possible fault locations for a lockout of one protective device, then faults will be harder to locate. Faults on the ends of long circuits are going to have less-accurate locations. Intermittent faults, especially short-duration blips, are more difficult to find.

**Question 16.** Can you estimate a range of accuracy (say 4 to 4.5 miles with 80% probability) on the answer rather than just one location?

**Response:** We have some idea of the overall accuracy of the fault-location algorithms that we have tested, but we are not yet at the point where we can claim to be able to estimate a range of accuracy for *one particular event* (predicting the performance of an overall set and predicting a range for an individual event are different). We hope to be able to produce such an estimate with further research an analysis of more data.

**Question 17.** Are the built-in algorithms on relays suitable?

**Response:** The built-in algorithms in relays can give useful location estimates. It is certainly among the easiest ways to get fault location estimates, but it has limitations. For example, the SEL relays must have both voltage and current, and the Takagi algorithm that they use is one of the poorer methods for distribution faults based on the data we have evaluated.

**Question 18.** Can feeder devices (even simple ones in customer meters) improve fault location accuracy?

**Response:** We are hopeful that feeder devices can help improve fault locations. They could help by providing downstream data points. On circuits with branching, having data from multiple data sources would help narrow down the choices of possible fault locations. Any fault location system should consider ways to include downstream data sources. Unfortunately, we have not found any utilities with a significant quantity of good downstream data sources. Utility E provided some downline recloser data, but the recloser only recorded faults downstream of itself. To be more useful, a feeder device should also record voltage sags, so it can help locate upstream or lateral faults. We are hopeful that we can find more data to help evaluate the benefit of downstream devices and the best ways to integrate that data into fault-locating algorithms.

# *7*
# IMPLEMENTATION VISION

Fault-location algorithms are only one component of an integrated system to locate faults. In fact, the algorithms may be the easiest part. A fault location system must be integrated with the monitoring event database and the system circuit information (see Figure 7-1). This must be brought together and presented to the operator. The event data must be made available within minutes to be most useful to dispatchers.
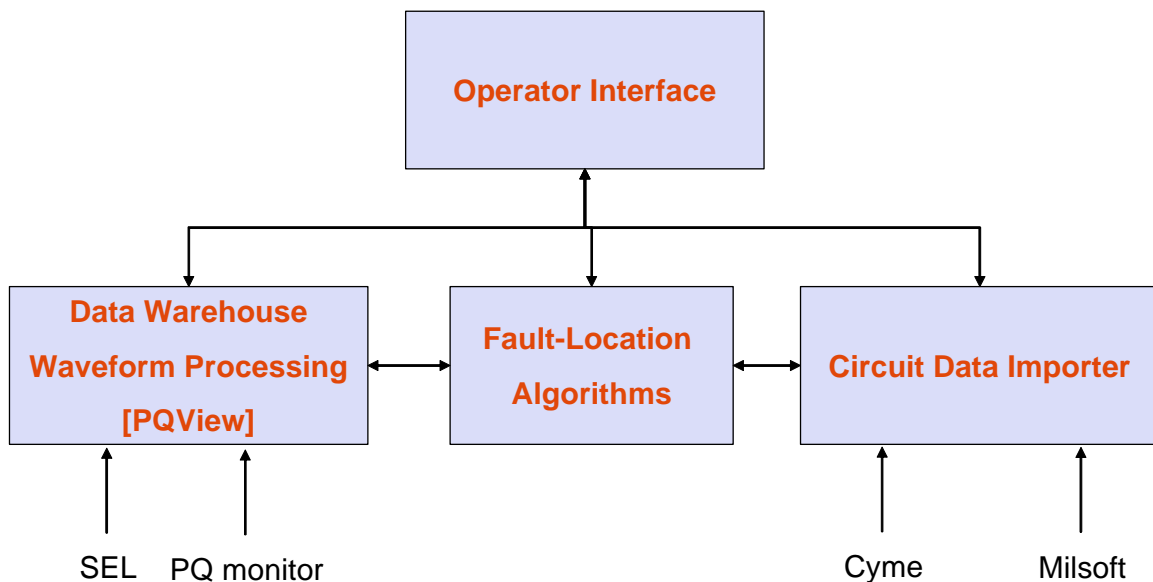


**Figure 7-1**
**Fault-Location System Components**

Each of these components must work together, and they must be integrated with other systems at a utility. Because of the level of integration between the fault-location system and other databases or interfaces, a fault-location system cannot be a shrink-wrapped standalone piece of software. Custom interfacing will always be necessary. The main goal will be to ease that integration as much as possible. Standardized, simplification, and documentation are the main ways to make integration easier. Supporting the most likely interfaces out-of-the-box will also make integration easier. This includes SEL relays and common PQ recorders on the monitoring side. On the circuit data side, import routines for Cyme and possibly other common programs are important.

## Monitor Interfacing and Event Data Storage

PQView will serve as the focal point for data storage and data collection. PQView can interface with many recording devices, including a large number of relays, power-quality recorders, and meters. PQView can now handle or will soon be able to handle a number of formats, including:

- IEEE COMTRADE

- IEEE PQDIF

- SEL raw formats

- Dranetz BMI 3100, 7010, and 8100

For some monitors, PQView's data manager can directly access and download event data. This is possible with power quality recorders such as the Dranetz/BMI PQNode. For some devices, PQView will rely on external software to download events. For example, one way to collect and store Schweitzer relay data is to use Schweitzer's SEL-5040 ACSELERATOR Report Server software can be set up to download the event data in Comtrade format. From there, a PQView data handler can read the Comtrade files collected by the SEL-5040 software.

Adding monitoring for fault locating has a number of extra benefits, including identifying miscoordination and misoperation of protective devices, tracking down customer power quality complaints, identifying problem areas, tracking fault rates, and identifying conductor slapping faults.

## Interfacing With Circuit Models

Utilities have circuit data in a variety of formats that would need to be accessed by a fault-location system. A number of distribution analysis programs are used widely, including those by Cyme, Milsoft, and Advantica. Some utilities may primarily store their data in a GIS system. Table 7-1 summarizes the data storage techniques for several common distribution analysis programs. Database storage is the most common, and most of the database table structures are straightforward, so writing data-import or conversion routines should not be complicated for most distribution analysis programs. While not difficult, there are always complications with data conversion such as when software publishers change formats between versions. The circuit model needed for fault location is a simplification of what is normally stored by distribution analysis programs. For fault location, only connectivity and impedance information are needed, not loads, regulators, capacitor banks, or any protective devices. Reading data from GIS systems or other systems may be more complicated.

**Table 7-1**
**Data Storage Format of Common Distribution Analysis Programs**

| Program | Data Storage Format |
|---------|---------------------|
| ABB FeederAll | Microsoft Access database |
| Advantica/Stoner Synergee | Microsoft Access or SQL Server or Oracle database |
| Cyme Cymdist | Microsoft Access or SQL Server or Oracle database |
| Milsoft | Advantage database |
| Siemens PTI PSS/Adept | Binary format |

The interface to distribution circuit data can be done in a number of ways. One possibility is to have a standalone converter service that run periodically to update the circuit model in the fault location system.

## Fault-Identification and Location Algorithm(s)

A fault identification algorithm is needed to separate fault events and nonfault events recorded by the monitors. The main components of a fault-identification algorithm include:

- Determine if the event is actually a fault. Filter out and/or possibly classify voltage sags and inrush.

- Determine the phase or phases faulted.

- Possibly determine additional fault parameters based on the fault-location algorithm results, including fault current magnitude, duration, whether the fault evolved to multiple phases, distance to the fault, and whether the event had significant arc voltage.

- Provide a concise summary of fault parameters for the system operator.

The fault-location portion of the system will use the voltages and currents from the monitoring storage module and use that to predict fault locations on the circuit model. One or more algorithms may be chosen, depending on further testing and evaluation of performance. One type of algorithm may work better for some systems than others, so having more than one fault-location method in the toolbox is advantageous.

The fault-identification and location system will likely be implemented as a standalone library that interfaces with the PQView data warehousing application and the operator interface.

## Operator Interface

The operator interface is the focal point of the system. The interface should display recent fault events. As much as possible, the selection of fault events and location of faults should be automatic. For a fault location, the interface should display the fault and circuit graphically as well as provide pole numbers or manhole numbers or other physical location notation. If

operators normally use some mapping software, one possibility is to forward fault-location information to the operator's normal mapping software for display and manipulation there. We envision that the operator interface will be a relatively simple web-based program. Ease of use and simplicity are important.

## Future Work Plan

As part of the commercialization of the fault-location technology, work will proceed in 2007 with the following tasks:

*Prototypes*—The major effort for 2007 will include prototyping the modules in a fault-location system. We will finalize the best fault identification and location algorithms through more testing. Interfacing to PQView will allow us to directly interface with a large number of monitors. For the circuit data, we will test one or more converter services, depending on the direction of volunteer funders.

*Data collection*—While we already have a fantastic collection of data, we will follow up and try to fill some areas. We could use longer term data accumulated over several years at a small number of locations. This would let us test ways to "tune" fault locations to improve performance once we get a certain number of events, and it might tell us how many events are needed for "tuning." Data from multiple sources on a circuit is also something we are looking for; this will help us explore how to incorporate multiple data sources to improve fault locations. Lines with significant branching are where the most benefit could be gained from downline devices. We could also use more fault data from relays and more 34.5-kV fault data.

*Advanced algorithms*—Most of the algorithms tested to date have been relatively simple (except perhaps for the nonlinear arc model). We may try more advanced algorithms published in the literature if they seem to offer improvements.

# 8
# REFERENCES

1. Baran, M. E. and Kim, J., "A classifier for distribution feeder overcurrent analysis," *IEEE Transactions on Power Delivery*, vol. 21, pp. 456-462, 2006.

2. Benmouyal, G., "Removal of DC-offset in current waveforms using digital mimic filtering," *IEEE Transactions on Power Delivery*, vol. 10, pp. 621-630, 1995.

3. Burke, J. J. and Lawrence, D. J., "Characteristics of Fault Currents on Distribution Systems," *IEEE Transactions on Power Apparatus and Systems*, vol. PAS-103, pp. 1-6, 1984.

4. Cobine, J. D., *Gaseous Conductors*: McGraw-Hill Book Company, 1941.

5. Diaz, H. and Lopez, M., "Fault Location Techniques for Electrical Distribution Networks: A Literature Survey," presented at Fifth IASTAD Conference on Power and Energy Systems, Benalmadena, Spain, 2005.

6. Drouet, M. G. and Nadeau, F., "Pressure Waves Due to Arcing Faults in a Substation," *IEEE Transactions on Power Apparatus and Systems*, vol. PAS-98, pp. 1632-5, 1979.

7. *Distribution Fault Current Analysis*. Electric Power Research Institute, Palo Alto, CA: 1983. EPRI 1209-1.

8. *An Assessment of Distribution System Power Quality: Volume 2: Statistical Summary Report*. Electric Power Research Institute, Palo Alto, CA: 1996. EPRI TR-106294-V2.

9. *An Assessment of Distribution System Power Quality: Volume 3: Library of Distribution System Power Quality Monitoring Case Studies*. Electric Power Research Institute, Palo Alto, CA: 1996. EPRI TR-106294-V3.

10. Eriksson, L., Saha, M. M., and Rockefeller, G. D., "An Accurate Fault Locator With Compensation for Apparent Reactance in the Fault Resistance Resulting From Remote-end Infeed [transmission Line Faults]," *IEEE Transactions on Power Apparatus and Systems*, vol. PAS-104, pp. 424-36, 1985.

11. Fletcher, R. and Reeves, C. M., "Function Minimization by Conjugate Gradients," *Computer Journal*, pp. 148-54, 1964.

12. General Electric GER-3963, "Evaluation of a Phasor-Based Fault Location Algorithm," 1996.

13. Girgis, A. A., Fallon, C. M., and Lubkeman, D. L., "A Fault Location Technique for Rural Distribution Feeders," *IEEE Transactions on Industry Applications*, vol. 29, pp. 1170-5, 1993.

14. Glinkowski, M. and Wang, N., "ANNs pinpoint underground distribution faults," *IEEE Computer Applications in Power*, vol. 8, pp. 31-34, 1995.

15. Goda, Y., Iwata, M., Ikeda, K., and Tanaka, S., "Arc Voltage Characteristics of High Current Fault Arcs in Long Gaps," *IEEE Transactions on Power Delivery*, vol. 15, pp. 791-5, 2000.

16. Hizman, H., Crossley, P., Gale, P., and Bryson, G., "Fault section identification and location on a distribution feeder using travelling waves," *Power Engineering Society Summer Meeting*, vol. 3, 2002.

17. IEEE Std C37.114-2004, *IEEE Guide for Determining Fault Location on AC Transmission and Distribution Lines*.

18. Jarventausta, P., Verho, P., and Partanen, J., "Using fuzzy sets to model the uncertainty in the fault location process of distribution networks," *IEEE Transactions on Power Delivery*, vol. 9, pp. 954-960, 1994.

19. Kim, J., Baranowski, J. F., and Lampley, G. C., "Estimation of Fault Location on Distribution Feeders using PQ Monitoring Data," presented at SPEC Power Electronics and Power System Seminar, Raleigh, NC, 2006.

20. Koch, B. and Christophe, P., "Arc Voltage for Arcing Faults on 25(28)-kV Cables and Splices," *IEEE Transactions on Power Delivery*, vol. 8, pp. 779-88, 1993.

21. Lampley, G. C., "Fault Detection and Location on Electrical Distribution System Case Study," presented at IEEE Rural Electric Power Conference, 2002.

22. Peele, G. S., "Using monitoring to improve the utility system," presented at IEEE Power Engineering Society Summer Meeting, 2001.

23. Peele, S., "Faults Per Feeder Mile," presented at PQA Conference, 2001.

24. Radojevic, Z. M., Koglin, H.-J., and Terzija, V. V., "A novel approach to the distance protection, fault location and arcing faults recognition," presented at IEEE PES Power Systems Conference and Exposition, 2004.

25. Radojevic, Z. M., Lee, C. J., Shin, J. R., and Park, J. B., "Numerical algorithm for fault distance calculation and blocking unsuccessful reclosing onto permanent faults," presented at IEEE Power Engineering Society General Meeting, 2005.

26. Radojevic, Z. M., Terzija, V. V., and Djuric, N. B., "Numerical algorithm for overhead lines arcing faults detection and distance and directional protection," *IEEE Transactions on Power Delivery*, vol. 15, pp. 31-37, 2000.

27. Reineri, C. A. and Alvarez, C., "Load research for fault location in distribution feeders," *Generation, Transmission and Distribution, IEE Proceedings-*, vol. 146, pp. 115-20, 1999.

28. Rizk, F. A. and Nguyen, D. H., "AC Source-Insulator Interaction in HV Pollution Tests," IEEE Transactions on Power Apparatus and Systems, vol. PAS-103, pp. 723-32, 1984.

29. Sachdev, M. S. and Agarwal, R., "A Technique for Estimating Transmission Line Fault Locations From Digital Impedance Relay Measurements," *IEEE Transactions on Power Delivery*, vol. 3, pp. 121-9, 1988.

30. Santoso, S., Dugan, R. C., Lamoree, J., and Sundaram, A., "Distance Estimation Technique for Single Line-to-Ground Faults in a Radial Distribution System," presented at IEEE Power Engineering Society Winter Meeting, 2000.

31. Schweitzer Engineering Laboratories, "SEL-251-1 Instruction Manual," 2002.

32. Schweitzer, E. O., "A Review of Impedance-Based Fault Locating Experience," presented at Fourteenth annual Iowa-Nebraska system protection seminar, Omaha, NE, 1990.

33. Schweitzer, E. O., III and Hou, D., "Filtering for protective relays," presented at IEEE WESCANEX 93. 'Communications, Computers and Power in the Modern Environment.' Conference Proceedings, 1993.

34. Short, T. A., *Electric Power Distribution Handbook*. Boca Raton, FL: CRC Press, 2004.

35. Slepian, J., "Extinction of a Long AC Arc," *AIEE Transactions*, vol. 49, pp. 421-30, 1930.

36. Stergiou, P. V., "Substation Monitoring to Locate Distribution Feeder Faults," presented at PQA Conference, 2005.

37. Stergiou, P. V., "Fault Location for Underground Systems," presented at PQA, 2006.

38. Strom, A. P., "Long 60-Cycle Arcs in Air," *AIEE Transactions*, vol. 65, pp. 113-8, 1946.

39. Takagi, T., Yamakoshi, Y., Yamaura, M., Kondow, R., and Matsushima, T., "Development of a New Type Fault Locator Using the One-terminal Voltage and Current Data," *IEEE Transactions on Power Apparatus and Systems*, vol. PAS-101, pp. 2892-8, 1982.

40. Xiangjun, Z., Li, K., Zhengyi, L., and Xianggen, Y., "Fault location using traveling wave for power networks," *Industry Applications Conference*, vol. 4, 2004.

41. Zimmerman, K. and Costello, D., "Impedance-Based Fault Location Experience," presented at 58th Annual Conference for Protective Relay Engineers, 2005.

**Export Control Restrictions**

Access to and use of EPRI Intellectual Property is granted with the specific understanding and requirement that responsibility for ensuring full compliance with all applicable U.S. and foreign export laws and regulations is being undertaken by you and your company. This includes an obligation to ensure that any individual receiving access hereunder who is not a U.S. citizen or permanent U.S. resident is permitted access under applicable U.S. and foreign export laws and regulations. In the event you are uncertain whether you or your company may lawfully obtain access to this EPRI Intellectual Property, you acknowledge that it is your obligation to consult with your company's legal counsel to determine whether this access is lawful. Although EPRI may make available on a case-by-case basis an informal assessment of the applicable U.S. export classification for specific EPRI Intellectual Property, you and your company acknowledge that this assessment is solely for informational purposes and not for reliance purposes. You and your company acknowledge that it is still the obligation of you and your company to make your own assessment of the applicable U.S. export classification and ensure compliance accordingly. You and your company understand and acknowledge your obligations to make a prompt report to EPRI and the appropriate authorities regarding any access to or use of EPRI Intellectual Property hereunder that may be in violation of applicable U.S. or foreign export laws or regulations.

**The Electric Power Research Institute (EPRI)**

The Electric Power Research Institute (EPRI), with major locations in Palo Alto, California, and Charlotte, North Carolina, was established in 1973 as an independent, nonprofit center for public interest energy and environmental research. EPRI brings together members, participants, the Institute's scientists and engineers, and other leading experts to work collaboratively on solutions to the challenges of electric power. These solutions span nearly every area of electricity generation, delivery, and use, including health, safety, and environment. EPRI's members represent over 90% of the electricity generated in the United States. International participation represents nearly 15% of EPRI's total research, development, and demonstration program.

Together...Shaping the Future of Electricity

*Program:*

Power Delivery Asset Management

1012438